

PDF hosted at the Radboud Repository of the Radboud University Nijmegen

The following full text is a publisher's version.

For additional information about this publication click this link.

<http://hdl.handle.net/2066/156479>

Please be advised that this information was generated on 2017-12-05 and may be subject to change.

A close-up photograph of a deer antler, showing the texture and branching structure. The antler is light brown and appears to be in the early stages of growth, with some darker, velvet-like material visible at the base.

CALCIUM
PHOSPHATE
CERAMICS

Eva R. Urquía Edreira

CALCIUM PHOSPHATE CERAMICS FOR BONE REGENERATION

“A substance that has been engineered to take a form which, alone or as part of a complex system, is used to direct, by control of interactions with components of living systems, the course of any therapeutic or diagnostic procedure, in human or veterinary medicine”.

ONE
GENERATION

Calcium phosphate ceramics for bone regeneration

Proefschrift

ter verkrijging van de graad van doctor
aan de Radboud Universiteit Nijmegen
op gezag van de rector magnificus,
volgens besluit van het college van decanen
in het openbaar te verdedigen op vrijdag 1 april 2016
om 12.30 uur precies

door

Eva R. Urquia Edreira

geboren op 7 maart 1981

te Madrid, Spanje

Promotor:

Prof. dr. ir. J.A. Jansen

Copromotoren: Dr. J.G.C. Wolke

Dr. J.J.J.P. van den Beucken

Manuscriptcommissie:

Prof. dr. J. Hoenderop

Prof. dr. ir. I.C. Heyligers

Dr. R. De Gelder

Calcium phosphate ceramics for bone regeneration

Doctoral Thesis

to obtain the degree of doctor
from Radboud University Nijmegen
on the authority of the Rector Magnificus,
according to the decision of the Council of Deans
to be defended in public on Friday, April 1, 2016
at 12.30 hours

by

Eva R. Urquia Edreira

Born on March 7, 1981

in Madrid (Spain)

Supervisor:

Prof. dr. ir. J.A. Jansen

Co-supervisors:

Dr. J.G.C. Wolke

Dr. J.J.J.P. van den Beucken

Doctoral Thesis Committee:

Prof. dr. J. Hoenderop

Prof. dr. ir. I.C. Heyligers

Dr. R. De Gelder

Cover design: Ignacio Cid Edreira (contacto@elchinoviene.com)

Thesis Layout: Eva R. Urquia Edreira

© Eva R. Urquia Edreira, Nijmegen 2016.

Printed by: www.proefschriftmaken.nl

“A mi familia”

“To my family”

This research forms part of the Project **P2.04 BONE-IP** of the research program of the **BioMedical Materials** institute, co-funded by the **Dutch Ministry of Economic Affairs, Agriculture and Innovation**.

CONTENTS

CHAPTER 1 | 9

General introduction.

CHAPTER 2 | 55

Instructive coatings for biological guidance of bone implants.

CHAPTER 3 | 95

Effects of calcium phosphate composition in sputter coatings on *in vitro* and *in vivo* performance.

CHAPTER 4 | 131

Residual stress evaluation within hydroxyapatite coatings of different micrometer thicknesses.

CHAPTER 5 | 153

Substrate geometry directs the mineralization the *in vitro* mineralization of calcium phosphate ceramics.

CHAPTER 6 | 181

Influence of ceramic disk material, surface hemispheres, and SBF volume on *in vitro* mineralization.

CHAPTER 7 | 207

Effect of Calcium Phosphate Ceramics Substrate Geometry on Cellular Organization, and Differentiation.

CHAPTER 8 | 239

English summary, Dutch summary, closing remarks, and future perspectives.

CHAPTER 9 | 261

Acknowledgments, Curriculum Vitae, and list of publications.

1

GENERAL INTRODUCTION

1. Introduction

In recent decades, the increase in both life-expectancy and associated bone-related diseases has consistently brought forth greater medical challenges in the field of bone regeneration. Material science research for healthcare applications has been stimulated to respond to this greater need for bone substitute materials. These materials, when applied for healthcare, are commonly known as “biomaterials”. A biomaterial can be defined as “a substance that has been engineered to take a form which, alone or as part of a complex system, is used to direct, by control of interactions with components of living systems, the course of any therapeutic or diagnostic procedure, in human or veterinary medicine”[1].

To improve the clinical performance of biomaterials, input from a number of scientific disciplines is required. Consequently, both scientists and engineers have focused on improving the design, properties, long-term survivability and development of new types of biomaterials to repair, replace or regenerate bone tissues [2, 3]. Biomaterials can be derived from metals, polymers, human or animal bones, corals, synthetic ceramics and composites [4].

2. Inorganic materials

Nowadays, autografts (a tissue or organ that is grafted into a new position in the body of the individual from which it was removed) remain the most effective option for bone repair and substitution followed by allografts (a tissue

or organ obtained from one member of a species and grafted to a genetically dissimilar member of the same species). However, despite the advantage of being osteogenic and osteoinductive, autografts and allografts present important drawbacks, such as high costs and limited availability. Consequently, there is a great need to develop synthetic alternative biomaterials for bone replacement or substitution. Synthetic inorganic materials have been applied clinically to repair or substitute bone tissue. These substitute materials need to possess appropriate mechanical and biological properties in order to be used for load-bearing applications and to achieve a strong fixation of the implant with bone tissue [4].

Biomaterials can be classified as bioactive or bioinert depending on their ability to bond to and stimulate bone tissue. Bioactive materials, such as calcium phosphate ceramics, several classes of bioglasses, calcium carbonates and calcium sulfates, stimulate bone tissue formation and directly bond to bone without an intervening soft tissue layer. On the other hand, bioinert materials such as titanium, aluminum oxide, stainless steel, cobalt-chromium, alloys and some ceramics (e.g. alumina, zirconia and carbon) do not bond directly to bone. Another property of major importance for biomaterials is osteoinductivity, which is “the mechanism of cellular differentiation towards bone of one tissue due to the physicochemical effect or contact with another tissue” [5]. This has aroused intense interest in the biomaterials field, and it will be further discussed in this chapter [4, 6]. The most common commercially available bone substitutes materials are inorganic (metallic and non-metallic), such as titanium and its alloys and calcium phosphate ceramics and their composites [7]. In the

CALCIUM PHOSPHATE CERAMICS FOR BONE REGENERATION

following paragraphs, the biomedical applications of these inorganic materials will be discussed.

Metallic materials, such as titanium and its alloys, are commonly used as implants for orthopedic and dental applications to replace hard tissue. This is due to their biocompatibility, high strength, low modulus of elasticity and low density. However, the high stiffness and fracture toughness of metallic materials are not optimal for the distribution of load to the surrounding bone tissue, which can reach low levels at certain areas at the interface and induce stress shielding. In these areas, the lack of load transfer can result in bone resorption and consequently implant loosening and failure.

For optimization of interaction with bone tissue at the interface, implant material surface modifications to enhance the surface biocompatibility and osseointegrative properties of these metallic implants have been extensively investigated. The physico-chemical properties of implant materials can be modified in order to increase the biological fixation of implant materials made of titanium and its alloys to bone [8]. Chemical pre-treatments on the titanium surface, such as alkali treatment or ions removal, have proved to enhance the bone-bonding strength [9]. Another approach has been the physical treatment of the metal by modifying the specific macrostructure and microstructure, e.g. titanium foam, which allows osteoblast cells to grow into an interconnected porosity [10]. Furthermore, the surface roughness of the material has been observed to significantly influence its ability to promote apatite nucleation and cell attachment compared to smooth surfaces [11-13].

Ceramics are common materials for dental and medical applications (e.g. repair of periodontal defects, augmentation of alveolar bone, sinus lifts, tooth replacement, repair of large bone defects, spinal fusion, and ear and eye implants) due to their appropriate biological properties, such as biodegradability, bioactivity and osteoconductivity. These ceramic materials are similar in composition to the bone mineral phase and are characterized by their hardness, strength, low electrical conductivity, and brittleness. However, due to their inferior mechanical properties, their application under load-bearing conditions is limited. One exception to this is long-term clinical performance of α -alumina (Al_2O_3) for orthopedic purposes (e.g. total hip prostheses) [14, 15] which has been in use for over three decades. However, in most cases ceramics are used as coatings on mechanically strong bioinert or biotolerant implants. These ceramic coatings and the main pros and cons of each coating technique will be discussed in detail in this section.

3. Structure and properties of bioceramics

All inorganic non-metallic solids prepared from powdered materials and created by the application of high temperature are classed as ceramics. Due to the mixed ionic-covalent bonding between the atoms, there are consistent properties that characterize ceramic materials: strength and hardness but brittleness at room temperature, resistance to chemical corrosion and high temperatures more than polymers and metals, and possession of low electrical

CALCIUM PHOSPHATE CERAMICS FOR BONE REGENERATION

conductivity. The majority of ceramics have many and varied crystal structures resulting in an extremely wide range of properties [16]. Due to their unique properties, ceramic materials are widely used in engineering and biomedical applications. Synthetic ceramics used for repair, reconstruction or replacement of damaged human body parts, or to function in intimate contact with living tissue are called “bioceramics”. For biomedical applications, a number of parameters have to be considered, including density, biocompatibility, strength and wear performance. Different types of bioceramics are detailed below, including polycrystalline ceramics (e.g. alumina or calcium phosphates), zirconia ceramics, bioactive composites, bioactive glasses and glass-ceramics [17].

Aluminum oxide, also known as alumina (Al_2O_3), is widely used in engineering bioceramics, for example in orthopedics and dentistry. Because of the strong bonding between the atoms, alumina has to be produced at a very high sintering temperature. It is usually white but is sometimes pink (88 % alumina) or brown (96 % alumina) depending on impurities or additives. The composition of aluminum oxide can be easily changed to enhance certain desirable material characteristics, such as the hardness or color. It also has excellent size and shape capability, which is advantageous for bioengineering applications. The low friction, wettability and hydrophilic surface of alumina (i.e. alumina crystal structure bonds with water) give it a superior load-bearing surface in a physiological environment. Similar to the majority of ceramics, its use as a structural material is restricted by its brittleness. To help alleviate this,

it can be toughened or reinforced by combining with composites of other materials with suitable mechanical properties (e.g. alumina matrix composite) [18].

Zirconia ceramics have good mechanical properties and low temperature degradation. This ceramic has a stress-induced phase transformation that results in a resistance to crack-propagation. This is due to a change in crystallographic structure depending on the temperature (at temperatures below 1170 °C, zirconia exists in monoclinic form, at the temperature 1170 °C monoclinic structure transforms to tetragonal form which is stable up to 2370 °C and tetragonal crystal structure transforms to cubic structure at 2370 °C) [19]. However, this phase transformation also occurs at the surface of the ceramic when present in body fluid, causing a progressive roughening (i.e. aging) that compromises the lifetime of zirconia implants. Currently, alumina-zirconia composites are being investigated as possible materials for orthopedic applications [20, 21].

Bioactive glass is a silicate glass-based, amorphous material. The first bioactive glass is known as 45S5 and was developed by Hench in the early 70s [22]. This bioactive glass was produced by melting high purity oxides (SiO_2 , Na_2CO_3 , CaCO_3 and P_2O_5) at very high temperatures. Bioactive glass releases ions when in contact with body fluid. Consecutive reactions with these ions occur on the surface of bioactive glass leading to the formation of a carbonated hydroxyapatite layer similar to bone mineral that creates a strong bond with soft and hard tissue [23]. Recently, the development of bioactive glasses based on

CALCIUM PHOSPHATE CERAMICS FOR BONE REGENERATION

borate and borosilicate compositions has been investigated due to the faster chemical release of ions compared to silicate 45S5 bioactive glass [24-26].

Glass ceramics are materials with higher mechanical strength than bioactive glass due to the different crystalline phases of various types of glass [27]. The main characteristic of glass ceramics (phosphate based glasses) is that they have a high ion dissolution rate. In order to control the degradation rate, the composition of glass ceramics can be changed by adding metal oxides (such as TiO_2 , Al_2O_3 , B_2O_3) [28-30]. These additives are incorporated into the phosphate based glass composition to stabilize the glass network resulting in a slower degradation of the glass [24].

Lastly, calcium phosphates are bioactive materials that can resorb over time when in contact with hard tissue [31, 32]. Like most ceramics, calcium phosphates have poor mechanical properties and for this reason they are mostly used as coatings and filler materials. As already mentioned, these calcium phosphate ceramics are similar to the mineral component of bone and therefore are not harmful and can remain in a biological system [2].

4. Bioactivity, osteoconductivity and osteoinductivity of calcium phosphate ceramics

Synthetic bone implant materials made of calcium phosphate ceramics have shown certain capacity for stimulating bone tissue. Depending on their physicochemical properties upon implantation, they are considered to be

bioactive, osteoconductive and/or osteoinductive. The following paragraphs discussed each of these mentioned properties.

Bioactive ceramics for load-bearing applications are used as coatings for titanium and its alloys to improve the biocompatibility of metal implants [2]. Calcium phosphate ceramics are known to allow direct physicochemical bonding with bone and to enhance bone tissue formation [4]. This phenomenon occurs when part of the CaP ceramics is dissolved in form of ions into the microenvironment. Once these liberated ions are released, protein adsorption and precipitation of the biological apatite crystals takes place creating a layer on the surface of the calcium phosphate biomaterial. This creates a favorable environment for the surface colonization by osteoblastic cells, which produce newly formed mineralized bone tissue in direct contact with the ceramic material [33]. Bioactive coatings accelerate stability by promoting a rapid fixation of implants with the bone. Among the bioactive ceramics most commonly investigated for use in bone regeneration are β -tricalcium phosphate (β -TCP), hydroxyapatite (HA) and bioactive glass, which are also biocompatible and osteoconductive but differ in resorption rate. By changing surface properties of CaP ceramics, bone integration and bonding can be influenced [34, 35].

Osteoconductivity was defined by Wilson-Hench as the process by which bone is directed so as to conform to a material's surface [36]. This apparent growth of bone tissue along an implant surface is essential for the stability of long-term orthopedic and dental implants [33]. All bioactive materials are also

CALCIUM PHOSPHATE CERAMICS FOR BONE REGENERATION

osteoconductive and they participate in the phenomenon that takes place at the bone/implant interface [4].

Some synthetic materials have the capacity to induce bone and are therefore considered osteoinductive materials [37]. This property has been defined as “the mechanism of cellular differentiation towards bone of one tissue due to the physicochemical effect or contact with another tissue” [5]. Calcium phosphate ceramics are commonly known for being osteoconductive, however, in the past decade a variety of studies have reported the intrinsic osteoinductive properties of diverse calcium phosphate ceramics. These CaP osteoinductive materials include porous synthetic HA [38-40], β -TCP [41], porous biphasic calcium phosphate (BCP) which is the mixture of HA and TCP [42, 43] and coral-derived hydroxyapatite [40]. Moreover, to further enhance the osteoinductive capacity, these materials can be subjected to some engineered modifications of physicochemical properties such as geometry, topography (i.e. surface structure), macroporosity, microporosity, particle size and chemical composition [4]. Finally, the selected model, implantation site, procedure and study duration to investigate osteoinduction may also influence this property [37].

5. Calcium phosphate ceramics used as coatings

Bioceramics can be produced in crystalline and amorphous forms and generally can be classified based on their chemical composition into two groups: calcium phosphates (CaPs) and others. CaP ceramics comprise a family

of compounds with different chemical compositions, crystallographic structures and solubility (See Table 1). Bone and calcium phosphate ceramics share common properties in mineral phase that make them excellent candidates for tissue replacement including biodegradability, bioactivity and osteoconductivity [4]. However, the use of CaP ceramics presents difficulties with degradation rate control and resorption. These issues are due to their limited solubility in the body fluid and no apparent degradation by cellular activity (i.e. bone resorbing cells) [44, 45]. Also, it is known that the use of CaP ceramics in parts of the body where substantial mechanical loading is experienced is not feasible due to their poor mechanical properties.

CaP ceramics are frequently used as bioactive coatings to modify the surface of bioinert metals or polymers. This modification facilitates the use of implants under loaded conditions and integrates the implant with the surrounding tissue. An ion-exchange reaction occurs between the bioactive implant surface and surrounding body fluid, initiating the formation of a carbonate apatite layer that leads to active bone growth onto the implant surface.

Improving the properties of coating materials relative to the bulk material can facilitate the clinical application of these implants. Biological characteristics of the coating can differ between coatings applied with different techniques. For this reason, it is essential to understand the coating deposition technique. Furthermore, the coated layers must be adequately adjusted by a post-treatment (e.g. heat treatment to increase crystallization). It has been

CALCIUM PHOSPHATE CERAMICS FOR BONE REGENERATION

demonstrated in several reports that cellular behavior and implant fixation can be controlled by material properties [46, 47]. Material surface modifications in both implant and CaP ceramic coatings can be applied by varying material properties such as surface topography, elasticity, chemistry, surface roughness, coating fatigue and stress and post and pre-treatments of the materials.

The most commonly investigated synthetic CaP ceramic materials for use in bone regeneration are hydroxyapatite ($\text{Ca}_5(\text{PO}_4)_3\text{OH}$, HA), which is the mineral that occurs naturally in bone tissue and the most abundant inorganic phase in the human body, and β -tricalcium phosphate ($\text{Ca}_3(\text{PO}_4)_2$, TCP). To deposit such coatings, several techniques can be used, including biomimetic deposition, electrostatic spray deposition, pulsed laser deposition, ion beam deposition, sputter deposition and plasma spray, which are discussed in more detail in the next section.

6. Coating techniques

Different coating deposition techniques can be used for the modification of bone implant surfaces. The most commonly used coating techniques are by dry coating deposition, although a recent trend involves the development of wet-chemical deposition (i.e. biomimetic deposition) for both inorganic and organic coatings.

- **Biomimetic deposition**

The biomimetic deposition technique, which mimics the natural deposition of biologic apatite, has opened up a new way to develop biomaterials. The apatite-like CaP coating is deposited by placing the substrates to be coated into simulated body fluid (SBF) medium kept at 37 °C. The SBF solution allows the in situ chemical precipitation from a metastable supersaturated solution similar in ion concentrations to those of human blood plasma with respect to the apatite nucleation [48].

Some of the advantages of this technique are its simplicity, the possibility to coat complex geometrical shapes at room temperature, coating with more similar chemistry with the biological one, and the deposition time. This makes the technique suitable for covering polymeric substrates. However, the main disadvantage is that the adhesion of the CaP coating, especially on inert polymeric substrates, is very poor [49, 50].

- **Plasma-spraying**

Plasma-spraying was the first coating technique for biomedical applications; this technique is also very successful technique for applying CaP coatings on implants due to its high deposition rate. The coating process consists in a DC (direct current) electric arc, which is stuck between two electrodes, while a mixed stream of gasses passes through this arc turning the gasses into a plasma of high temperature (which rapidly decreases as a function of distance) and high speed. Appropriated cooling techniques keep the temperature of surface to be coated below 100 to 150 °C. Plasma spraying

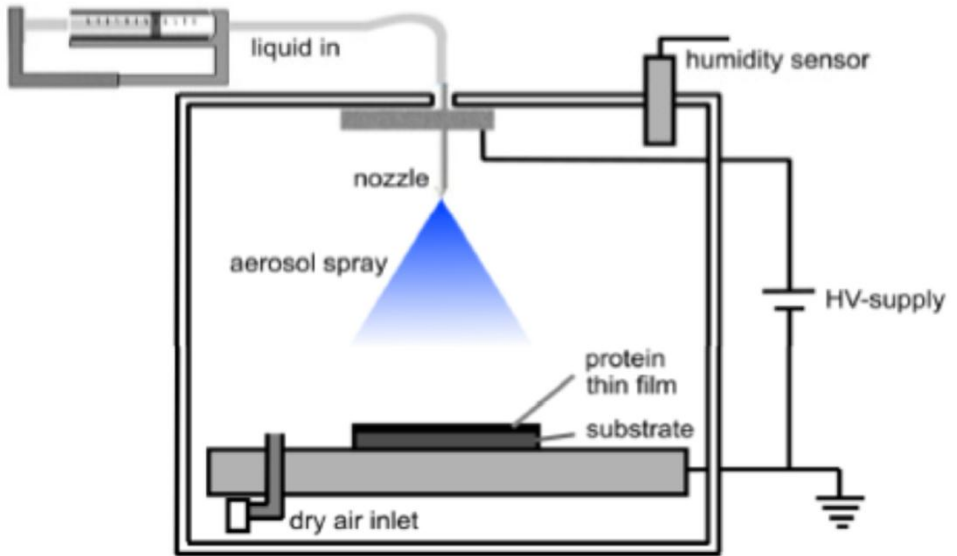


Figure 1. A representative ESD process

produces coatings with desired chemistry and crystallinity, despite poor control of the thickness and surface morphology [51].

- **Electrostatic spray deposition**

The principle of electrostatic spray deposition (ESD) technique is based on the generation of a dispersion of solid or liquid particles in a gas under the influence of a high voltage. The liquid is pumped through a nozzle and a spherical droplet is then formed, when high voltage is applied between the nozzle and the substrate a spray of highly charged droplets are attracted onto the surface of the substrate depositing a thin layer. A representative ESD process is shown in **Figure 1**.

This technique has several advantages, such as simplicity, wide choice of CaP phases to be sprayed, extensive control over surface property and high deposition efficiency [52, 53]. Some of this technique disadvantages are chemical homogeneity in the deposited coating and substrate adhesion.

- **Pulsed laser deposition**

Laser deposition is a technique in which intense ultraviolet laser beam pulses are used to evaporate CaP ceramic from a rotatory target situated inside of a vacuum chamber. The substrates are located at a certain distance parallel to the target on a heated substrate holder.

This technique allows deposition of thin, dense, well adhering coatings with controlled chemistry and crystallinity [54, 55]. A major advantage of this technique is the possibility of coating CaP ceramics on polymeric substrates at low temperature [56]. However, a non-uniform coverage makes this technique not very well suited for large area deposition [57].

- **Ion beam deposition**

Ion beam deposition is a technique, in which CaP target material and substrates are placed in a vacuum chamber; there is bombardment by a beam from an ion gun. The generated ions are accelerated in an electric field and deposited onto the substrates in a cold plasma atmosphere. However, the deposited CaP coatings have inherent properties and the chemical composition of the coating may differ from that of the bulk material [58-60]. The CaP coating presents an amorphous phase after deposition that can be post-heat

CALCIUM PHOSPHATE CERAMICS FOR BONE REGENERATION

treated to increase crystallization and high adhesion to the substrate materials [61].

- **Sputter deposition**

Sputtering deposition is a deposition technique that takes place in a vacuum environment. CaP target material is irradiated with high energetic ions, accelerated by high voltage, which bombard and collide with atoms on the target surface. Subsequently, the atoms of the target material are ejected a very high speed onto the substrate surface. As a result, a thin coating chemically bonded with the substrate is deposited [62].

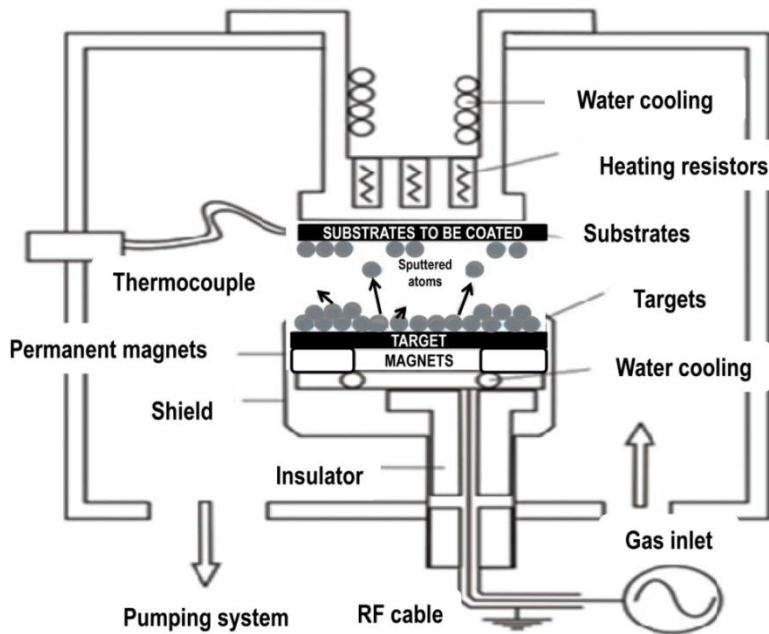


Figure 2. Typical experimental system for RF magnetron sputtering.

There are several modes of sputtering, such as radiofrequency (RF) magnetron sputtering, RF diode sputtering, ion-beam sputtering[63], direct current (DC) sputtering [64] and reactive DC sputtering. RF magnetron sputter deposition is used to deposit CaP ceramic; this is due to the insulator properties of ceramics. This mode of sputtering uses an alternative current source and is further enhance by a magnetic field. Typical experimental system for Radiofrequency (RF) magnetron sputtering is shown in **Figure 2**.

This deposition technique allows the use of a wide range of materials and produces thin, uniform coatings with excellent adhesive properties.

7. Biological properties of inorganic coatings

7.1. Bone healing around the implant surface

Bone implants are surgically placed within the bone tissue. The process of bone growth around the implant is following the same biological cascades of bone defect healing [65]. Bone is one of tissues that have the ability to undergo complete regeneration [66]. Bone healing is divided into three overlapping phases: inflammation, repair, and remodeling. The inflammatory phase begins immediately after the initial tissue damage to bone and surrounding soft tissues, and persists for 3-4 days until the formation of bone is initiated [67]. The traumatic interruption of the blood vessels leads to ischemic necrosis of bone tissue,

CALCIUM PHOSPHATE CERAMICS FOR BONE REGENERATION

histologically characterized by the presence of empty lacunae. Consequently, a fibrin-rich clot forms at the defect site, known as hematoma, and initiates spontaneous wound healing. The hematoma acts as a scaffold for cells, and sets the stage for the repair phase by releasing growth factors, stimulating angiogenesis and bone formation [68]. Platelets are likely to be the first source of healing factors at a traumatized site. In addition to coagulation factors, they release platelet-derived growth factor (PDGF) and transforming growth factor- β 1 (TGF- β 1), both of which stimulate the osteogenesis process [69]. The angiogenic properties of the defect hematoma appear to be mediated via vascular endothelial growth factor (VEGF) and angiopoietin proteins. VEGF is an essential endothelial-cell-specific mediator of neo-angiogenesis, whereas angiopoietin-1 and -2 directly control vascular growth [44, 45]. Angiopoietin proteins are also suggested to act during the whole period of new bone tissue formation. They seem to be related to the formation of larger vessel structures and the development of lateral branches from existent vessels. Indeed, the branches of blood vessels emerging from surrounding tissue, are necessary for revascularizing the hypoxic defect site [45]. Macrophages, generated by the differentiation of monocytes, are attracted to the defect site and assist in the removal of necrotic bone as well as initiate early bone resorption by osteoclasts. Resorption of necrotic bone fragments is particularly important as initiation for bone formation processes [48]. Within a few days, the osteogenesis phase starts and coincides with recruitment of mesenchymal stem cells. Proliferation and differentiation of these stem cells into osteoprogenitor cells is stimulated by

numerous growth factors, among which TGF- β 1 and bone morphogenic proteins (BMPs) play a major role [66]. Osteoprogenitor cells differentiate into osteoblasts [68]. After two weeks, the blood supply is well established and osteoblasts deposit layer upon layer of woven bone, which are subsequently replaced with mature bone [48]. At the end of the repair phase, bone remodeling starts and lamellar bone is deposited in the defect. Therefore, the remodeling phase is characterized by a morphological adaptation of new bone to the original tissue [67].

7.2. Cellular response to bioactive ceramics

The use of ceramic materials, mainly CaPs, for implant surface coatings provides a physical matrix suitable for deposition of more new bone (**Figure 3**). Bone formation on the implant surface may be directly influenced by the quality of such coatings, and osteogenic cell interactions and behavior. CaP coatings display growth-guiding properties inducing, osteoblast proliferation, differentiation, extracellular matrix (ECM) production and mineralization of new bone [70].

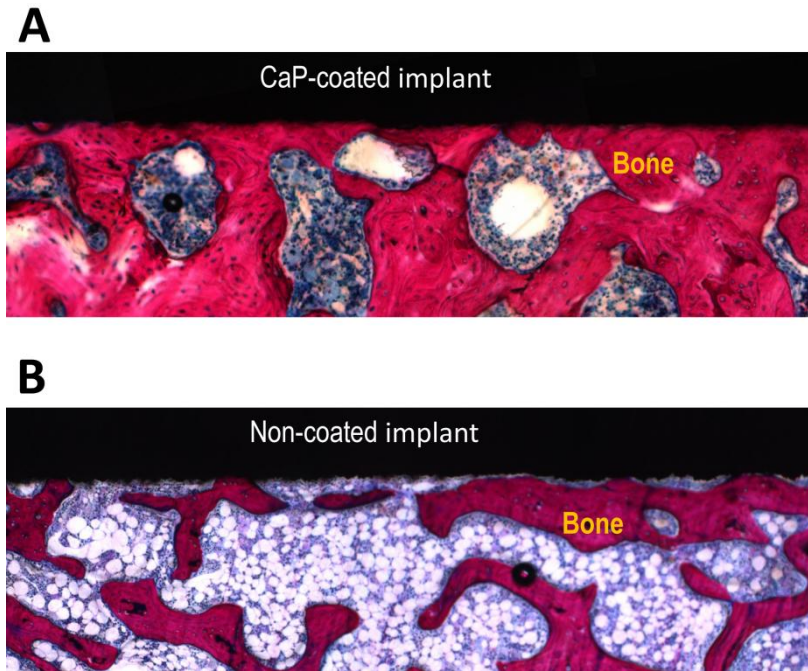


Figure 3. Light micrographs showing an apparent difference in bone contact between (A) CaP-coated implant surface and (B) non-coated implant surface (original magnification $\times 10$).

Generally, CaP implant coatings are suggested to improve the cellular reactions to the implant surface as a direct result of CaP incorporation with protein molecules, facilitate cell attachment and adhesion (**Figure 4**) [71, 72].

Immediately after implantation, CaP coatings are found to increase the protein adsorption to the implant surface. This adsorbed protein layer will subsequently mediate the interaction of the implant material with the cells arriving from the surrounding tissue [73].

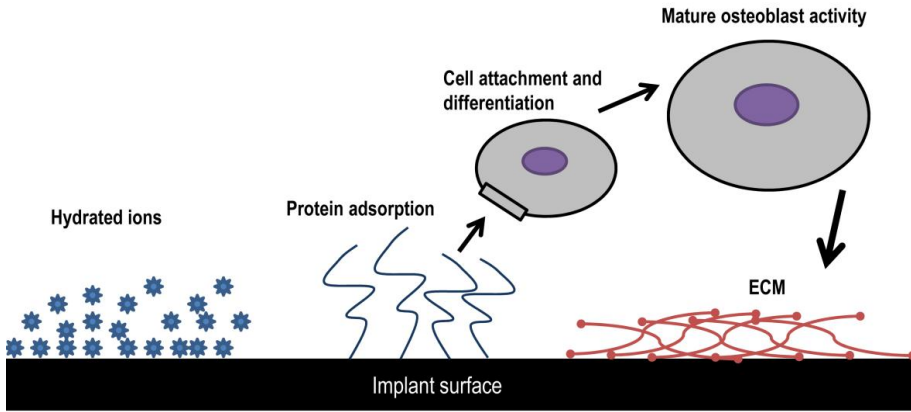


Figure 4. Schematic drawing of biological reactions to the implant surface. After implantation, hydrated ions are incorporated into the surface, followed by adsorption of proteins, leading to osteoblastic cells attachment, differentiation, and production of the extracellular matrix (ECM).

Cellular interactions with extracellular proteins are mediated by integrins. These specific cell membrane molecules transduce signals from the extracellular matrix (ECM) to the cell and vice versa. Then, the signaling pathways through integrins can regulate cell activity to a certain extent [74]. Integrins consist of two glycoprotein subunits, the α -chain and the β -chain, which are non-covalent bonds. Both subunits contain extracellular and intercellular tails (**Figure 5**). Integrins interact with the ECM proteins through their extracellular tails and receive signaling through their intracellular tails [75]. Consequently, integrins are suggested to mediate cellular-substrate interactions including cell attachment, adhesion, spreads, proliferation, and differentiation [76, 77]. Osteoblasts are capable of expressing a wide variety of

CALCIUM PHOSPHATE CERAMICS FOR BONE REGENERATION

integrins, which bind to specific amino acid sequences, such as the tripeptide amino acid sequence arginine-glycine-aspartic acid (RGD) recognition motif present in many ECM proteins, including collagen, fibronectin, vitronectin, bone sialoprotein, and osteopontin [78]. The interaction of integrins with ECM ligands is necessary for the expression of osteoblastic-specific genes [79]. After the binding of a protein ligand, intercellular signaling will be initiated. This signaling pathway inside the cell is complex, and involves the accumulation of several proteins, like focal adhesion kinase (FAK), src, vinculin, and actin filaments. FAK and vinculin are the cytoplasmic side of focal adhesion and seem to be responsible for transmitting signals to actin filaments. Both FAK and vinculin molecules require the interaction between integrins and the ECM ligands for their expression [78, 79].

Using osteoblast-like cells culture, the number of FAK-positive focal adhesions increased continuously on CaP-coated substrate, whereas the number of vinculin-positive adhesions decreased [80-83]. It may be that the production of vinculin molecules is inhibited after the cells become stably attached to CaP surface. Although it is unclear why the number of vinculin-positive focal adhesions decreased, it is likely that vinculin is inhibited after the cells become stably attached to the CaP surface faster than non-coated surface [84]. Differences in integrin expression have been also shown for cells when cultured on titanium substrates coated with a CaP layer [83]. The differences in integrin expression can possibly be explained by the differences in adsorbed proteins conformation [73].

CaP-coated implants have been reported to adsorb more specific ECM proteins, mainly vitronectin and fibronectin, compared to non-coated implants [85]. As CaP ceramics can affect protein conformation, the biological activity of these proteins may increase and then the cellular integrin expression also increase [73, 86]. Beside the ligand-binding activities, integrins are able to cooperate with many additional enzymes and growth factors that are expected to accumulate on the implant surface, which subsequently results in the regulation of cell cycle progression and mobility [78, 79]. Moreover, CaP coatings were found to stimulate the expression of proteins that are known to be features of the osteoblasts lineage. The release of Ca^{2+} and PO_4^- ions from the coating is speculated to regulate the initiation of messenger ribonucleic acid (mRNA) transcription of cellular differentiation to osteoblasts [87]. These ions may also stimulate several intracellular signaling molecules in osteoblasts and favor the mineralization process during bone formation [88]. Furthermore, the presence of a CaP coating is found to induce the precipitation of bone-like apatite on the implant surface. The osteogenic cells might, in turn, recognize the bone-like apatite layer and be more activated to initiate osteogenesis [89, 90]. Beside the chemical composition, it has been proposed that the use of nano-CaP granules for implant coatings increases the concentration of vitronectin and collagen [91]. Again, the presence of these proteins on the implant surface enhances the osteogenic cell integrin-signaling pathways [92, 93].

Osteogenic cell

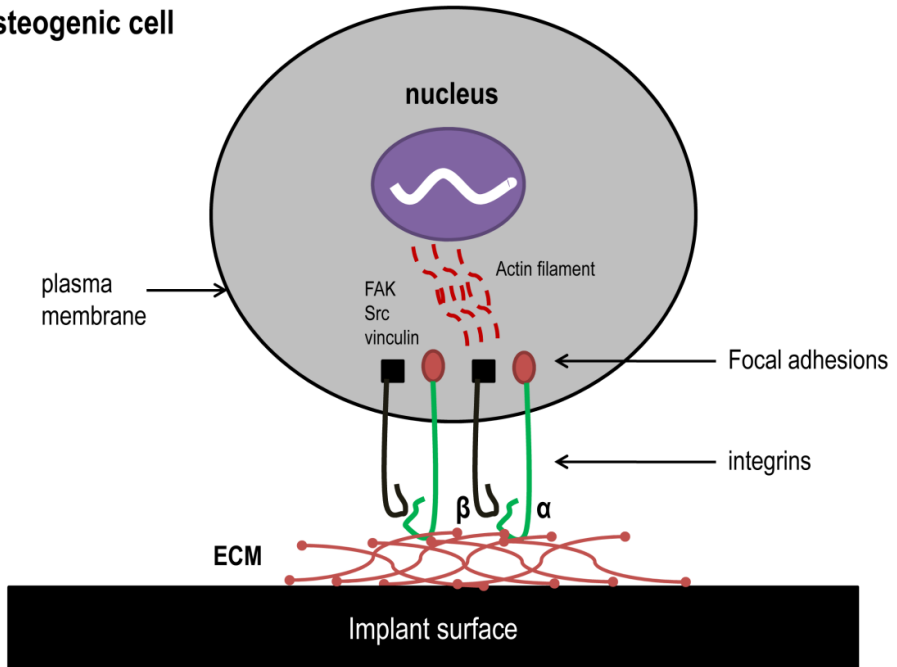


Figure 5. Integrins-mediated cell adhesion to extracellular matrix (ECM) on the implant surface. The subunits structure of the integrin (α -chain and β -chain) bind ECM proteins ligands. Focal adhesions assembly is containing signaling components regulating osteoblastic cell functions.

As can be concluded from the above, it is important to realize that protein adsorption as well as integrin expression are very dynamic processes *in vivo*. The adsorbed proteins to the implant surface are enzymatically degraded and undergo several changes that may also alter the integrin expression during the various stages of osteogenesis [73]. Other parameters involved in the protein-cellular interactions include the techniques used to deposit CaP coating, the

thickness of the applied coating, and the final physicochemical characteristics of the coating [70, 94].

7.3. Bone-bonding to calcium phosphate ceramics

When a biomaterial is implanted in the body, a reaction takes place at the material/tissue interface. This reaction leads to changes in both tissue and surface material. It is essential to understand the *in vivo* host response to the material and the attachment mechanism between implant and tissue, to ensure a long functional life of the biomaterial [2, 17].

All biomaterials evoke a response from living tissue, which classifies them generally as first, second and third generation biomaterials. A first generation biomaterial aims to “achieve a suitable combination of physical properties to match those of the replaced tissue with a minimal toxic response in the host” [95]. A shift in research focus from investigating only bioinert tissue response to bioactive materials yielded the second generation of biomaterials. Some of these second generation biomaterials are CaP ceramics; their bonding mechanism is through the formation of a carbonate apatite layer on the biomaterial surface, which is chemically and crystallographically equivalent to the bone tissue mineral phase. This carbonate apatite layer creates an ideal environment for cellular attachment and subsequent new bone formation with strong bonding to the material surface [17, 95]. Biomaterials with certain capacities to stimulate adsorption of proteins and specific cellular responses are

CALCIUM PHOSPHATE CERAMICS FOR BONE REGENERATION

currently of interest. Such stimulating biomaterials constitute the third generation of biomaterials [95].

Failures of implanted biomaterials occur at the biomaterial-tissue interface. When biomaterials are almost inert and the interface is not chemically or biologically bonded, there is relative movement due to lack of interfacial mechanical stability which isolates the material from the body tissue [2]. This movement influences the deterioration in function of the implant or of the tissue at the interface or of both, and it may differ depending on both the material and the extent of relative motion [17]. In healthy patients, bone implants are quite successful, however, it has been observed that the rate of implant failure is substantially higher in elderly patients. This could be due to volume or bone density deficiency or impaired vascularization, which provokes lack of osseointegration and further implant failure [96].

7.4. Degradation of calcium phosphate ceramics

Synthetic bioresorbable materials have been developed for medical applications, however, it is a challenge to match material resorption rates with body tissue remodeling by self-healing.

Bioactive ceramics can be degraded either by biochemical dissolution ion processes or by acidic environments due to cellular bone remodeling processes (i.e. osteoclastic activity) [44, 45]. As already mentioned in this chapter, the most commonly investigated synthetic calcium phosphate ceramics are

hydroxyapatite (HA), β -tricalcium phosphate (β -TCP) and biphasic calcium phosphate (BCP). One distinguishing aspect of CaP ceramics are their resorption rates. Hydroxyapatite resorbs very slowly and more closely resembles natural bone hydroxyapatite than β -TCP and therefore is being more commonly used for bone ingrowth. However, HA's slow resorption rate can be a disadvantage when new bone is formed in the porous HA network because it cannot experience the mechanical loading that it needs to remodel if the HA remains strong. If the initial material would degrade and allow the bone to be loaded, long-term persistent remodeled bone would be more likely to occur [17, 65]. In the case of BCP, biodegradation kinetics depend on the HA/TCP ratio; the higher the ratio, the lower the degradation rate.

When the process of bone resorption (i.e. osteoclast activity) takes place, the environment becomes acidic. Therefore, the *in vivo* behavior of CaPs can be predicted to a large extent by their solubility (Table 1 shows the solubility of CaPs compounds). To mimic the degradation of calcium phosphate ceramics *in vivo*, an *in vitro* experiment is usually performed by measuring the amount of Ca^{2+} ions released over time when soaking the material in an acidic buffer (pH 5) [2].

In order to control the solubility of calcium phosphate ceramics, different ions can be incorporated. CO_3^{2-} , Mg^{2+} , or Sr^{2+} ions can increase the solubility-biodegradability when incorporated in the hydroxyapatite matrix while F^- ions can decrease it. In contrast, the solubility of β -TCP is decreased by incorporation of either Mg^{2+} or Zn^{2+} ions [2, 44]. Furthermore, the degradation

CALCIUM PHOSPHATE CERAMICS FOR BONE REGENERATION

of calcium phosphate ceramics also depends on several parameters such as their composition, particle size, crystallinity, both design and preparation conditions and technique used to apply the calcium phosphate coating. Further investigation should be done to control the biodegradation of calcium phosphate ceramics.

8. Objectives of this thesis

Calcium phosphate (CaP) based ceramics are synthetic materials commonly used as bone substitutes and for bone implant surface modification [97]. Specific properties, including biodegradability, bioactivity, osteoconductivity, and osteoinductivity, make CaPs biologically appealing materials for bone implantology applications [98, 99]. The dissolution behavior of bulk ceramics due to chemical composition (CaP phase) has been associated with osteoinductive potential *in vivo* [100]. More specifically, hydroxyapatite (HA), tricalcium phosphate (TCP) and biphasic calcium phosphate (BCP) are CaPs that have shown varying degrees of osteoinductive capacity, which inversely corresponds to their biological stability (i.e. TCP > BCP > HA) [100]. In addition to compositional effects, surface morphologies have been shown to affect biological performance [101, 102]. Micro- and nano-scale morphology of the CaP surface can strongly influence osteoblast and stem cell adhesion, proliferation, and differentiation [103-105].

Although the development of CaP ceramics as either coatings or bulk materials *in vitro* and *in vivo* has been widely studied, material properties related to the biological performance of CaP ceramics are still not well understood. For instance, only few attempts have been made to evaluate the biological potential of CaP phases, such as TCP or TTCP sputter coatings *in vivo*. Additionally, the biological effects of CaP surface morphology has only recently become a topic of research (yuan et al., Ripamonti et al.), while the power of a pure materials-based treatment option for bone regenerative medicine basically relies on the instructive capacity of material properties on the biological surrounding. Therefore, the main objective of this thesis was to study the physicochemical and biological properties of various calcium phosphate ceramics as either CaP coatings or bulk CaP ceramics for their use in biomedical applications, with major focus on CaP composition and surface morphology.

The following research questions were addressed:

1. What is the current knowledge on coatings using inorganic and/or organic materials and which techniques are available for the deposition of such coatings on metallic materials? (Chapter 2)
2. What are the effects of CaP composition in sputter coatings on *in vitro* and *in vivo* performance? (Chapter 3)
3. What is the influence of calcium phosphate target composition on surface and mechanical properties of sputtered coatings? (Chapter 4)

CALCIUM PHOSPHATE CERAMICS FOR BONE REGENERATION

4. What is the role of hemispherical concavities on the *in vitro* mineralization of bioceramic materials? (Chapter 5)
5. What is the influence of SBF volume change, disk material, and surface hemispheres on mineralization? (Chapter 6)
6. How do cells populate hemispherical concavities and to what extent does concavity size influence 3-dimensional cellular organization? (Chapter 7)

References

1. Williams, D.F., Secondary author, *On the nature of biomaterials. Biomaterials*, 2009. 30(30): p. 5897-5909.
2. Dorozhkin, S.V., Secondary author, *Bioceramics of calcium orthophosphates. Biomaterials*, 2009. 31(7): p. 1465-1485.
3. Put, P.J.v.d., ed. *The inorganic chemistry of materials: how to make things out of elements*. 1998, Springer;.
4. LeGeros, R.Z., Secondary author, *Calcium Phosphate-Based Osteoinductive Materials. Chemical Reviews*, 2008. 108(11): p. 4742-4753.
5. Urist, M.R., et al., Secondary author, *The bone induction principle. Clin Orthop Relat Res*, 1967. 53: p. 243-83.
6. Habibovic, P., et al., Secondary author, *Osteoinduction by biomaterials—Physicochemical and structural influences. Journal of Biomedical Materials Research Part A*, 2006. 77A(4): p. 747-762.
7. Li, Z. and M. Kawashita, Secondary author, *Current progress in inorganic artificial biomaterials. Journal of Artificial Organs*: p. 1-8.
8. Wang, W., Y. Ouyang, and C.K. Poh, Secondary author, *Orthopaedic implant technology: biomaterials from past to future. Ann Acad Med Singapore*, 2011. 40(5): p. 237-8.
9. Fujibayashi, S., et al., Secondary author, *Bioactive titanium: Effect of sodium removal on the bone-bonding ability of bioactive titanium*

CALCIUM PHOSPHATE CERAMICS FOR BONE REGENERATION

- prepared by alkali and heat treatment. Journal of Biomedical Materials Research, 2001. 56(4): p. 562-570.*
10. *Muller, U., et al., Secondary author, Do human osteoblasts grow into open-porous titanium? Eur Cell Mater, 2006. 11: p. 8-15.*
 11. *Mihalko, W.M., et al., Secondary author, Effects of hydroxyapatite on titanium foam as a bone ingrowth surface in acetabular shells: a canine study. J Long Term Eff Med Implants, 2010. 20(1): p. 35-42.*
 12. *Singh, R.G., Secondary author, Evaluation of the bioactivity of titanium after varied surface treatments using human osteosarcoma osteoblast cells: an in vitro study. Int J Oral Maxillofac Implants, 2011. 26(5): p. 998-1003.*
 13. *Fujibayashi, S., et al., Secondary author, Osteoinduction of porous bioactive titanium metal. Biomaterials, 2004. 25(3): p. 443-450.*
 14. *Sugano, N., et al., Secondary author, Eleven- to 14-year Follow-up Results of Cementless Total Hip Arthroplasty Using a Third-generation Alumina Ceramic-on-ceramic Bearing. The Journal of Arthroplasty, (0).*
 15. *Laurent, M.P., et al., Secondary author, In vivo wear of a squeaky alumina-on-alumina hip prosthesis: a case report. J Bone Joint Surg Am, 2011. 93(7): p. e27.*
 16. *Callister, W.D. and D.G. Rethwisch, Fundamentals of Materials Science and Engineering: An Integrated Approach. 2011: John Wiley & Sons.*

17. *Hench, L.L., Secondary author, Bioceramics. Journal of the American Ceramic Society, 1998. 81(7): p. 1705-1728.*
18. *Masson, B., Secondary author, Emergence of the alumina matrix composite in total hip arthroplasty. International Orthopaedics, 2009. 33(2): p. 359-363.*
19. *Door Hua-Tay Lin, D.Z., Tatsuki Ohji, Andrew Wereszczak, ed. Advanced Ceramic Coatings and Interfaces. 2008, John Wiley and Sons, Inc.*
20. *Chevalier, J., et al., Secondary author, Reliability assessment in advanced nanocomposite materials for orthopaedic applications. Journal of the Mechanical Behavior of Biomedical Materials, 2011. 4(3): p. 303-314.*
21. *Pezzotti, G., et al., Secondary author, On the role of oxygen vacancies and lattice strain in the tetragonal to monoclinic transformation in alumina/zirconia composites and improved environmental stability. Biomaterials, 2010. 31(27): p. 6901-6908.*
22. *Hench, L.L., et al., Secondary author, Bonding mechanisms at the interface of ceramic prosthetic materials. Journal of Biomedical Materials Research, 1971. 5(6): p. 117-141.*
23. *Rahaman, M.N., et al., Secondary author, Bioactive glass in tissue engineering. Acta Biomaterialia, 2011. 7(6): p. 2355-2373.*
24. *Hoppe, A., N.S. Gldal, and A.R. Boccaccini, Secondary author, A review of the biological response to ionic dissolution products from*

CALCIUM PHOSPHATE CERAMICS FOR BONE REGENERATION

- bioactive glasses and glass-ceramics. Biomaterials, 2011. 32(11): p. 2757-2774.*
25. *Pan, H.B., et al., Secondary author, Strontium borate glass: potential biomaterial for bone regeneration. J R Soc Interface, 2010. 7(48): p. 1025-31.*
 26. *Zhao, D., et al., Secondary author, Mechanism for converting Al₂O₃-containing borate glass to hydroxyapatite in aqueous phosphate solution. Acta Biomaterialia, 2009. 5(4): p. 1265-1273.*
 27. *Kokubo, T., Secondary author, Bioactive glass ceramics: properties and applications. Biomaterials, 1991. 12(2): p. 155-63.*
 28. *Ahmed, I., et al., Secondary author, Processing, characterisation and biocompatibility of iron-phosphate glass fibres for tissue engineering. Biomaterials, 2004. 25(16): p. 3223-3232.*
 29. *Franks, K., I. Abrahams, and J.C. Knowles, Secondary author, Development of soluble glasses for biomedical use Part I: In vitro solubility measurement. Journal of Materials Science: Materials in Medicine, 2000. 11(10): p. 609-614.*
 30. *Saravanapavan, P., et al., Secondary author, Bioactivity of gel-glass powders in the CaO-SiO₂ system: A comparison with ternary (CaO-P₂O₅-SiO₂) and quaternary glasses (SiO₂-CaO-P₂O₅-Na₂O). Journal of Biomedical Materials Research Part A, 2003. 66A(1): p. 110-119.*

31. *Sergey V, D., Secondary author, Biphasic, triphasic and multiphasic calcium orthophosphates. Acta Biomaterialia, (0).*
32. *Sergey V, D., Secondary author, Amorphous calcium (ortho)phosphates. Acta Biomaterialia, 2010. 6(12): p. 4457-4475.*
33. *Blokhuis, T.J. and J.J.C. Arts, Secondary author, Bioactive and osteoinductive bone graft substitutes: Definitions, facts and myths. Injury, 2011. In Press, Corrected Proof.*
34. *Hamlet, S. and S. Ivanovski, Secondary author, Inflammatory cytokine response to titanium chemical composition and nanoscale calcium phosphate surface modification. Acta Biomaterialia, 2011. 7(5): p. 2345-2353.*
35. *Paital, S., et al., Secondary author, Laser surface modification for synthesis of textured bioactive and biocompatible Ca–P coatings on Ti–6Al–4V. Journal of Materials Science: Materials in Medicine, 2011. 22(6): p. 1393-1406.*
36. *Albrektsson, T.A. and C.J. Johansson, Secondary author, Osteoinduction, osteoconduction and osseointegration. European Spine Journal, 2001. 10(0): p. S96-S101.*
37. *Barradas, A.M.C., ed. Osteoinductive biomaterials: current knowledge of properties, experimental models and biological mechanisms. Vol. 21. 2011, European cells and materials. 22.*

CALCIUM PHOSPHATE CERAMICS FOR BONE REGENERATION

38. Gotz, W., et al., Secondary author, *A preliminary study in osteoinduction by a nano-crystalline hydroxyapatite in the mini pig. Folia Histochem Cytobiol*, 2010. 48(4): p. 589-96.
39. Ugo, R., Secondary author, *Osteoinduction in porous hydroxyapatite implanted in heterotopic sites of different animal models. Biomaterials*, 1996. 17(1): p. 31-35.
40. Ripamonti, U., et al., Secondary author, *The induction of bone formation by coral-derived calcium carbonate/hydroxyapatite constructs. Biomaterials*, 2009. 30(7): p. 1428-39.
41. Yuan, H., et al., Secondary author, *Osteoinduction by calcium phosphate biomaterials. J Mater Sci Mater Med*, 1998. 9(12): p. 723-6.
42. Yang, R.N., et al., Secondary author, *Osteoinduction by Ca-P biomaterials implanted into the muscles of mice. J Zhejiang Univ Sci B*, 2011. 12(7): p. 582-90.
43. Cheng, L., et al., Secondary author, *Osteoinduction of hydroxyapatite/beta-tricalcium phosphate bioceramics in mice with a fractured fibula. Acta Biomater*, 2010. 6(4): p. 1569-74.
44. Suri, C., et al., Secondary author, *Requisite role of angiopoietin-1, a ligand for the TIE2 receptor, during embryonic angiogenesis. Cell*, 1996. 87(7): p. 1171-80.
45. Carano, R.A.D. and E.H. Filvaroff, Secondary author, *Angiogenesis and bone repair. Drug discovery today*, 2003. 8(21): p. 980-989.

46. Ayala, R., et al., Secondary author, *Engineering the cell-material interface for controlling stem cell adhesion, migration, and differentiation. Biomaterials*, 2011. 32(15): p. 3700-11.
47. Li, C.X., A. Hussain, and A. Kamali, Secondary author, *A hip simulator study of metal-on-metal hip joint device using acetabular cups with different fixation surface conditions. Proc Inst Mech Eng H*, 2011. 225(9): p. 877-87.
48. Kalfas, I.H., Secondary author, *Principles of bone healing. Neurosurgical Focus*, 2001. 10(4): p. 1-4.
49. Sepahvandi, A., et al., Secondary author, *Photoluminescence in the characterization and early detection of biomimetic bone-like apatite formation on the surface of alkaline-treated titanium implant: state of the art. Colloids Surf B Biointerfaces*, 2011. 86(2): p. 390-6.
50. Duarte, L.T., et al., Secondary author, *Preparation and characterization of biomimetically and electrochemically deposited hydroxyapatite coatings on micro-arc oxidized Ti-13Nb-13Zr. J Mater Sci Mater Med*, 2011. 22(7): p. 1663-70.
51. Kurzweg, H., et al., Secondary author, *Development of plasma-sprayed bioceramic coatings with bond coats based on titania and zirconia. Biomaterials*, 1998. 19(16): p. 1507-11.
52. Leeuwenburgh, S.C., et al., Secondary author, *Influence of precursor solution parameters on chemical properties of calcium phosphate*

CALCIUM PHOSPHATE CERAMICS FOR BONE REGENERATION

- coatings prepared using Electrostatic Spray Deposition (ESD). Biomaterials, 2004. 25(4): p. 641-9.*
53. *Hou, X., K.L. Choy, and S.E. Leach, Secondary author, Processing and in vitro behavior of hydroxyapatite coatings prepared by electrostatic spray assisted vapor deposition method. J Biomed Mater Res A, 2007. 83(3): p. 683-91.*
54. *Cleries, L., J.M. Fernandez-Pradas, and J.L. Morenza, Secondary author, Bone growth on and resorption of calcium phosphate coatings obtained by pulsed laser deposition. J Biomed Mater Res, 2000. 49(1): p. 43-52.*
55. *Rajesh, P., et al., Secondary author, Laser surface modification of titanium substrate for pulsed laser deposition of highly adherent hydroxyapatite. J Mater Sci Mater Med, 2011. 22(7): p. 1671-9.*
56. *Lackner, J.M., et al., Secondary author, Hemocompatible, pulsed laser deposited coatings on polymers. Biomed Tech (Berl), 2010. 55(1): p. 57-64.*
57. *Rajesh, P., et al., Secondary author, Pulsed laser deposition of hydroxyapatite on titanium substrate with titania interlayer. J Mater Sci Mater Med, 2011. 22(3): p. 497-505.*
58. *Park, Y.S., et al., Secondary author, The effects of ion beam-assisted deposition of hydroxyapatite on the grit-blasted surface of endosseous implants in rabbit tibiae. Int J Oral Maxillofac Implants, 2005. 20(1): p. 31-8.*

59. Wang, C.X., et al., Secondary author, Ion-beam-sputtering/mixing deposition of calcium phosphate coatings. I. Effects of ion-mixing beams. *J Biomed Mater Res*, 2001. 55(4): p. 587-95.
60. Choi, J.M., H.E. Kim, and I.S. Lee, Secondary author, Ion-beam-assisted deposition (IBAD) of hydroxyapatite coating layer on Ti-based metal substrate. *Biomaterials*, 2000. 21(5): p. 469-73.
61. Ong, J.L. and L.C. Lucas, Secondary author, Post-deposition heat treatments for ion beam sputter deposited calcium phosphate coatings. *Biomaterials*, 1994. 15(5): p. 337-41.
62. Jansen, J.A., et al., Secondary author, Application of magnetron sputtering for producing ceramic coatings on implant materials. *Clin Oral Implants Res*, 1993. 4(1): p. 28-34.
63. Ho, J.J., et al., Secondary author, Ion-assisted sputtering deposition of antireflection film coating for flexible liquid-crystal display applications. *Appl Opt*, 2005. 44(29): p. 6176-80.
64. Wu, K.R., et al., Secondary author, Photoelectrochemical properties of N/C-codoped TiO₂ film electrodes prepared by reactive DC magnetron sputtering. *J Nanosci Nanotechnol*, 2010. 10(2): p. 1057-64.
65. Bra-nemark, P.I., et al., Secondary author, Tissue-integrated prostheses. *Osseointegration in clinical dentistry. Plastic and Reconstructive Surgery*, 1986. 77(3): p. 496.

CALCIUM PHOSPHATE CERAMICS FOR BONE REGENERATION

66. *Ferguson, C.M., et al., Secondary author, Common molecular pathways in skeletal morphogenesis and repair. Annals of the New York Academy of Sciences, 1998. 857(1): p. 33-42.*
67. *Gerstenfeld, L.C., et al., Secondary author, Fracture healing as a post-natal developmental process: Molecular, spatial, and temporal aspects of its regulation. Journal of Cellular Biochemistry, 2003. 88(5): p. 873-884.*
68. *Dimitriou, R., E. Tsiridis, and P.V. Giannoudis, Secondary author, Current concepts of molecular aspects of bone healing. Injury, 2005. 36(12): p. 1392-1404.*
69. *Lieberman, J.R., A. Daluiski, and T.A. Einhorn, Secondary author, The role of growth factors in the repair of bone: biology and clinical applications. Journal of bone and joint surgery. American volume, 2002. 84(6): p. 1032-1044.*
70. *de Jonge, L.T., et al., Secondary author, Organic–inorganic surface modifications for titanium implant surfaces. Pharmaceutical Research, 2008. 25(10): p. 2357-2369.*
71. *LeGeros, R.Z., Secondary author, Properties of osteoconductive biomaterials: calcium phosphates. Clinical Orthopaedics and Related Research, 2002. 395: p. 81.*
72. *Kim, H.W., et al., Secondary author, Calcium phosphates and glass composite coatings on zirconia for enhanced biocompatibility. Biomaterials, 2004. 25(18): p. 4203-4213.*

73. Siebers, M., et al., Secondary author, *Integrins as linker proteins between osteoblasts and bone replacing materials. A critical review. Biomaterials*, 2005. 26(2): p. 137-146.
74. García, A.J. and C. Reyes, Secondary author, *Bio-adhesive surfaces to promote osteoblast differentiation and bone formation. Journal of Dental Research*, 2005. 84(5): p. 407-413.
75. Gumbiner, B.M., Secondary author, *Cell adhesion: the molecular basis of tissue architecture and morphogenesis. Cell*, 1996. 84(3): p. 345.
76. Ahmad, M., et al., Secondary author, *Differential response of human osteoblast-like cells to commercially pure (cp) titanium grades 1 and 4. Journal of Biomedical Materials Research*, 1999. 46(1): p. 121-131.
77. Anselme, K. and M. Bigerelle, Secondary author, *Topography effects of pure titanium substrates on human osteoblast long-term adhesion. Acta Biomaterialia*, 2005. 1(2): p. 211-222.
78. Ruoslahti, E. and M.D. Pierschbacher, Secondary author, *New perspectives in cell adhesion: RGD and integrins. Science*, 1987. 238(4826): p. 491.
79. Ruoslahti, E., Secondary author, *RGD and other recognition sequences for integrins. Annual Review of Cell and Developmental Biology*, 1996. 12(1): p. 697-715.
80. Liu, X., et al., Secondary author, *Influence of substratum surface chemistry/energy and topography on the human fetal osteoblastic cell*

CALCIUM PHOSPHATE CERAMICS FOR BONE REGENERATION

- line hFOB 1.19: phenotypic and genotypic responses observed in vitro. Biomaterials, 2007. 28(31): p. 4535-4550.*
81. *Di Palma, F., et al., Secondary author, Physiological strains induce differentiation in human osteoblasts cultured on orthopaedic biomaterial. Biomaterials, 2003. 24(18): p. 3139-3151.*
82. *Itthichaisri, C., et al., Secondary author, Comparative in vitro study of the proliferation and growth of human osteoblast-like cells on various biomaterials. Journal of Biomedical Materials Research Part A, 2007. 82(4): p. 777-787.*
83. *Ter Brugge, P. and J. Jansen, Secondary author, Initial interaction of rat bone marrow cells with non-coated and calcium phosphate coated titanium substrates. Biomaterials, 2002. 23(15): p. 3269-3277.*
84. *Ellingsen, J.E., P. Thomsen, and S.P. Lyngstadaas, Secondary author, Advances in dental implant materials and tissue regeneration. Periodontology 2000, 2006. 41(1): p. 136-156.*
85. *Bombonato-Prado, K.F., et al., Secondary author, Microarray-based gene expression analysis of human osteoblasts in response to different biomaterials. Journal of Biomedical Materials Research Part A, 2009. 88(2): p. 401-408.*
86. *Ong, J., G. Raikar, and T. Smoot, Secondary author, Properties of calcium phosphate coatings before and after exposure to simulated biological fluid. Biomaterials, 1997. 18(19): p. 1271-1275.*

87. Mo, M.J., et al., Secondary author, *Biological Responses of Osteoblastic HOS Cells to Titanium-and Calcium Phosphate-Coated Films. JOURNAL OF INDUSTRIAL AND ENGINEERING CHEMISTRY-SEOUL-*, 2005. 11(4): p. 507.
88. Bender, S., et al., Secondary author, *Effect of protein on the dissolution of HA coatings. Biomaterials*, 2000. 21(3): p. 299-305.
89. Abe, Y., T. Kokubo, and T. Yamamuro, Secondary author, *Apatite coating on ceramics, metals and polymers utilizing a biological process. Journal of materials science: Materials in medicine*, 1990. 1(4): p. 233-238.
90. Kokubo, T. and H. Takadama, Secondary author, *How useful is SBF in predicting in vivo bone bioactivity? Biomaterials*, 2006. 27(15): p. 2907-2915.
91. Kommireddy, D.S., et al., Secondary author, *Stem cell attachment to layer-by-layer assembled TiO₂ nanoparticle thin films. Biomaterials*, 2006. 27(24): p. 4296-4303.
92. Leeuwenburgh, S.C.G., et al., Secondary author, *In vitro and in vivo reactivity of porous, electrosprayed calcium phosphate coatings. Biomaterials*, 2006. 27(18): p. 3368-3378.
93. Habibovic, P., et al., Secondary author, *Osteoinduction by biomaterials—physicochemical and structural influences. Journal of Biomedical Materials Research Part A*, 2006. 77(4): p. 747-762.

CALCIUM PHOSPHATE CERAMICS FOR BONE REGENERATION

94. De Bruijn, J., C. Van Blitterswijk, and J. Davies, *Secondary author*, *Initial bone matrix formation at the hydroxyapatite interface in vivo. Journal of Biomedical Materials Research*, 1995. 29(1): p. 89-99.
95. Hench, L.L. and I. Thompson, *Secondary author*, *Twenty-first century challenges for biomaterials. J R Soc Interface*, 2010. 7 Suppl 4: p. S379-91.
96. Marco, F., et al., *Secondary author*, *Peri-implant osteogenesis in health and osteoporosis. Micron*, 2005. 36(7-8): p. 630-44.
97. Dorozhkin, S.V. and M. Epple, *Secondary author*, *Biological and medical significance of calcium phosphates. Angew Chem Int Ed Engl*, 2002. 41(17): p. 3130-46.
98. Dorozhkin, S.V., *Secondary author*, *Biphasic, triphasic and multiphasic calcium orthophosphates. Acta Biomaterialia*, 2012. 8(3): p. 963-977.
99. Surmenev, R.A., *Secondary author*, *A review of plasma-assisted methods for calcium phosphate-based coatings fabrication. Surface and Coatings Technology*, 2012. 206(8-9): p. 2035-2056.
100. Yuan, H., et al., *Secondary author*, *Osteoinductive ceramics as a synthetic alternative to autologous bone grafting. Proc Natl Acad Sci U S A*, 2010. 107(31): p. 13614-9.
101. Tampieri, A., G. Celotti, and E. Landi, *Secondary author*, *From biomimetic apatites to biologically inspired composites. Analytical and Bioanalytical Chemistry*, 2005. 381(3): p. 568-576.

102. Schouten, C., et al., Secondary author, *Effects of implant geometry, surface properties, and TGF-beta 1 on peri-implant bone response: an experimental study in goats. Clinical Oral Implants Research, 2009. 20(4): p. 421-429.*
103. Li, B., et al., Secondary author, *Effect of nanostructure on osteoinduction of porous biphasic calcium phosphate ceramics. Acta Biomaterialia, 2012. 8(10): p. 3794-3804.*
104. Prodanov, L., et al., Secondary author, *The effect of nanometric surface texture on bone contact to titanium implants in rabbit tibia. Biomaterials, 2013. 34(12): p. 2920-2927.*
105. Graziano, A., et al., Secondary author, *Concave Pit-Containing Scaffold Surfaces Improve Stem Cell-Derived Osteoblast Performance and Lead to Significant Bone Tissue Formation. Plos One, 2007. 2(6).*

CALCIUM PHOSPHATE CERAMICS FOR BONE REGENERATION

2

INSTRUCTIVE COATINGS FOR BIOLOGICAL GUIDANCE OF BONE IMPLANTS

1. Introduction

Load-bearing bone implants for dental and orthopedic applications to replace hard tissue are generally made from bioinert materials, including titanium, stainless steel, cobalt-chromium, alloys or certain ceramics (e.g. alumina and zirconia). Extensive efforts have been dedicated to the optimization of the interaction with bone tissue at the implant interface via surface modifications to enhance the surface biocompatibility and osteoconductive properties of these implants. Still, implant failure remains a problem for especially clinical cases characterized by compromised local or systemic conditions (e.g. osteoporosis and diabetes) [1].

Biomaterials research is evolving from the use of bioinert and biologically passive implants toward actively interacting implants that stimulate tissue regeneration. Currently, there is an increasing interest in biomaterials that are capable of activating protein adsorption processes and specific cellular responses. Surface physico-chemical properties need to be modified in order to transform passive inert implant surfaces into active ones able to instruct the biological environment toward regeneration of bone tissue (**Fig. 1**). For instance, physical surface modifications in topography or macrostructural properties have been reported to concentrate more bone morphogenetic proteins (BMPs) and stimulate osteogenesis [2,3]. On the other hand, chemical surface modifications have been shown to play an essential role in bone tissue responses [4-10]. For ceramic coatings, the liberation of certain ions from the

implant surface into the surroundings increases local super-saturation of the biologic fluid causing precipitation of carbonated apatite that incorporates calcium, phosphate and other ions, as well as proteins, and other organic compounds [11]. Furthermore, the immobilization of biomolecules into the coating materials allows implants to deliver drugs and growth factors [12].

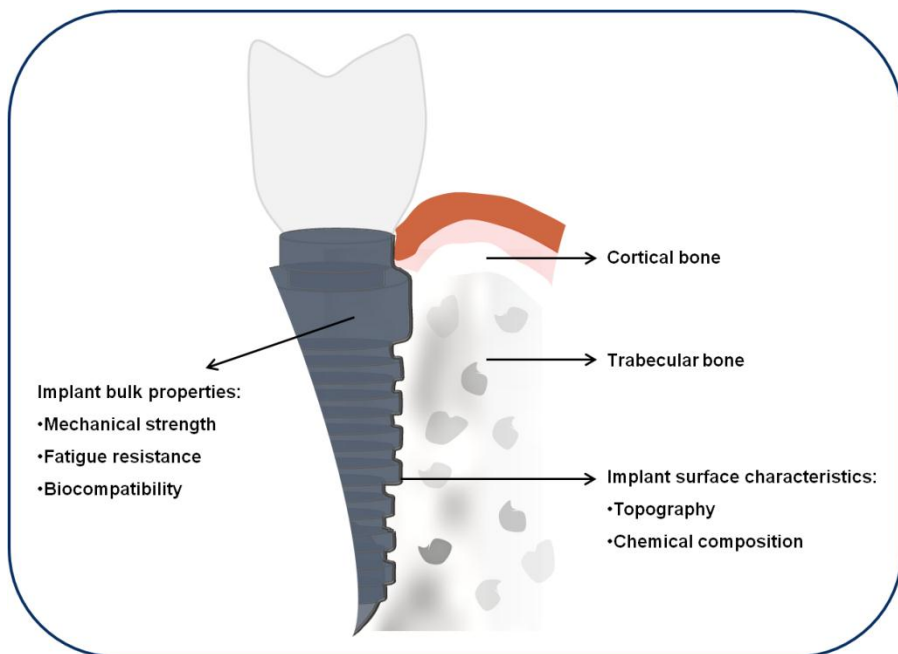


Figure 1. Schematic overview of a bone implant.

In addition, when referring to organic coatings, the use of organic compounds derived from the extracellular matrix (ECM) of bone attempts to

CALCIUM PHOSPHATE CERAMICS FOR BONE REGENERATION

stimulate mineralization and/or adhesion of cells onto the bone implant surfaces.

This review aims to provide an overview of surface modifications for load-bearing bone implants. Special attention is devoted to the most recent developments of inorganic and organic coatings for bone implants that actively interact with bone tissue to aid skeletal repair and reconstruction.

2. Inorganic coatings

Bone tissue is a composite that exhibits a rich hierarchical structure. The cells within bone tissue are embedded in an extracellular matrix made of organic and inorganic compounds, which permit bone tissue to remodel and adapt its structure in response to mechanical stress (**Fig. 2**). More specifically, the strength of bone tissue is related to the orderly interspersed inorganic crystals within the organic compounds [13,14]. These crystals have an apatite structure (i.e. $\text{Ca}_{10}(\text{PO}_4)_6(\text{OH})_2$ for hydroxyapatite), in which calcium and phosphate are the most prominent elements. Synthetic inorganic materials have therefore been extensively explored to mimic the mineral part of bone tissue for bone implantology applications.

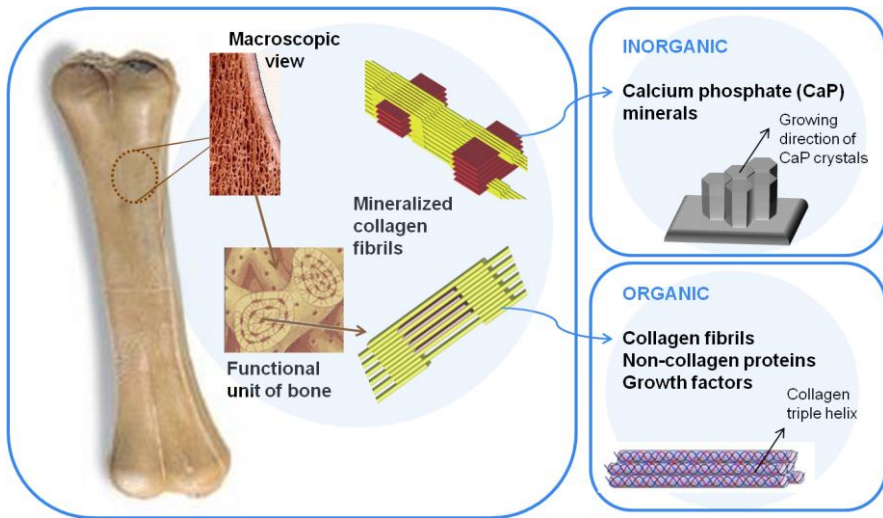


Figure 2. Hierarchical levels of bone structure.

2.1. Properties and bonding mechanism of CaP-based ceramics

Calcium phosphate (CaP) ceramics are synthetic materials that share common mineral phase properties with bone tissue and are biodegradable, bioactive and osteoconductive [15]. CaP ceramic materials are characterized by their hardness, strength, low electrical conductivity, brittleness and inferior mechanical properties. Due to their inferior mechanical properties, the application of CaP ceramics as bulk materials under load-bearing conditions is limited. Used as implant surface coatings, these CaP ceramics provide a physical matrix at the implant surface suitable for interaction with bone tissue.

CALCIUM PHOSPHATE CERAMICS FOR BONE REGENERATION

CaP ceramics bond to bone tissue through the release of ions from the implant surface inducing apatite nucleation, followed by the formation of a carbonated apatite layer on the biomaterial surface [16]. This apatite layer at the surface is chemically and crystallographically equivalent to the bone tissue mineral phase. As such, this carbonated apatite layer creates an ideal environment for protein and cellular attachment and subsequent strongly bonded bone formation. Several parameters of CaP ceramics, either in bulk or coating form, have been demonstrated to alter protein binding, cell-material interactions and implant resorption rate. These inherent parameters include chemical composition, crystallinity, surface area, surface charge, surface topography and porosity, elasticity and fatigue of the implant surface.

2.1.1. Pure CaP-based coatings

CaP-based ceramic coatings were originally developed to improve bone-implant attachment and enhance surface reactivity, for example of dental implants and metallic prostheses, because of their favorable bioactivity and osteoconductivity. Surface properties of the implant material such as coatings roughness, chemical purity, and topography should be optimized to improve osseointegration. Bioactive materials, such as CaP ceramics, several classes of bioglasses, calcium carbonates and calcium sulfates, evoke specific biological responses, stimulate bone tissue formation and directly bond to adjacent bone tissue.

There are several CaP phases, the most commonly used for bone ingrowth has been hydroxyapatite (HA; $\text{Ca}_{10}(\text{PO}_4)_6\text{OH}_2$), which has crystalline and molecular structure similarities to the inorganic phase of bones and teeth [17-19]. Other structures include brushite (DCPD, $\text{CaHPO}_4 \cdot \text{H}_2\text{O}$), and tricalcium phosphate (α -TCP and β -TCP, $\text{Ca}_3(\text{PO}_4)_2$) have been used as bioactive coatings to modify the surface of bioinert metals or polymers [20]. At physiological pH (between 7.2-7.6), HA is the most stable CaP phase. The partial dissolution of the ceramic (i.e. release of ions) initiates the re-precipitation of biological apatite crystals and subsequent proteins and cells attachment to the implant surface. Amorphous CaP coatings have higher dissolution and re-precipitation rates than the crystalline CaP coatings and present faster bone formation²¹ and produce higher cell differentiation *in vitro* studies [21,22]. However, crystalline CaP coatings are preferred when long-term stability of the implant is desirable. The biological properties of these CaP-based ceramic coatings are related to their chemical composition, Ca/P ratio, crystallographic structures and solubility. Consequently, the release of ions and the interaction with body fluid, cells and tissue of CaP implant coatings differs related to specific CaP coating structure [23,24].

2.1.2. Incorporation of active ions into CaP-based ceramic coatings

CALCIUM PHOSPHATE CERAMICS FOR BONE REGENERATION

In an attempt to further increase the biological performance of CaP-based ceramic coatings, research focused on the incorporation of ions into the ceramic lattice. Ionic doping not only changes the chemical composition but also physicochemical properties, such as morphology and crystallinity. Numerous articles have claimed that silicon (Si) substitution into the crystal structure of CaP ceramics, in particular HA, positively influences the biological response compared to pure CaP coatings [25-27]. For example, Patel et al. [26] compared granules of pure HA and Si-substituted HA when implanted in a rabbit model; more bone ingrowth and bone-implant coverage were found with the incorporation of silicate ions into the HA structure. Similar results were obtained by Hing et al. [27] using porous HA and silicate-substituted HA scaffolds. The authors claimed that the presence of Si ions is responsible for an increased collagen deposition, cells differentiation, bone ingrowth and repair. However, a recent critical review on Si-substituted CaP coatings has shown that there is no experimental evidence that Si ions are released (at sufficiently high concentrations) from the CaP lattice *in vitro* or *in vivo* studies [25]. The heterogeneity of studies based on Si-substituted CaP remain inconclusive regarding the cause for the positive biological responses: topographical effects or the release of Ca ions instead of the Si ions release. A mayor criticism is moved concerning the analysis of the effective principle through Si ions could enhance bone deposition or formation [25]. The incorporation of magnesium (Mg) ions into HA in an *in vivo* study has shown that Mg-substituted HA enhances the osteoconductivity and resorption compared to commercial HA.

Landi and Tampieri highlighted how Mg substituted hydroxylapatite (HA) has chemico-physical properties that increase solubility compared to synthetic HA that resemble more the characteristics of natural HA [28]. Experiments substituting calcium by strontium (Sr) ions have been performed in several calcium phosphate ceramics, such as HA [29, 30], β -TCP³¹ and α -TCP [32]. Fielding et al. showed that the addition of silver (Ag) and Sr dopants to the HA coating enhanced cell proliferation and differentiation activity compared with pure HA coating [33]. Lithium (Li) incorporation into the CaP coating changes the coating morphology and interferes with the CaP crystallization. The presence of lithium has been demonstrated to enhance MG63 cell attachment and early proliferation [34]. Lastly, zinc (Zn) incorporation has also been widely studied. *In vivo* studies demonstrated more bone apposition when using low concentrations of zinc (~0.3 wt.%), whereas long-term implantation studies with low concentrations of zinc or high concentrations of zinc (~0.6 wt.%) led to an increased resorption of bone [35,36].

2.1.3. CaP-based ceramic coatings with entrapment of biomolecules

HA ceramics have been used as a delivery system for chemicals [37], antibiotics [38] and anticancer drugs [39]. A final approach toward inorganic surface modifications with enhanced biological performance involves the

CALCIUM PHOSPHATE CERAMICS FOR BONE REGENERATION

entrapment of biomolecules into a ceramic coating, enabling active release of drugs

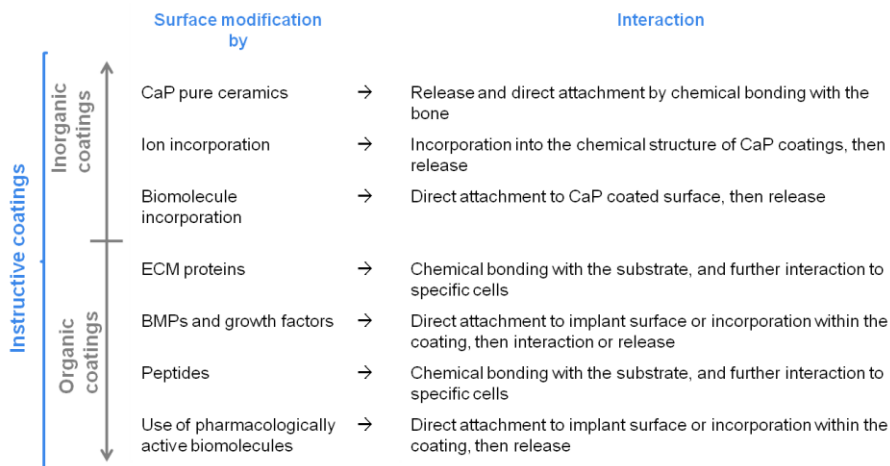


Figure 3. Classification and interaction of instructive coatings.

(e.g. anti-microbial coatings). By local delivery of antibiotic drugs from a coated implant, the occurrence of post-surgery infections can be reduced, enhancing the short and long term stability of a bone implant [12]. The use of CaP coatings as delivery vehicles for antimicrobial agents such as chlorhexidine has already reported its efficacy in an *in vitro* study by Campbell et al. In this study the incorporation of chlorhexidine within the hydroxyapatite (HA) coatings showed an initial rapid release followed by a period of slower sustained release. The *in vitro* evaluation results showed that a large “inhibition zone” was formed around the HA/chlorhexidine coating compared to HA coating [10]. Moreover, for compromised situations such as osteoporosis, the

incorporation of bisphosphonate drugs (e.g. alendronate) into the inner layers of CaP coatings has shown beneficial results on osteoblast cells differentiation [40]. CaP coatings used as local delivery of drugs or antimicrobial agents offers the possibility of improving efficacy (i.e. dosage near the affected site) and reduce the treatment duration.

A classification of the different instructive inorganic and organic coating materials and their interaction when implanted is shown in **Fig. 3**.

3. Organic coatings

The bone tissue extracellular matrix (ECM) is composed of a hierarchical and complex structure of inorganic and organic phases. The inorganic or crystalline phase of bone represents 50% of the total volume and 70% of the weight, and mainly consists of a stiff, carbonated and nano-sized apatite. The organic phase of bone tissue constitutes the remaining volume, which comprises collagen (40% in volume of the organic phase) and other proteins, such as proteoglycans, glycoproteins (alkaline phosphatase, osteonectin), bone sialoproteins and growth factors.

In the last decades, organic biomolecules derived from the ECM have been increasingly considered a fundamental source in the development of organic bone implant coatings [41]. Bone implants surfaces can be enriched [42-44] using organic biomolecules to obtain instructive medical devices able induce a biological response at the tissue-implant interface. Organic-based coatings

CALCIUM PHOSPHATE CERAMICS FOR BONE REGENERATION

involve immobilization of structural proteins, Bone Morphogenetic Proteins (BMPs) and growth factors and peptides to stimulate cell adhesion onto implant surfaces [45, 46] and an approach on the use of pharmacologically active biomolecules.

3.1. Surface modifications by ECM proteins

Collagen is the main component of the bone tissue organic phase and it has a fundamental structural and functional role. The minimum element is the collagen fibril that is composed of a structured repetition of tropocollagen molecules (300 nm size) that are interconnected in a right-helix structure. Between tropocollagen molecules, there is a gap zone, in which the nano-sized hydroxyapatite crystals can start nucleation and mineralization. Moreover, the structural presence of collagen in the ECM is fundamental to obtain the mechanical properties of bone tissue.

Collagen has been used as a coating material to retain biomolecules at the implant surface and improve their activity. Collagen-based coatings are able to bind an important ECM protein called fibronectin, which plays a major role in the interaction between implant surfaces and the surrounding biological medium (e.g. cell adhesion, growth, migration and differentiation) [47]. Different research groups have also tried to use collagen to increase proliferation or differentiation of osteoblasts and osteoprogenitor cells. Douglas et al. showed the positive effect of a layer of collagen promoting osteoblasts

focal adhesion. Rammelt et al. showed a comparison between collagen and other biomolecules in an *in vivo* experiment on a rat model. Their analysis is not focus on the biochemical mechanism of action of these biomolecules but it remarks the efficacy of the coated samples in new bone formation [48-50].

Osteoblasts (bone forming) and osteoclasts (bone resorbing) are the most important cell types in bone tissue. These cells maintain the balance between dissolved and deposited mineral phase. This balance between osteoclasts and osteoblasts is defined as *bone turn over* and it is controlled through several signaling pathways. The key element to regulate the *bone turn over* is to affect cell differentiation and proliferation. Lastly, *in vivo* experiments using collagen-coated bone implants have reported successful results, evidenced by an improved bone implant contact, bone density and bone formation [51-53].

3.2. Surface modifications by growth factors and biomolecules

Osteotropic biomolecules (e.g. growth factors, GFs) have been used to improve tissue response and bone formation. GFs are widely used to obtain cell differentiation in *in vitro* procedures. Several GFs, including bone morphogenetic protein (BMP), transforming growth factor-beta (TGF- β), fibroblast growth factor (FGF), platelet-derived growth factor (PDGF), and insulin-like growth factor (IGF), have shown an active role in bone tissue formation also after their immobilization onto implants surface [54-56].

CALCIUM PHOSPHATE CERAMICS FOR BONE REGENERATION

Stadlinger *et al.* investigated GFs that belong to the TGF- β superfamily (e.g. BMP-2, BMP-4, BMP-7 and TGF- β 1) and showed successful results in terms of bone to implant contact, bone density and osteoinduction in a pre-clinical study[57].

The synergistic effects of collagen and other biomolecules, such as GFs, bone sialoproteins or with hydroxyapatite, have shown potential as initiators of mineralization by deposition of calcium phosphate onto implant surfaces [41, 58, 59].

3.3. Surface modifications by peptides

The use of complete proteins as a coating material can introduce biological effects that can become an obstacle to bone cells recruitment or to bone initial contact. The immobilization of these biomolecules is often associated with their tendency to lose their 3D-conformation and hence impedes with their biological activity. As such, their adsorption to an implant surface often decreases the efficacy of immobilized proteins. The use of short peptide sequences derived from entire proteins as coating material can offer a solution to this problem [60, 61]. The Arg–Gly–Asp RGD peptide sequence [62, 63] has been widely used and presents a predominant binding site for cells via integrin receptors. Various other peptide sequences have been used similarly onto implanted materials. Bone implants surfaces enriched with a

layer of these peptides demonstrated improved biological effects *in vitro* in terms of cells proliferation, mineralization and adhesion [64-66].

3.4. Use of pharmacologically active biomolecules

An alternative selection of molecules for bone implant coatings is offered by pharmaceutical research. Especially for compromised health conditions (e.g. patients with osteoporosis, osteopenia or diabetes) pharmaceutical drugs can be used for surface modifications in order to provide a localized therapy. Molecules with specific active properties, defined as active principles, represent the fundamental material in drugs composition. The use of active principles in reduced amounts and *in situ* (i.e. local administration instead of systemic administration) is a challenge for several medical fields. Adsorption of locally deliverable drugs onto bone implants can be obtained through immersion of implants in a solution that contains active principles prior to implantation. Anti-osteoporotic drugs, such as bisphosphonates [67] or antibiotics like chlorhexidine [68], are currently adopted to enhance the biological performance of implants used in compromised bone conditions [69]. Bone implants can be coated with active biomolecules to become able to face lower bone density in osteoporotic patients or reduce fibrotic tissue formation in diabetic conditions. Bisphosphonates can be added as a coating material to reduce the number or the activity of osteoclasts in order to modify the balance between bone forming and bone resorbing cells.

CALCIUM PHOSPHATE CERAMICS FOR BONE REGENERATION

Immobilization of active biomolecules onto bone implants is the most recent development in surface engineering to obtain instructive coatings [70]. A recent review on bisphosphonates (BPs) showed that BPs that have an affinity for CaP materials can be incorporated into CaP coatings by soaking the implants into BPs solution and achieve stronger primary fixation by the inhibition of osteoclast action [71].

4. Coating deposition techniques

The most commonly used coating techniques are physical coating deposition methods, although there is a trend toward the utilization of wet-

	Deposition technique	Type of coating material	Coating thickness	Advantages	Disadvantages
Wet-chemical deposition	Biomimetic	osteocalcin, fibronectin and poly (L-lysine). BMP-2 incorporated into biomimetic CaP coatings	< 30 μm	Coating of complex geometries; co-deposition of biomolecules	Time consuming; requires controlled pH
	Sol-gel	Aluminosilicate, fluoridated hydroxyapatite (HA), Si-substituted HA and bioglass	< 1 μm	Coating of complex geometries; low processing temperature	Requires controlled atmosphere processing; expensive raw materials
	Electrospray	HA, Nano HA, ALP, biomolecules-HA composite collagen	0.1-5 μm	Co-depositon of biomolecules; control over coating composition and morphology	Low mechanical strength; line of sight technique
Physical deposition	RF magnetron sputtering	HA, Si-HA, carbonated HA, and Zn, Mg, and Al-doped CaPs	0.5-5 μm	Uniform and dense coating; strong adhesion	Line of sight technique; time consuming; low deposition rates
	Plasma spray	HA, Si-HA and antibacterial Ag-HA composite coatings	50-250 μm	High deposition rates	Non-uniform coating crystallinity; line of sight technique
	Pulsed laser	HA resistant to dissolution in SBF, Ag-HA, HA and fluorinated-HA, alendronate-doped HA	0.05-5 μm	Control over coating chemistry and morphology	Line of sight technique
	Ion beam dynamic mixing	Calcium phosphate (CaP)	0.05-1 μm	High adhesive strength	Line of sight technique; requires high sintering temperatures
	Ion beam assisted deposition	CaP	0.02-10 μm	Increased tensile bond strength	Line of sight technique

Table 1. Characteristics of deposition techniques.

chemical deposition techniques (e.g. biomimetic and sol-gel deposition techniques) for inorganic and organic coatings (**Table 1**). The deposition of uniform and adherent coatings of any organic biomolecule requires a deposition technique that does not cause damage to the biomolecule. The major drawbacks of biomolecules used for surface modification include the sensitivity of these biomolecules to physicochemical conditions and hence the requirement of controlled settings during deposition.

In fact, high temperatures or exposure to ion beams or plasmas can alter the organic structure of the biomolecules reducing their activity. Several wet-chemical deposition techniques that allow preservation of biomolecule activity have been explored in the past few decades [46].

4.1. Wet-chemical deposition techniques

Biomimetic deposition mimics the natural deposition of biological apatite and opened up a new way to develop biomaterials. It was introduced by Kokubo et al. in 1990 and the system originally involved simple immersion of (pre-treated) titanium substrates into a so-called simulated body fluid (SBF) to obtain deposition onto the surface of the substrates of a biologically active bone-like CaP layer [72]. The deposition is performed under physiological conditions (37°C, pH 7.4, $p(\text{CO}_2)=0.05$ atmosphere and appropriate electrolyte concentrations) [73] and biomolecules can be dissolved in the liquid and hence be incorporated in the growing coating. Several reports have shown the cell and

CALCIUM PHOSPHATE CERAMICS FOR BONE REGENERATION

tissue response (i.e. differentiation of stem cells into osteoblasts that deposit bone matrix on the ceramic surface) by the incorporation of biomolecules in combination to CaP coatings using the biomimetic deposition technique [74-76]. One of the main advantages of biomimetic deposition, in fact, is the possibility of co-precipitating ceramic (nano)particles with biomolecules (e.g. osteogenic agents) [77]. Bone implants have been immersed in a suspension containing antibiotics⁷⁸ or active principles like bisphosphonates [79-81] to obtain adsorption of these bioactive biomolecules onto the implant surface. Each application showed different response according with the expected role of the active agent incorporated onto implants through biomimetic deposition.

The sol-gel coating technique involves the immersion of a substrate into a concentrated solution with a gel-like texture [82-83]. This technique provides a resourceful approach to synthesize inorganic polymer and organic-inorganic hybrid materials under mild conditions. Moreover, sol-gel technique includes inherent advantages such as single step manufacturing process, material homogeneity at the molecular level and chemical bonding between the substrate and the coating [84].

The electrospray deposition (ESD) technique is an electrochemical coating method with promising applicability for inorganic and organic coatings. ESD, schematically represented in **Fig. 4**, shares the benefits of preserving biomolecules as the wet chemical deposition methods, such as biomimetic or sol-gel, and the deposition control of dry methods described for inorganic coating materials.

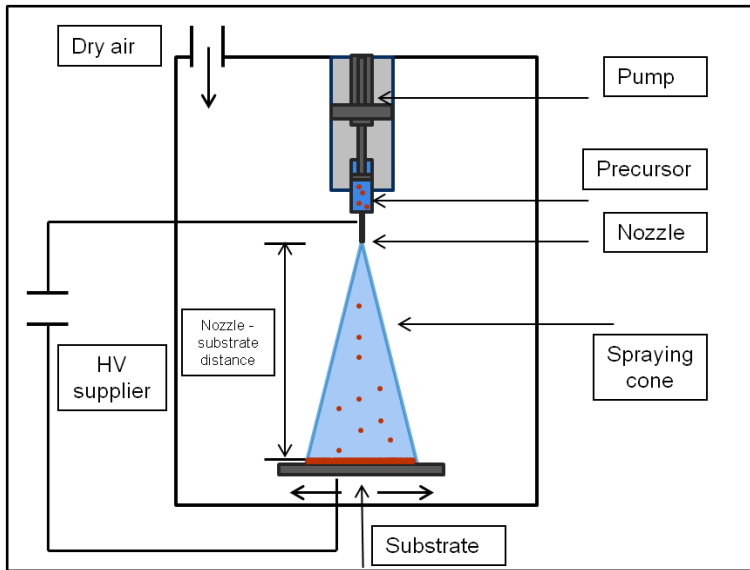


Figure 4. Schematic representation of electro spray deposition (ESD) apparatus.

ESD method is applicable to solutions or suspensions containing precursor that precursors are particles or molecules that carry an electrical charge or that can be dispersed in electrolytic solutions. Also the targets, onto which the coating is applied, have to be conductive. ESD allows for a strong control over physicochemical coating properties such as thickness or chemical composition [87].

CALCIUM PHOSPHATE CERAMICS FOR BONE REGENERATION

Although dip coating [88], sol–gel and biomimetic coatings are suitable for coating a complex shape (e.g. porous, 3D, etc.), all these techniques suffer from weak adhesive strength.

4.2. Physical deposition techniques

Other physical coating techniques such as plasma-spraying, pulsed laser deposition, ion beam deposition and sputter deposition offer advantages over wet-chemical depositions with respect to interfacial strength and crystallinity.

Plasma-spraying was the first coating technique for biomedical applications; this technique is also very successful for applying CaP coatings on implants due to its high deposition rate. Plasma spraying produces coatings with desired chemistry and crystallinity, despite poor control of the thickness and surface morphology [89]. Pulsed laser is a technique that allows deposition of thin, dense, well adhering coatings with control chemistry and crystallinity [90]. Ion beam deposition technique (**Fig. 5 A**) is a vacuum technique used to deposit coatings from precursor materials vaporized. Inherent properties and chemical composition of the coating may differ from that of the bulk material due to the high energy involved [91]. Lastly, one of the most frequently applied techniques used to prepare CaP coatings by physical vapor deposition process is radio-frequency (RF) magnetron sputtering (**Fig. 5 B**).

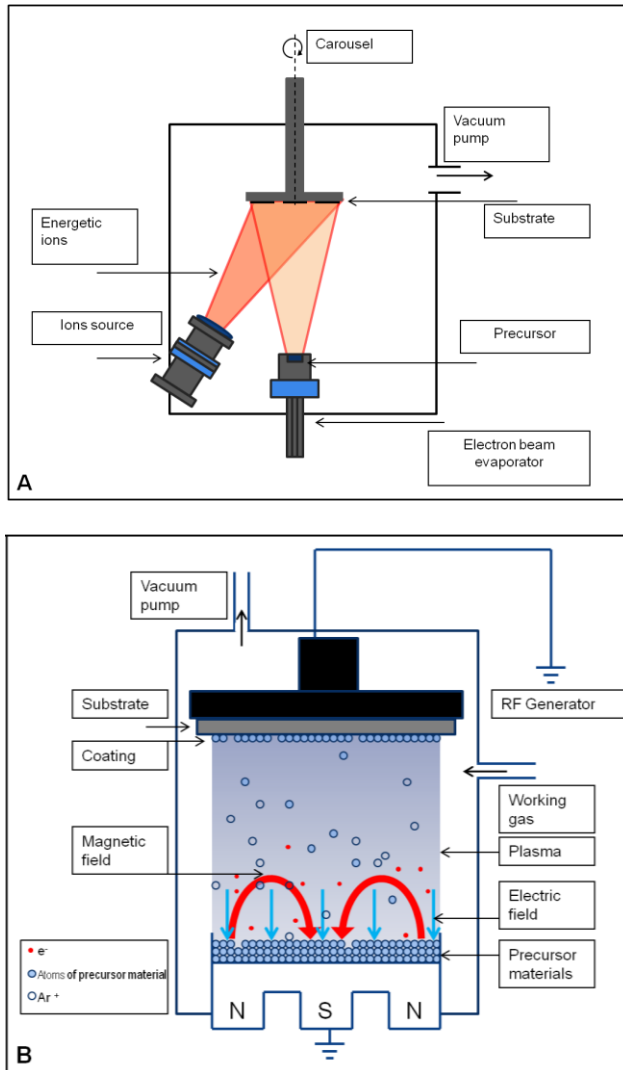


Figure 5. Schematic representation of physical deposition technique. (A) Ion beam deposition scheme. (B) Radio frequency magnetron sputtering apparatus.

This technique deposits thin coatings chemically bonded with the substrate which improves adhesion between the coatings and the substrate [92].

5. Future perspectives

The science of surface modification has shown significant progress in clinical applications through the development of more active inorganic and organic coating materials on implant surfaces. However, many scientific and technological challenges remain in biomaterials research. Further research and full understanding of fundamental aspects of the field such as the process of bone formation, attachment of proteins and specific cells, cell adhesion, bone stimulation or induction by inorganic and organic coatings are essential.

The use of CaP as a bone implant surface coating is well established in the field of biomaterials research, although the validity and efficacy of efforts focused on substitution within the crystal lattice have yet to be thoroughly explored. CaP-based coatings employed as a local delivery system of antimicrobials or pharmaceuticals offer great potential for medical applications, but still more precise control on local release kinetics is required.

Deposition of coating materials can strongly modify implant surface characteristics. Different coatings are obtained by selecting precursor materials for deposition, but also the coating techniques have a strong role in the final surface modifications. A deposited layer of calcium phosphate can assume totally different nano-, micro- and macromorphology if biomimetic, electrospray or RF magnetron sputtering deposition technique is used (**Fig. 6A-C**).

Incorporation of organic compounds into coatings, such as proteins derived from ECM, BMPs and other growth factors, peptides or pharmacologically active biomolecules have shown to play an effective role in stimulating cell adhesion to implant surfaces. Nevertheless, optimization of coating degradation, immobilization of biomolecules and effective concentrations are needed to improve functionality and biological efficacy. A representation of surfaces treated with biomolecules with two different methods is given in **Fig. 6 D and E**.

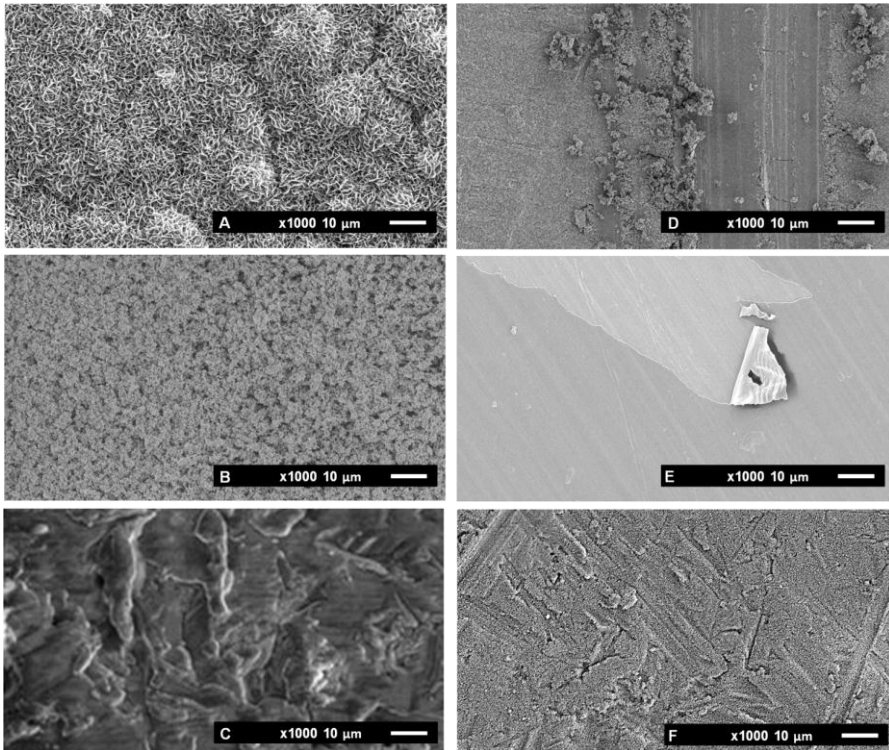


Figure 6. Overview of scanning electron microscopy images of surfaces of coated titanium sample substrates. Different coating techniques are considered and different precursor materials. Inorganic coating: (A) Calcium phosphate

CALCIUM PHOSPHATE CERAMICS FOR BONE REGENERATION

biomimetic deposition. (B) Calcium phosphate electrospray deposition (C) Calcium phosphate RF magnetron sputtering deposition. Organic coating: (D) Wet chemical deposition of biomolecules (Alkaline Phosphatase) (E) Collagen deposited with electro spray deposition. Composite coating: (F) Calcium phosphate and collagen electrospray deposition.

The heterogeneity of available biomaterials and deposition methods is leading to a continuous evolution of surface modifications that combine different techniques and materials to obtain solutions for specific needs, such as improved retention of deposited materials or to create composite coating layers (**Fig. 6F**).

Finally, initial research steps have been taken regarding the optimization of surface properties for bone implants to be used in compromised situations (e.g. osteoporosis and diabetes research). More reactive surfaces, with direct tissue interaction, have been engineered to improve bone quality. Future research strategies should consider validating therapeutic safety and effectiveness of therapeutic coatings.

Acknowledgement:

This research forms part of the Project **P2.04 BONE-IP** of the research program of the **BioMedical Materials** institute, co-funded by the **Dutch Ministry of Economic Affairs, Agriculture and Innovation**.

References

1. Bornstein, M. M.; Cionca, N.; Mombelli, A., *Systemic conditions and treatments as risks for implant therapy. Int J Oral Maxillofac Implants* **2009**, 24 Suppl, 12-27.
2. Ripamonti, U.; Roden, L. C.; Renton, L. F., *Osteoinductive hydroxyapatite-coated titanium implants. Biomaterials* **2012**, 33, (15), 3813-3823.
3. Habibovic, P.; Gbureck, U.; Doillon, C. J.; Bassett, D. C.; van Blitterswijk, C. A.; Barralet, J. E., *Osteoconduction and osteoinduction of low-temperature 3D printed bioceramic implants. Biomaterials* **2008**, 29, (7), 944-953.
4. Hing, K. A.; Revell, P. A.; Smith, N.; Buckland, T., *Effect of silicon level on rate, quality and progression of bone healing within silicate-substituted porous hydroxyapatite scaffolds. Biomaterials* **2006**, 27, (29), 5014-5026.
5. Brook, I.; Freeman, C.; Grubb, S.; Cummins, N.; Curran, D.; Reidy, C.; Hampshire, S.; Towler, M., *Biological evaluation of nano-hydroxyapatite-zirconia (HA-ZrO₂) composites and strontium-hydroxyapatite (Sr-HA) for load-bearing applications. Journal of Biomaterials Applications* **2011**.
6. Yang, F.; Dong, W.-j.; He, F.-m.; Wang, X.-x.; Zhao, S.-f.; Yang, G.-l., *Osteoblast response to porous titanium surfaces coated with zinc-*

CALCIUM PHOSPHATE CERAMICS FOR BONE REGENERATION

- substituted hydroxyapatite. Oral Surgery, Oral Medicine, Oral Pathology and Oral Radiology* **2012**, 113, (3), 313-318.
7. Bigi, A.; Boanini, E.; Capuccini, C.; Fini, M.; Mihailescu, I. N.; Ristoscu, C.; Sima, F.; Torricelli, P., *Biofunctional alendronate–Hydroxyapatite thin films deposited by Matrix Assisted Pulsed Laser Evaporation. Biomaterials* **2009**, 30, (31), 6168-6177.
 8. Müller, L.; Conforto, E.; Caillard, D.; Müller, F. A., *Biomimetic apatite coatings—Carbonate substitution and preferred growth orientation. Biomolecular Engineering* **2007**, 24, (5), 462-466.
 9. Ferro, D.; Barinov, S. M.; Rau, J. V.; Teghil, R.; Latini, A., *Calcium phosphate and fluorinated calcium phosphate coatings on titanium deposited by Nd:YAG laser at a high fluence. Biomaterials* **2005**, 26, (7), 805-812.
 10. Campbell, A. A.; Song, L.; Li, X. S.; Nelson, B. J.; Bottoni, C.; Brooks, D. E.; DeJong, E. S., *Development, characterization, and anti-microbial efficacy of hydroxyapatite-chlorhexidine coatings produced by surface-induced mineralization. Journal of Biomedical Materials Research* **2000**, 53, (4), 400-407.
 11. LeGeros, R. Z., *Calcium phosphate-based osteoinductive materials. Chem Rev* **2008**, 108, (11), 4742-53.
 12. Bose, S.; Tarafder, S., *Calcium phosphate ceramic systems in growth factor and drug delivery for bone tissue engineering: A review. Acta Biomaterialia* **2012**, 8, (4), 1401-1421.

13. Currey, J. D., *Bone architecture and fracture. Curr Osteoporos Rep* **2005**, 3, (2), 52-6.
14. Currey, J. D., *Bones: structure and mechanics. In Press, P. U., Ed.* 2002.
15. LeGeros, R. Z., *Calcium Phosphate-Based Osteoinductive Materials. Chemical Reviews* **2008**, 108, (11), 4742-4753.
16. Hench, L. L., *Bioceramics. Journal of the American Ceramic Society* **1998**, 81, (7), 1705-1728.
17. Kamitakahara, M.; Ohtsuki, C.; Miyazaki, T., *Coating of bone-like apatite for development of bioactive materials for bone reconstruction. Biomed Mater* **2007**, 2, (4), R17-23.
18. Voigt, J. D.; Mosier, M., *Hydroxyapatite (HA) coating appears to be of benefit for implant durability of tibial components in primary total knee arthroplasty. Acta Orthop* **2011**, 82, (4), 448-59.
19. Kim, K. H.; Ramaswamy, N., *Electrochemical surface modification of titanium in dentistry. Dent Mater J* **2009**, 28, (1), 20-36.
20. Leeuwenburgh, S. C.; Wolke, J. G.; Schoonman, J.; Jansen, J. A., *Influence of precursor solution parameters on chemical properties of calcium phosphate coatings prepared using Electrostatic Spray Deposition (ESD). Biomaterials* **2004**, 25, (4), 641-9.
21. Wang, J.; Layrolle, P.; Stigter, M.; de Groot, K., *Biomimetic and electrolytic calcium phosphate coatings on titanium alloy:*

CALCIUM PHOSPHATE CERAMICS FOR BONE REGENERATION

- physicochemical characteristics and cell attachment. Biomaterials* **2004**, 25, (4), 583-92.
22. Ehara, A.; Ogata, K.; Imazato, S.; Ebisu, S.; Nakano, T.; Umakoshi, Y., *Effects of alpha-TCP and TetCP on MC3T3-E1 proliferation, differentiation and mineralization. Biomaterials* **2003**, 24, (5), 831-6.
23. Yao, Z. Q.; Ivanisenko, Y.; Diemant, T.; Caron, A.; Chuvilin, A.; Jiang, J. Z.; Valiev, R. Z.; Qi, M.; Fecht, H. J., *Synthesis and properties of hydroxyapatite-containing porous titania coating on ultrafine-grained titanium by micro-arc oxidation. Acta Biomaterialia* **2010**, 6, (7), 2816-2825.
24. Pan, Y. K.; Chen, C. Z.; Wang, D. G.; Yu, X., *Microstructure and biological properties of micro-arc oxidation coatings on ZK60 magnesium alloy. Journal of Biomedical Materials Research Part B: Applied Biomaterials* **2012**, n/a-n/a.
25. Bohner, M., *Silicon-substituted calcium phosphates - a critical view. Biomaterials* **2009**, 30, (32), 6403-6.
26. Patel, N.; Best, S. M.; Bonfield, W.; Gibson, I. R.; Hing, K. A.; Damien, E.; Revell, P. A., *A comparative study on the in vivo behavior of hydroxyapatite and silicon substituted hydroxyapatite granules. J Mater Sci Mater Med* **2002**, 13, (12), 1199-206.
27. Hing, K. A.; Revell, P. A.; Smith, N.; Buckland, T., *Effect of silicon level on rate, quality and progression of bone healing within silicate-*

- substituted porous hydroxyapatite scaffolds. Biomaterials* **2006**, *27*, (29), 5014-26.
28. Landi, E.; Logroscino, G.; Proietti, L.; Tampieri, A.; Sandri, M.; Sprio, S., *Biomimetic Mg-substituted hydroxyapatite: from synthesis to in vivo behaviour. J Mater Sci Mater Med* **2008**, *19*, (1), 239-47.
29. Verberckmoes, S. C.; Behets, G. J.; Oste, L.; Bervoets, A. R.; Lamberts, L. V.; Drakopoulos, M.; Somogyi, A.; Cool, P.; Dorriné, W.; De Broe, M. E.; D'Haese, P. C., *Effects of Strontium on the Physicochemical Characteristics of Hydroxyapatite. Calcified Tissue International* **2004**, *75*, (5), 405-415.
30. Christoffersen, J.; Christoffersen, M. R.; Kolthoff, N.; Barenholdt, O., *Effects of strontium ions on growth and dissolution of hydroxyapatite and on bone mineral detection. Bone* **1997**, *20*, (1), 47-54.
31. Kannan, S.; Pina, S.; Ferreira, J. M. F., *Formation of Strontium-Stabilized β -Tricalcium Phosphate from Calcium-Deficient Apatite. Journal of the American Ceramic Society* **2006**, *89*, (10), 3277-3280.
32. Saint-Jean, S. J.; Camire, C. L.; Nevsten, P.; Hansen, S.; Ginebra, M. P., *Study of the reactivity and in vitro bioactivity of Sr-substituted alpha-TCP cements. J Mater Sci Mater Med* **2005**, *16*, (11), 993-1001.
33. Fielding, G. A.; Roy, M.; Bandyopadhyay, A.; Bose, S., *Antibacterial and biological characteristics of silver containing and strontium doped plasma sprayed hydroxyapatite coatings. Acta Biomater* **2012**, *8*, (8), 3144-52.

CALCIUM PHOSPHATE CERAMICS FOR BONE REGENERATION

34. Wang, J.; de Groot, K.; van Blitterswijk, C.; de Boer, J., *Electrolytic deposition of lithium into calcium phosphate coatings. Dent Mater* **2009**, 25, (3), 353-9.
35. Kawamura, H.; Ito, A.; Miyakawa, S.; Layrolle, P.; Ojima, K.; Ichinose, N.; Tateishi, T., *Stimulatory effect of zinc-releasing calcium phosphate implant on bone formation in rabbit femora. J Biomed Mater Res* **2000**, 50, (2), 184-90.
36. Kawamura, H.; Ito, A.; Muramatsu, T.; Miyakawa, S.; Ochiai, N.; Tateishi, T., *Long-term implantation of zinc-releasing calcium phosphate ceramics in rabbit femora. J Biomed Mater Res A* **2003**, 65, (4), 468-74.
37. Bajpai, P. K.; Benghuzzi, H. A., *Ceramic systems for long-term delivery of chemicals and biologicals. J Biomed Mater Res* **1988**, 22, (12), 1245-66.
38. Shinto, Y.; Uchida, A.; Korkusuz, F.; Araki, N.; Ono, K., *Calcium hydroxyapatite ceramic used as a delivery system for antibiotics. J Bone Joint Surg Br* **1992**, 74, (4), 600-4.
39. Uchida, A.; Shinto, Y.; Araki, N.; Ono, K., *Slow release of anticancer drugs from porous calcium hydroxyapatite ceramic. J Orthop Res* **1992**, 10, (3), 440-5.
40. Zhou, H.; Lawrence, J. G.; Touny, A. H.; Bhaduri, S. B., *Biomimetic coating of bisphosphonate incorporated CDHA on Ti6Al4V. J Mater Sci Mater Med* **2012**, 23, (2), 365-74.

41. *de Jonge, L. T.; Leeuwenburgh, S. C.; Wolke, J. G.; Jansen, J. A., Organic-inorganic surface modifications for titanium implant surfaces. Pharm Res* **2008**, *25*, (10), 2357-69.
42. *Sumner, D. R.; Turner, T. M.; Purchio, A. F.; Gombotz, W. R.; Urban, R. M.; Galante, J. O., Enhancement of bone ingrowth by transforming growth factor- β . Journal of Bone and Joint Surgery - Series A* **1995**, *77*, (8), 1135-1147.
43. *Puleo, D. A., Biochemical surface modification of Co-Cr-Mo. Biomaterials* **1996**, *17*, (2), 217-222.
44. *Endo, K., Chemical modification of metallic implant surfaces with biofunctional proteins (Part 1). Molecular structure and biological activity of a modified NiTi alloy surface. Dental materials journal* **1995**, *14*, (2), 185-198.
45. *Schliephake, H.; Scharnweber, D., Chemical and biological functionalization of titanium for dental implants. Journal of Materials Chemistry* **2008**, *18*, (21).
46. *Nijhuis, A. W. G.; Leeuwenburgh, S. C. G.; Jansen, J. A., Wet-Chemical Deposition of Functional Coatings for Bone Implantology. Macromolecular Bioscience* *10*, (11), 1316-1329.
47. *Petrie, T. A.; García, A. J., Extracellular Matrix-derived Ligand for Selective Integrin Binding to Control Cell Function Biological Interactions on Materials Surfaces. In Puleo, D. A.; Bizios, R., Eds. Springer US: 2009; pp 133-156.*

CALCIUM PHOSPHATE CERAMICS FOR BONE REGENERATION

48. Muller, R.; Abke, J.; Schnell, E.; Macionczyk, F.; Gbureck, U.; Mehrl, R.; Ruszczak, Z.; Kujat, R.; Englert, C.; Nerlich, M.; Angele, P., *Surface engineering of stainless steel materials by covalent collagen immobilization to improve implant biocompatibility. Biomaterials* **2005**, 26, (34), 6962-6972.
49. Douglas, T.; Heinemann, S.; Hempel, U.; Mietrach, C.; Knieb, C.; Bierbaum, S.; Scharnweber, D.; Worch, H., *Characterization of collagen II fibrils containing biglycan and their effect as a coating on osteoblast adhesion and proliferation. Journal of Materials Science: Materials in Medicine* **2008**, 19, (4), 1653-1660.
50. Rammelt, S.; Illert, T.; Bierbaum, S.; Scharnweber, D.; Zwipp, H.; Schneiders, W., *Coating of titanium implants with collagen, RGD peptide and chondroitin sulfate. Biomaterials* **2006**, 27, (32), 5561-5571.
51. Schliephake, H.; Scharnweber, D.; Dard, M.; Sewing, A.; Aref, A.; Roessler, S., *Functionalization of dental implant surfaces using adhesion molecules. Journal of Biomedical Materials Research Part B: Applied Biomaterials* **2005**, 73B, (1), 88-96.
52. Bernhardt, R.; van den Dolder, J.; Bierbaum, S.; Beutner, R.; Scharnweber, D.; Jansen, J.; Beckmann, F.; Worch, H., *Osteoconductive modifications of Ti-implants in a goat defect model: characterization of bone growth with SR β -CT and histology. Biomaterials* **2005**, 26, (16), 3009-3019.

53. Alghamdi, H. S.; van Oirschot, B.; Bosco, R.; den Beucken, J. J. J. P.; Aldosari, A. A. F.; Anil, S.; Jansen, J. A., *Biological response to titanium implants coated with nanocrystals calcium phosphate or type I collagen in a dog model. Clinical Oral implants Research* **2012**.
54. Solheim, E., *Growth factors in bone. Int Orthop* **1998**, 22, (6), 410-6.
55. Hall, J.; Sorensen, R. G.; Wozney, J. M.; Wikesjo, U. M., *Bone formation at rhBMP-2-coated titanium implants in the rat ectopic model. J Clin Periodontol* **2007**, 34, (5), 444-51.
56. Siebers, M. C.; Walboomers, X. F.; Leewenburgh, S. C.; Wolke, J. C.; Boerman, O. C.; Jansen, J. A., *Transforming growth factor-beta1 release from a porous electrostatic spray deposition-derived calcium phosphate coating. Tissue Eng* **2006**, 12, (9), 2449-56.
57. Stadlinger, B.; Pilling, E.; Mai, R.; Bierbaum, S.; Berhardt, R.; Scharnweber, D.; Eckelt, U., *Effect of biological implant surface coatings on bone formation, applying collagen, proteoglycans, glycosaminoglycans and growth factors. Journal of Materials Science: Materials in Medicine* **2008**, 19, (3), 1043-1049.
58. de Jonge, L. T.; van den Beucken, J. J. J. P.; Leeuwenburgh, S. C. G.; Hamers, A. A. J.; Wolke, J. G. C.; Jansen, J. A., *In vitro responses to electrosprayed alkaline phosphatase/calcium phosphate composite coatings. Acta Biomaterialia* **2009**, 5, (7), 2773-2782.
59. Stadlinger, B.; Pilling, E.; Mai, R.; Bierbaum, S.; Berhardt, R.; Scharnweber, D.; Eckelt, U., *Effect of biological implant surface*

CALCIUM PHOSPHATE CERAMICS FOR BONE REGENERATION

- coatings on bone formation, applying collagen, proteoglycans, glycosaminoglycans and growth factors. J Mater Sci Mater Med* **2008**, *19*, (3), 1043-9.
60. Shin, H.; Jo, S.; Mikos, A. G., *Biomimetic materials for tissue engineering. Biomaterials* **2003**, *24*, (24), 4353-64.
61. Morra, M., *Biochemical modification of titanium surfaces: peptides and ECM proteins. Eur Cell Mater* **2006**, *12*, 1-15.
62. Elmengaard, B.; Bechtold, J. E.; Soballe, K., *In vivo effects of RGD-coated titanium implants inserted in two bone-gap models. J Biomed Mater Res A* **2005**, *75*, (2), 249-55.
63. Schliephake, H.; Scharnweber, D.; Dard, M.; Sewing, A.; Aref, A.; Roessler, S., *Functionalization of dental implant surfaces using adhesion molecules. J Biomed Mater Res B Appl Biomater* **2005**, *73*, (1), 88-96.
64. Roessler, S.; Born, R.; Scharnweber, D.; Worch, H.; Sewing, A.; Dard, M., *Biomimetic coatings functionalized with adhesion peptides for dental implants. J Mater Sci Mater Med* **2001**, *12*, (10-12), 871-7.
65. LeBaron, R. G.; Athanasiou, K. A., *Extracellular matrix cell adhesion peptides: functional applications in orthopedic materials. Tissue Eng* **2000**, *6*, (2), 85-103.
66. Sreejalekshmi, K. G.; Nair, P. D., *Biomimeticity in tissue engineering scaffolds through synthetic peptide modifications* "Altering

- chemistry for enhanced biological response. In Wiley Online Library: Vol. 96, pp 477-491.*
67. Bigi, A.; Boanini, E.; Capuccini, C.; Fini, M.; Mihailescu, I. N.; Ristoscu, C.; Sima, F.; Torricelli, P., *Biofunctional alendronate-Hydroxyapatite thin films deposited by Matrix Assisted Pulsed Laser Evaporation. Biomaterials* **2009**, 30, (31), 6168-6177.
 68. Barbour, M. E.; O'Sullivan, D. J.; Jagger, D. C., *Chlorhexidine adsorption to anatase and rutile titanium dioxide. Colloids and Surfaces A: Physicochemical and Engineering Aspects* **2007**, 307, (1â€“3), 116-120.
 69. Abtahi, J.; Tengvall, P.; Aspenberg, P., *A bisphosphonate-coating improves the fixation of metal implants in human bone. A randomized trial of dental implants. Bone* **2012**, 50, (5), 1148-1151.
 70. Bosco, R.; Van Den Beucken, J.; Leeuwenburgh, S.; Jansen, J., *Surface Engineering for Bone Implants: A Trend from Passive to Active Surfaces. In 2012; Vol. 2, pp 95-119.*
 71. Cattalini, J. P.; Boccaccini, A. R.; Lucangioli, S.; Mourino, V., *Bisphosphonate-Based Strategies for Bone Tissue Engineering and Orthopedic Implants. Tissue Eng Part B Rev* **2012**.
 72. Kokubo, T.; Kushitani, H.; Sakka, S.; Kitsugi, T.; Yamamuro, T., *Solutions able to reproduce in vivo surface-structure changes in bioactive glass-ceramic A-W. J Biomed Mater Res* **1990**, 24, (6), 721-34.

CALCIUM PHOSPHATE CERAMICS FOR BONE REGENERATION

73. Kokubo, T.; Takadama, H., *How useful is SBF in predicting in vivo bone bioactivity? Biomaterials* **2006**, 27, (15), 2907-2915.
74. Gandolfi, M. G.; Ciapetti, G.; Perut, F.; Taddei, P.; Modena, E.; Rossi, P. L.; Prati, C., *Biomimetic calcium-silicate cements aged in simulated body solutions. Osteoblast response and analyses of apatite coating. J Appl Biomater Biomech* **2009**, 7, (3), 160-70.
75. Wu, G.; Liu, Y.; Iizuka, T.; Hunziker, E. B., *Biomimetic coating of organic polymers with a protein-functionalized layer of calcium phosphate: the surface properties of the carrier influence neither the coating characteristics nor the incorporation mechanism or release kinetics of the protein. Tissue Eng Part C Methods* **2010**, 16, (6), 1255-65.
76. Pasinli, A.; Yuksel, M.; Celik, E.; Sener, S.; Tas, A. C., *A new approach in biomimetic synthesis of calcium phosphate coatings using lactic acid-Na lactate buffered body fluid solution. Acta Biomater* **2010**, 6, (6), 2282-8.
77. Liu, Y.; Layrolle, P.; de Bruijn, J.; van Blitterswijk, C.; de Groot, K., *Biomimetic coprecipitation of calcium phosphate and bovine serum albumin on titanium alloy. Journal of Biomedical Materials Research* **2001**, 57, (3), 327-335.
78. Jahoda, D.; Nyc, O.; Pokorny, D.; Landor, I.; Sosna, A., *[Antibiotic treatment for prevention of infectious complications in joint*

- replacement]. *Acta Chir Orthop Traumatol Cech* **2006**, 73, (2), 108-14.
79. Denissen, H.; Van Beek, E.; Lowik, C.; Papapoulos, S.; Van Den Hooff, A., *Ceramic hydroxyapatite implants for the release of bisphosphonate. Bone and Mineral* **1994**, 25, (2), 123-134.
80. Seshima, H.; Yoshinari, M.; Takemoto, S.; Hattori, M.; Kawada, E.; Inoue, T.; Oda, Y., *Control of bisphosphonate release using hydroxyapatite granules. Journal of Biomedical Materials Research - Part B Applied Biomaterials* **2006**, 78, (2), 215-221.
81. Boanini, E.; Torricelli, P.; Gazzano, M.; Giardino, R.; Bigi, A., *Alendronate-hydroxyapatite nanocomposites and their interaction with osteoclasts and osteoblast-like cells. Biomaterials* **2008**, 29, (7), 790-796.
82. Shadanbaz, S.; Dias, G. J., *Calcium phosphate coatings on magnesium alloys for biomedical applications: A review. Acta Biomaterialia* **2012**, 8, (1), 20-30.
83. Ji, X.; Lou, W.; Wang, Q.; Ma, J.; Xu, H.; Bai, Q.; Liu, C.; Liu, J., *Sol-gel-derived hydroxyapatite-carbon nanotube/titania coatings on titanium substrates. Int J Mol Sci* **2012**, 13, (4), 5242-53.
84. Bagheri, H.; Piri-Moghadam, H.; Ahdi, T., *Role of precursors and coating polymers in sol-gel chemistry toward enhanced selectivity and efficiency in solid phase microextraction. Analytica Chimica Acta* **2012**, 742, (0), 45-53.

CALCIUM PHOSPHATE CERAMICS FOR BONE REGENERATION

85. W, S., *Corona spray pyrolysis: A new coating technique with an extremely enhanced deposition efficiency. Thin Solid Films* **1984**, 120, (4), 267-274.
86. Wilhelm, O.; Mädler, L.; Pratsinis, S. E., *Electrospray evaporation and deposition. Journal of Aerosol Science* **2003**, 34, (7), 815-836.
87. de Jonge, L. T.; Leeuwenburgh, S. C. G.; van den Beucken, J. J. P.; Wolke, J. G. C.; Jansen, J. A., *Electrosprayed Enzyme Coatings as Bioinspired Alternatives to Bioceramic Coatings for Orthopedic and Oral Implants. Advanced Functional Materials* **2009**, 19, (5), 755-762.
88. Aksakal, B.; Hanyaloglu, C., *Bioceramic dip-coating on Ti-6Al-4V and 316L SS implant materials. Journal of Materials Science: Materials in Medicine* **2008**, 19, (5), 2097-2104.
89. Kurzweg, H.; Heimann, R. B.; Troczynski, T.; Wayman, M. L., *Development of plasma-sprayed bioceramic coatings with bond coats based on titania and zirconia. Biomaterials* **1998**, 19, (16), 1507-11.
90. Cleries, L.; Fernandez-Pradas, J. M.; Morenza, J. L., *Bone growth on and resorption of calcium phosphate coatings obtained by pulsed laser deposition. J Biomed Mater Res* **2000**, 49, (1), 43-52.
91. Choi, J. M.; Kim, H. E.; Lee, I. S., *Ion-beam-assisted deposition (IBAD) of hydroxyapatite coating layer on Ti-based metal substrate. Biomaterials* **2000**, 21, (5), 469-73.

92. Wolke, J. G.; van Dijk, K.; Schaeken, H. G.; de Groot, K.; Jansen, J. A., *Study of the surface characteristics of magnetron-sputter calcium phosphate coatings. J Biomed Mater Res* **1994**, 28, (12), 1477-84.

CALCIUM PHOSPHATE CERAMICS FOR BONE REGENERATION

3

EFFECTS OF CALCIUM PHOSPHATE COMPOSITION IN SPUTTER COATING ON IN VITRO AND IN VIVO PERFORMANCE

CALCIUM PHOSPHATE CERAMICS FOR BONE REGENERATION

1. Introduction

Calcium phosphate (CaP) based ceramics are commonly used synthetic materials for bone substitutes and bone implant surface modification [1]. Properties including biodegradability, bioactivity, osteoconductivity, and osteoinductivity make calcium phosphates biologically appealing implant materials [2,3]. Differences in dissolution behavior of bulk ceramics are due to changes in chemical composition (CaP phase) and have been associated with osteoinductive potential *in vivo* [4]. More specifically, hydroxyapatite (HA), tricalcium phosphate (TCP) and biphasic calcium phosphate (BCP) have shown different levels of osteoinductive capacity that inversely correspond to their biological stability (i.e., TCP > BCP > HA) [4]. However, because of the inferior mechanical properties of bulk CaP ceramics, their application under load-bearing conditions is limited. Under load-bearing conditions, CaP ceramics are used as coating on mechanically strong bioinert implant materials, such as titanium (or titanium alloy), for optimization of the interaction with bone tissue at the interface [5].

Compared to bulk ceramics, as-deposited coatings possess distinctive network structures and properties (i.e., surface roughness, coating thickness, and crystallinity) and therefore can evoke a different response *in vivo*. The most commonly investigated synthetic CaP ceramic materials for use as coatings are HA ($\text{Ca}_{10}(\text{PO}_4)_6\text{OH}_2$) [6-8] and TCP ($\text{Ca}_3(\text{PO}_4)_2$) [9,10]. These CaP-based ceramics differ in composition, crystal structure and resorption rate. HA resorbs

slowly and resembles more closely natural bone mineral than TCP [11]. Therefore, HA is more commonly used for medical application. Among CaP-based ceramics, tetracalcium phosphate (TTCP; $\text{CaO} \cdot \text{Ca}_3(\text{PO}_4)_2$) has the highest solubility at $\text{pH} < 4.0$ and is the only CaP ceramic with a Ca/P ratio greater than HA [12]. TTCP is formed only by a solid-state reaction above $1300\text{ }^\circ\text{C}$ and in aqueous solutions complete hydrolysis of TTCP to HA occurs. However, very little research has been done on the use of TTCP as a CaP coating [13,14] and, to our knowledge, no attempts have been made to evaluate the performance of either TCP and TTCP sputtered coatings *in vivo*. Nevertheless, this seems to be interesting due to the suggested osteoinductive potential of the various CaP phases [4].

Plasma spraying of CaP ceramics onto metallic implants has been commonly used for biomedical applications, despite poor control of thickness and surface morphology [15-17]. However, radio frequency (RF) magnetron sputtering has several advantages over plasma spraying of CaP such as deposition of dense, uniform, and continuous coatings that have high CaP coating-substrate bonding strength [18]. After sputtering onto a metallic implant, the stoichiometry, CaP ratio, crystallinity, phase composition, and structure of the CaP ceramic are different relative to the bulk material. As a final step, post-annealing treatment is necessary to crystallize the coating, which also influences the final coating properties [19]. The resultant coating properties might enhance implant fixation and the bone formation processes.

CALCIUM PHOSPHATE CERAMICS FOR BONE REGENERATION

The aim of this study was to evaluate the effect of CaP-sputtered coatings with different phase composition on i) *in vitro* dissolution, and ii) *in vivo* bone response. For this purpose, three different CaP-based target materials (i.e. HA, TCP, and TTCP) were used for coating preparation, after which coating characterization, *in vitro* dissolution experiments, and *in vivo* implantation in a rabbit femoral condyle model (6 weeks implantation) were performed. We hypothesized that different CaP-based target materials affect coating properties and lead to coating-specific dissolution/precipitation behavior *in vitro* and bone response *in vivo*.

2. Materials and Methods

Materials

Commercially available pure Ti discs (thickness 1.5 mm, diameter 12 mm) and cylindrical Ti implants (length 8 mm, diameter 3.25 mm) were Al₂O₃ grit-blasted before deposition. The target materials used in the deposition process were HA granulated powder obtained from CAMCERAM[®] (CAM Bioceramics, Leiden, The Netherlands) and a copper disc provided with either a plasma-sprayed β-TCP or TTCP coating (CAM Bioceramics, Leiden, The Netherlands). The chemical composition and purity of the different target materials was confirmed by X-ray diffraction (XRD).

Coating deposition and characterization

The coatings for this study were deposited using RF magnetron sputtering equipment (Edwards High Vacuum ESM 100 system, Crawford, England) [18,20,21]. Substrates were cleaned ultrasonically in acetone and ethanol before deposition to remove impurities. Subsequently, substrates were placed on a rotating holder. The distance between target and implants was 80 mm. During deposition, argon pressure was kept at 5×10^{-3} mbar and a sputter power of 400 W with a coating thickness of 1 μm was used. A non-coated implant was used as control for the experiments.

After deposition, all coatings were subjected to an additional heat-treatment of 15 seconds in air at final heating temperature of up to 650 °C in an infrared furnace (Quad Ellipse Chamber, Model E4- 10-P, Research Inc, Minnesota, United States) [22]. The following ceramic coatings were generated:

1. HAH \rightarrow Coating deposited using HA as target material + HT
2. TCPH \rightarrow Coating deposited using β -TCP as target material + HT
3. TTCPH \rightarrow Coating deposited using TTCP as target material + HT

CaP-coated substrates were characterized using scanning electron microscopy (SEM, Jeol, SEM6310, Tokyo, Japan), reflection Fourier-transform infrared spectroscopy (FTIR, Perkin Elmer, Spectrum One, Groningen, The Netherlands) and thin-film X-ray diffraction (XRD, Philips, PW3710, Eindhoven, The Netherlands). To determine the Ca/P molar ratio, the coatings were dissolved in concentrated nitric acid. After digestion, the samples were diluted to 5 ml of 1% HNO_3 and the solution was analyzed by inductively

CALCIUM PHOSPHATE CERAMICS FOR BONE REGENERATION

coupled plasma optical emission spectroscopy (ICP-OES, iCAP 6000 Thermo Fischer Scientific Inc.) for Ca and P ions.

***In vitro* evaluation**

The *in vitro* dissolution of the CaP-based coatings was evaluated in conventional SBF with an ionic composition almost equal to human plasma [23]. Ionic concentrations of the SBF were 142.0 mM Na⁺, 5.0 mM K⁺, 1.5 mM Mg²⁺, 2.5 mM Ca²⁺, 147.8 mM Cl⁻, 4.2 mM HCO₃⁻², 1.0 mM HPO₄⁻², and 0.5 mM SO₄⁻². Tris-HCl served as a buffer to maintain a constant pH value of 7.4. The coated and uncoated discs (three specimens per time period per type of CaP coating) were immersed in 4 ml of SBF for 1, 2 and 4 weeks. In total, 36 CaP-coated discs were immersed in SBF (n=3 for HAH, TCPH, TTCPH and uncoated Ti-discs). SBF temperature was maintained at 37 °C and the solution was refreshed weekly. At each time point, the discs were removed from the SBF, washed with distilled water and dried at room temperature. Subsequently, all discs were characterized using XRD, FTIR, ICP-OES and SEM.

***In vivo* experiment**

Animals and regulations

The research protocol for animal experimental procedures was approved by the ethical committee of King Saud University (Riyadh, Kingdom of Saudi Arabia), and national guidelines for care and use of laboratory animals were

observed. A total of 20 New Zealand white rabbits (female; 6 months old) weighing between 3.2 and 5.1 kg were used.

Surgical procedure

Surgery was performed under general anesthesia by intramuscular injections of a combination of a dose of 35mg/kg ketamine and a dose of 5mg/kg xylazine. The rabbits were immobilized on their back and the hind limbs were shaved, washed and disinfected with povidone-iodine. The left and right femoral condyles were then exposed to a medial longitudinal incision. A hole (3.2 mm in diameter and 8 mm in depth) was created in the center of the condyle using a dental drill (KAVO, Intrasept 905, KAVO Nederland BV, Vianen, the Netherlands). A 2 mm drill bit was first used to establish a 2 mm diameter defect. The bone defect was gradually widened to a final diameter of 3.2 mm. Debris was removed from the defect by irrigation with physiological saline solution. The implants were placed into the defects. Subsequently, the periosteum and muscle were closed with a continuous 4-0 Vicryl suture. Finally, the skin was closed with continuous intracutaneous 4-0 Vicryl sutures. Post-surgery pain was controlled for two days postoperatively by the administration of Fynadyne[®] (Fynadine, Schering Plough Animal Health Benelux, Utrecht, the Netherlands) intramuscularly. To reduce the post-operative infection risk Enrofloxacin 5-10 mg /kg (Baytril, Bayvet Division, Chemagro Ltd, Etobicoke, Ontario; 5-10 mg/kg) was administered. The implants were randomized according to a balanced split plot design to exclude

CALCIUM PHOSPHATE CERAMICS FOR BONE REGENERATION

the effect of implantation location and possible variations in individual rabbits. Each rabbit received 2 implants, in total 40 implants were placed (n=10 for HAH, TCPH, TTCPH and uncoated implants). Rabbits were euthanized six weeks after implantation and the femoral condyles were harvested and fixed in 10% formaldehyde solution, and dehydrated in ethanol for evaluation.

Micro-computed tomography

For micro-computed tomography, harvested femoral condyles were wrapped in parafilm[®] to prevent drying. For quantitative 3D analysis, all specimens were vertically placed onto the sample holder, with the long axis of the implant perpendicular to the scanning beam, and scanned using Skyscan-1072 X-ray microtomograph, TomoNT version 3N.5, Skyscan[®], Belgium. Subsequently, a high resolution scan was recorded at a 30 μm voxel resolution. Then, using CT Analyzer (version 1.4, Skyscan[®]), a cone beam reconstruction was performed onto the projected files. The region of interest (ROI) was specified for distinct areas starting at the implant surface: inner (0-300 μm), middle (300-600 μm) and outer (600-900 μm) surrounding the implant over a constant length (4 mm). Thereafter, for all images a threshold was manually selected to discriminatively assign bone tissue and preserve its morphology, while excluding the metallic implant material. Per implant, the parameters of bone volume and tissue volume were measured, after which the amount of bone volume per zone was determined and expressed as a percentage.

Histological processing and analysis

Each specimen was hemisected along the longitudinal axis of the implant with a diamond saw blade. Subsequently, one half containing the implant was fixed in 4 % formaldehyde for 2 days, dehydrated in increasing ethanol concentrations (70-100 %) and embedded in methylmethacrylate (MMA). After polymerization in MMA, thin sections (10 μm) were sawed in a longitudinal direction to the axes using a modified sawing microtome technique [24]. MMA sections were stained with methylene blue/basic fuchsin, basic fuchsin was used to color mineralized and unmineralized bone tissue (i.e., osteoid) [25]. Implants from the second half of the specimens were carefully removed from the bone tissue to avoid interface damage. Afterwards, the specimens were decalcified with a specific-purpose apparatus (TDE30, Sakura; Sakura Finetek Europe B.V. Alphen aan den Rijn, The Netherlands) for three weeks, dehydrated through a graded series of ethanol, embedded in paraffin and cut into sections along the longitudinal axis of the implant. Using a microtome (Leica RM 2145), 5 μm thick sections were prepared and stained using elastic-van Gieson (EVG), Masson-Goldner, and tartrate-resistant acid phosphatase. All sections were examined with a light microscope (Leica Microsystems AG, Wetzlar, Germany).

Histomorphometrical analysis

CALCIUM PHOSPHATE CERAMICS FOR BONE REGENERATION

To evaluate the peri-implant bone response, histomorphometrical analyses were performed using a computer-based image analysis technique (Leica® Qwin Pro-image analysis system, Wetzlar, Germany). Sections of MMA-embedded specimens (n=3 per specimen) were quantitatively analyzed for the percentage of bone-to-implant contact (BIC) and peri-implant bone volume (BV). BIC was defined as the relative implant surface distance at which direct bone-to-implant contact was present. To determine the peri-implant BV, three zones surrounding the implant were defined starting at the implant surface, i.e., inner 0-300 μm , middle 300-600 μm and outer 600-900 μm over a length of 4 mm. Consecutive elastic-van Gieson stained sections were used to verify assignment of tissue as bone tissue in the ROI.

In addition, Masson-Goldner stained sections were analyzed (n=3 per specimen) to specifically determine the presence of unmineralized bone matrix (i.e., osteoids) in contact with the implant surface. To determine the presence of osteoclast-like cells in a peri-implant region of 900 μm (over 4 mm implant length) tartrate-resistant acid phosphatase (TRAP) staining was used. Results are presented as a percentage of TRAP-positive stained sections of the total number of sections analyzed.

Statistical analysis

All statistical analyses were performed with GraphPad Instat[®] 3.05 software (GraphPad Software Inc, San Diego, CA, USA), using analysis of variance (ANOVA) combined with a post-hoc Tukey-Kramer Multiple Comparisons Test. Results were considered significant at $p < 0.05$. Chi-square test was applied to assess the presence of TRAP-positive staining.

3.Results

Characterization and *in vitro* evaluation

Ca and P and the Ca/P ratio were determined by ICP-OES (**Table 1**). This analysis revealed that all the as-sputtered and heat-treated coatings had a higher Ca/P ratio compared to the theoretical value of the initial target materials. The Ca/P ratio for HAH, TCPH and TCPH coating was in the range of 2.07, 2.17 and 2.30 respectively.

Figure 1 shows the XRD patterns of the sputtered coatings before, during and after 4 weeks incubation in SBF. The XRD patterns of the as-sputtered coatings showed an amorphous structure without specific reflection lines (data not shown). Heat treatment at 650 °C changed the amorphous structure into a more random apatite structure with peaks at 25.9 °, 31.9 ° and 32.4 ° 2 θ (**Figure 1**, lower lines). The XRD-patterns of the HAH coating did not show any change during the four week incubation period (**Figure 1A**). Typical reflection peaks at 25.9°, 31.7°, 32.0° and 34.0° 2 θ were attributed to the apatite phase.

CALCIUM PHOSPHATE CERAMICS FOR BONE REGENERATION

Nomenclature	Chemical Formula	Abbreviation	Ca/P ratio*	Ca/P ratio after HT**
Hydroxyapatite	$\text{Ca}_{10}(\text{PO}_4)_6(\text{OH})_2$	HA	1.67	2.07 ± 0.01
β-Tricalcium phosphate	$\text{Ca}_3(\text{PO}_4)_2$	TCP	1.5	2.17 ± 0.01
Tetracalcium phosphate	$\text{CaO} \cdot \text{Ca}_3(\text{PO}_4)_2$	TTCP	2.0	2.30 ± 0.01

* Theoretical Ca/P ratio

** Experimentally determined Ca/P ratio by ICP-OES
after coating deposition + heat treatment (HT)

Table 1. Nomenclature, chemical formula and Ca/P ratio of CaP-based ceramics.

After 4 weeks incubation, the XRD patterns of the TCPH (**Figure 1B**) and TTCPH coatings (**Figure 1C**) showed an increase in crystallinity with more intense CaP diffraction peaks.

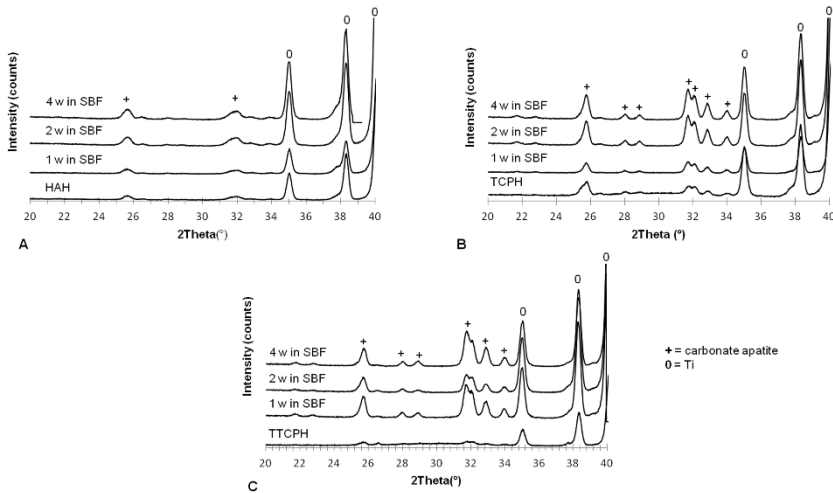


Figure 1. XRD pattern of HAH (A), TCPH (B) and TTCPH (C) coatings after 0, 1, 2 and 4 weeks of immersion in SBF.

The phase composition was confirmed by the FTIR analysis. HAH coating showed bands at 1090, 1050, 970, 670 and 575 cm^{-1} , which were assigned as the stretching and bending motion of phosphate characteristics for hydroxyapatite (**Figure 2A**). These P-O bonds remained present and unchanged throughout the four weeks incubation in SBF. For the spectrum of the TCPH and TTCPH coatings (**Figure 2B,C**), the bands present at 1090, 1050, 670 and 575 cm^{-1} split up into sharper bands. Furthermore, carbonate apatite ($\text{CO}_3\text{-AP}$) bands became apparent at wavelengths of 1454 and 1404 cm^{-1} with increasing incubation time, revealing that carbonate was mainly substituting for phosphate anions in a crystalline CaP environment.

CALCIUM PHOSPHATE CERAMICS FOR BONE REGENERATION

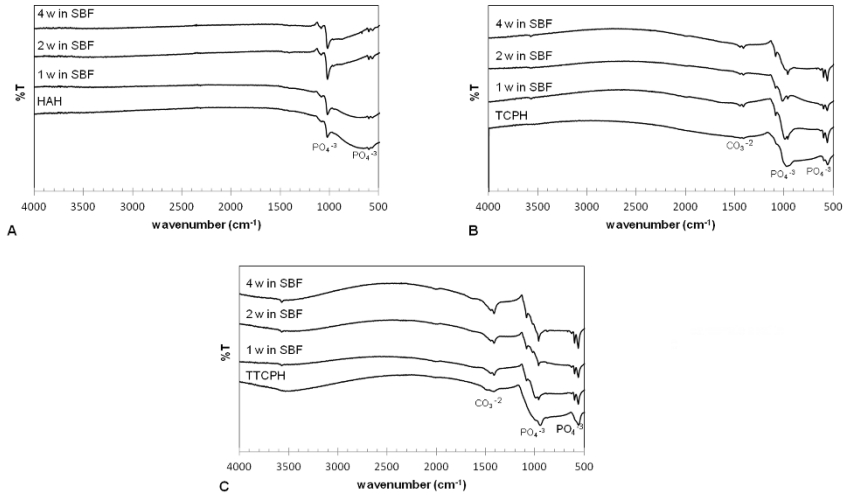


Figure 2. Fourier transform infrared of HAH (A), TCPH (B) and TTCPH (C) coatings after 0, 1, 2 and 4 weeks of immersion in SBF.

Scanning electron micrographs of the heat-treated and SBF incubated coatings are shown in **Figure 3**. SEM examination of the heat-treated coatings showed a homogeneous layer and a complete coverage of the substrate surface. After two weeks incubation in SBF, TCPH and TTCPH coatings showed morphological changes. For both coatings, local surface dissolution was observed, precipitates formed, and in the case of TTCPH coating the precipitate had a rod-like morphology (**Figure 3**, higher magnification).

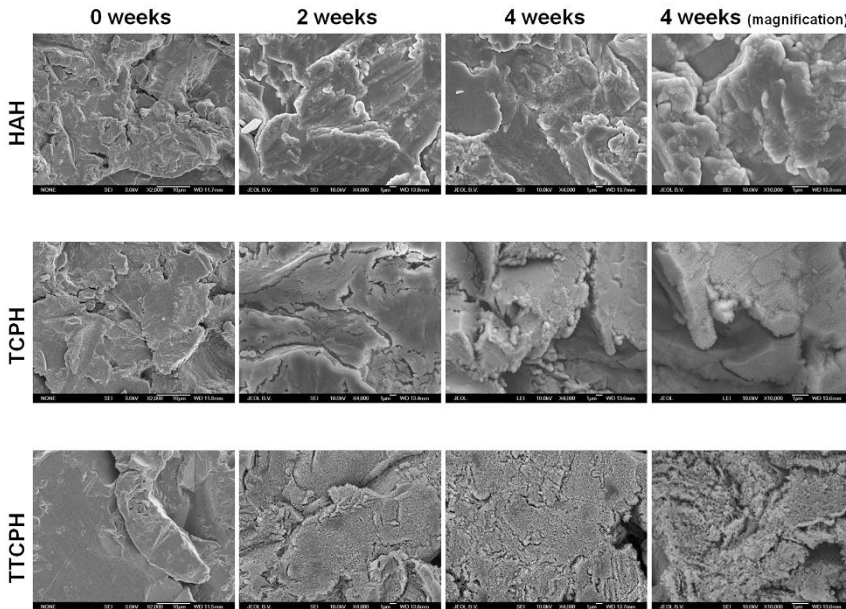


Figure 3. Scanning electron micrographs of HAH, TCPH and TTCPH coatings after immersion in SBF for 0 (magnification 1000x), 2 and 4 weeks (magnification 4000x). Right panels show higher magnifications (10000x) of the 4 week specimens.

This heterogeneous morphological appearance for TCPH and TTCPH coatings was maintained up to 4 weeks incubation. On the other hand, HAH coatings did not show any morphological changes during the 4 weeks incubation in SBF.

Changes in the concentration of calcium (Ca^+) and phosphate (PO_4^{3-}) ions in SBF of the CaP coatings during the 4-week incubation period are shown in **Figure 4**. HAH coating had stable Ca^+ ion concentrations during the first 3 weeks of incubation, after which the concentration of Ca^+ ions in SBF decreased. For the TCPH and TTCPH coatings, Ca^+ ion concentration increased

CALCIUM PHOSPHATE CERAMICS FOR BONE REGENERATION

over the first 2 weeks of incubation with a subsequent stabilizing Ca^+ ion concentration. HAH coatings showed an increase of PO_4^{3-} ion concentration during the 4-week incubation. TCP coatings showed an increase of PO_4^{3-} ion concentration during the first 2 weeks, after which the concentration in SBF solution decreased. TTCPH showed an increase of PO_4^{3-} ion concentration during the first 3 weeks, after which the concentration decreased.

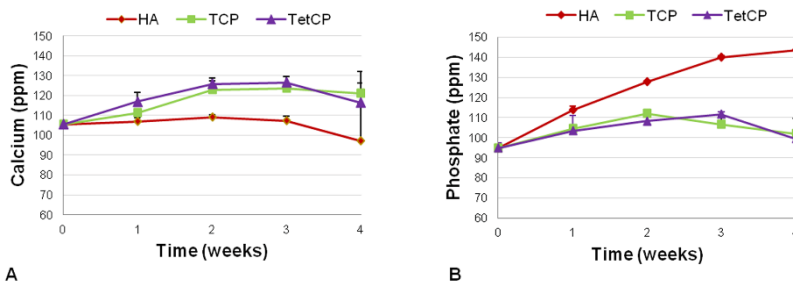


Figure 4. Calcium and phosphate ion concentration of the SBF solution during the 4-weeks incubation period of the different experimental coatings.

General observations of *in vivo* implantation

All 20 animals remained in good health and did not show any wound healing complications. At the end of the implantation period, a total of 40 implants were harvested. At retrieval, no signs of inflammatory or adverse tissue reaction were observed around the implants. Post-mortem radiographs as obtained via micro-CT imaging revealed that the implants were located in trabecular bone (**Figure 5 A-C**).

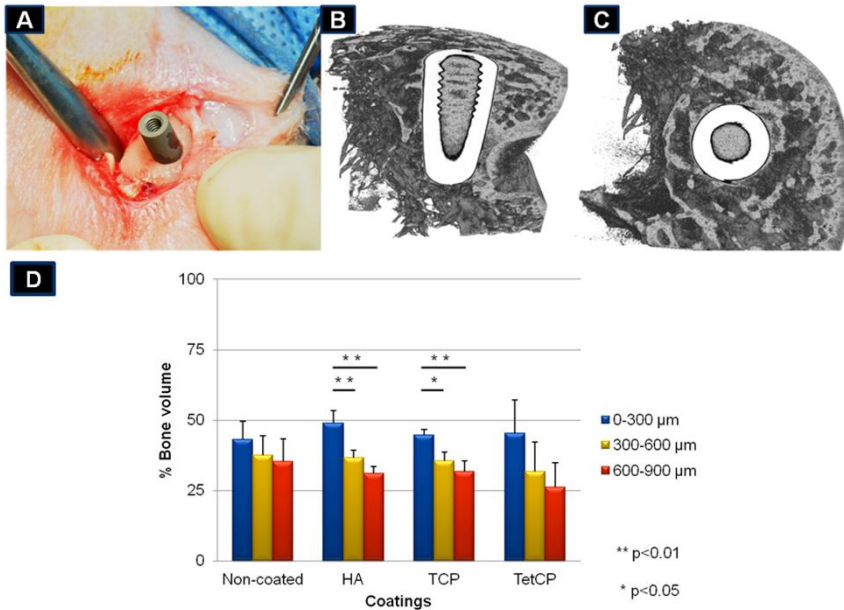


Figure 5. A) Surgical procedure of the titanium cylinder inserted in the femoral condyle of a rabbit. Post-sacrifice radiographs obtained with micro-computer tomography showing that the implants (i.e., metallic structures appear white) were mainly located in trabecular bone. B) cross-sectional view. C) top view of the implant. D) Results of micro-computed tomography (microCT) analysis of peri-implant BV percentage for the different experimental implants (non-coated, HAH, TCPH and TTCPH) in three different zones: inner (0-300 μm), middle (300-600 μm) and outer (600-900 μm). * p <0.05 and ** p <0.01.

Micro-CT analysis

Peri-implant BV measurements were performed for three different regions of interest: 0-300 μm (inner), 300-600 μm (middle) and 600-900 μm (outer).

Mean BV of the inner, middle and outer zone are depicted in **Figure 5D**. As a

CALCIUM PHOSPHATE CERAMICS FOR BONE REGENERATION

general trend, the highest BV (range: 43-49 %) was observed in the inner zone, intermediate BV (range: 31-37 %) in the middle zone and the lowest BV (range: 26-35 %) in the outer zone. Additionally, statistical analyses showed significant differences in BV for the inner zone compared to the middle (12.2 %, $p < 0.01$) and outer zone (17.7 %, $p < 0.01$) for HAH coatings and for the inner zone compared to the middle (9.2 %, $p < 0.05$) and outer zone (13 %, $p < 0.01$) for the TCPH coatings.

Descriptive histological evaluation

Histological examination was carried out to evaluate the peri-implant bone response using MMA-embedded and paraffin-embedded sections.

MMA-embedded specimens stained with methylene blue/basic fuchsin (MB/BF) showed no indications of an inflammatory response at the implant interface. MMA-embedded specimens showed new bone formation around and bone apposition to all experimental implants. The non-coated implants had apparently less new bone formation around the implant than the HAH, TCPH and TTCPH coated implants (**Figure 6**).



Figure 6. Representative histological sections (methylene blue/basic fuchsin stain) of the different experimental implants (non-coated, HAH, TCPH and TTCPH) after 6 weeks of implantation in the femoral condyle of rabbits.

Results from Elastica-van Gieson (EVG) staining performed on the paraffin embedded specimens showed bone formation and bone apposition around all coated implants (**Figure 7A**). Masson-Goldner staining showed presence of immature new bone tissue (osteoid; unmineralized; red staining) as well as mineralized bone tissue (blue staining) at all the implant-tissue interface (**Figure 7B**). Further, specimens displaying TRAP-positive staining contained osteoclast-like cells mainly close to the interface region of the implants (**Figure 7C**).

CALCIUM PHOSPHATE CERAMICS FOR BONE REGENERATION

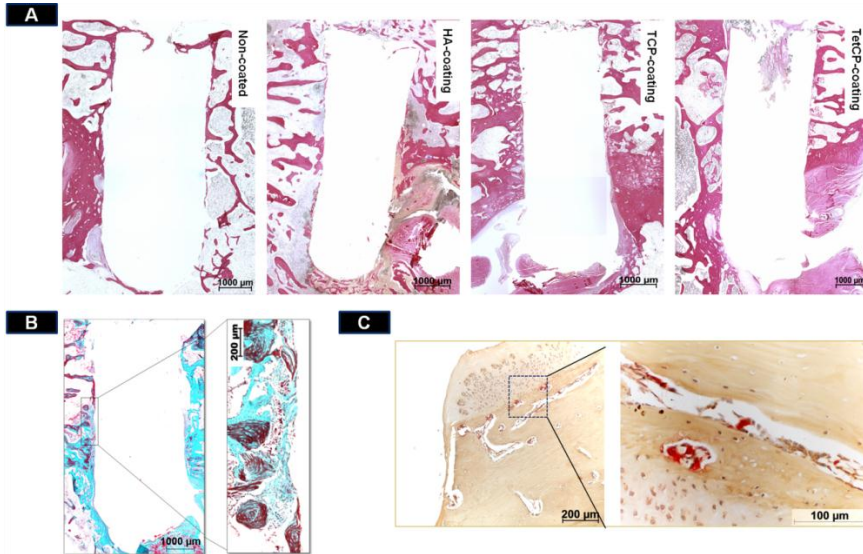


Figure 7. Histological sections after 6 weeks of implantation in the femoral condyle of rabbits: A) Elastica-van Gieson stain of the different experimental implants (non-coated, HAH, TCPH and TTCPH). White area represents the original implant location; implants were removed for subsequent decalcification, paraffin-embedding and sectioning. B) Masson-Goldner stain at a higher magnification of the interface. C) Tartrate-resistant acid phosphatase positive staining at a higher magnification that shows the presence of osteoclast.

Histomorphometry

BIC data for the different experimental groups are shown in **Figure 8A**. The results of BIC measurements showed a similar response (values range: 60-69 %) for all experimental coatings.

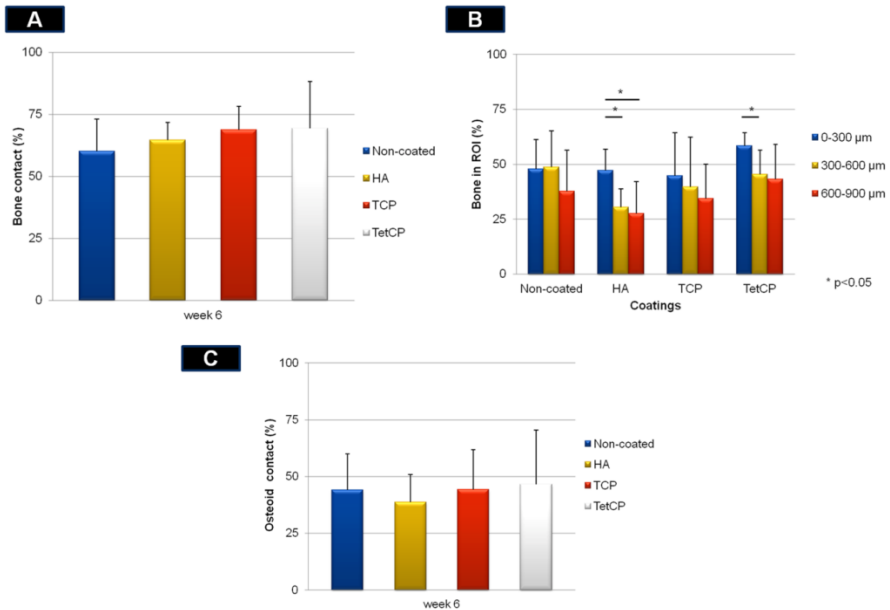


Figure 8. A) Results of histomorphometrical analysis of BIC percentage measurements for the different experimental implants (non-coated, HAH, TCPH and TTCPH). B) Peri-implant BV percentage measurements for the different experimental implants (non-coated, HAH, TCPH and TTCPH). * $p < 0.05$ C) Results of histomorphometrical analysis of osteoid-implant contact measurements of non-coated, HAH, TCPH and TTCPH.

Peri-implant BV was measured for distinct zones in the peri-implant region (**Figure 8B**). Significantly higher peri-implant BV was observed in the vicinity of the implant surface of the inner zone 0-300 μm compared to middle 300-600 μm for the HAH coating (difference 16.6 %, $p < 0.05$) and TTCPH coating

CALCIUM PHOSPHATE CERAMICS FOR BONE REGENERATION

(difference 13 %, $p < 0.05$). Further, similar peri-implant BV were found between the groups for individual zones in the peri-implant region ($p > 0.05$).

Osteoid-implant contact values were within a range of 38-46 % without significant differences between the experimental implants (**Figure 8C**). TRAP-positive staining was present in 17 % of the sections of non-coated, 40 % of the sections of HAH, 60 % of the sections of TCPH, 75 % of the sections of TTCPH coated implants (**Table 2**). Although a higher percentage of TRAP-positive staining was found in coated than non-coated specimens, no statistical differences were found ($p > 0.05$).

Groups	TRAP-positive presence percentage
Non-coated	17 %
HAH	40 %
TCPH	60%
TTCPH	75 %

Table 2. Percentage of specimens with TRAP-positive presence at the region close to the interface.

4. Discussion

The aim of this study was to evaluate the effect of phase composition of different CaP-sputtered coatings prepared with different CaP target materials on i) *in vitro* dissolution, and ii) *in vivo* bone response. We hypothesized that CaP-based target materials would lead to coating-specific dissolution/precipitation behavior *in vitro* and bone response *in vivo*. This study showed that the initially deposited coatings all have a similar apatitic structure based on XRD and FTIR analyses. However, when tested *in vitro*, the experimental groups showed

different dissolution/precipitation behavior. Furthermore, results from the *in vivo* test showed that despite similar BIC and peri-implant BV for all experimental implants, the presence of TRAP-positive staining in the peri-implant region suggests an apparent increase in bone remodeling around the implant surfaces with increasing coating dissolution (i.e., TTCP > TCP > HA).

In this study, sputtered coatings with specific CaP content and properties were obtained using various starting CaP targets with different stoichiometry (i.e., HA, β -TCP and TTCP). Phase purity of these targets was confirmed by X-ray diffraction patterns. SEM examination showed that all as-sputtered and heat treated coatings had a homogenous and dense structure. XRD measurements revealed that all the as-sputtered coatings were amorphous. In accordance with previous studies, after an additional heat treatment, the XRD of all the sputtered coatings changed to a random apatite structure [26-28]. Ca/P ratios of all coatings were higher than initial Ca/P ratios of the corresponding target materials as demonstrated by additional ICP-OES measurements (**Table 1**). The higher Ca/P ratio of these coatings can be explained by preferential sputtering of calcium in growing films [27], and by the fact that orthophosphate ions are more volatile than calcium ions during sputtering and are pumped away before being deposited on the substrate [3, 27-29]. In particular, TCPH had a higher Ca/P ratio than expected, which may be due to more orthophosphate ions in TCP than in HA or TTCP. Although several studies have examined the properties of HA and β -TCP sputtered coatings [29-32], as far as the authors are

CALCIUM PHOSPHATE CERAMICS FOR BONE REGENERATION

aware, only one study has been published dealing with TTCP sputtered coatings [19].

Solubility of the various types of coatings was investigated during *in vitro* incubation in SBF. Calcium and phosphate ion deposition and formation of a calcium phosphate layer when exposed to SBF are necessary to initiate the growth of bone-like apatite on biocompatible implants. Surface morphological differences were already observed for the TCPH and TTCPH coatings after two weeks of immersion indicating that precipitation had occurred. FTIR and XRD analyses revealed that the precipitate observed on the TCPH and TTCPH coatings was carbonate apatite, the amount of which increased with immersion time in SBF, while the HAH surface remained unchanged. Calcium and phosphate ions are released due to local surface dissolution of TCPH and TTCPH coatings, which supersaturates the SBF promoting apatite nucleation and subsequently apatite precipitation. This phenomenon was not observed for the HAH coating, but several studies of CaP precipitation have demonstrated that the dissolution rate of β -TCP and TTCP is higher than that of hydroxyapatite [33-35]. After heat treatment, a different calcium phosphate phase could be expected for each CaP coating given the initial differences in Ca/P ratio of the target material. However, XRD measurements revealed that the heat treatment only induced a random apatite structural formation for all the as-sputtered coatings. It could be argued that the energy during heat treatment requires adjustment for individual CaP phases to achieve a more crystalline phase for each coating type in the present study. Also, the differences in coating

dissolution are likely due to differences in atomic organization at the surface and the fraction of the as-sputtered CaP coating that was crystallized after the additional heat treatment.

The chemical composition of the coating surface is important, because the implant surface is the level at which the bone healing process starts. The femoral condyle rabbit model was chosen for the *in vivo* study because of its fast healing response and for comparison with other studies performed in our laboratory [36]. Previous work using RF magnetron sputtering to prepare bioactive CaP coatings showed accelerated implant stability by promoting rapid implant to bone fixation in different animal models, using rabbits [36-38], goats [32,39,40] dogs [41-44], rats [45], and primates [46]. A recent study showed favorable effects of CaP sputter-coatings on the bone implant interface in an osteoporotic rat model [45]. However, in this study measurements of BIC 6 weeks after implantation in the rabbit model showed no significant differences between CaP coatings and non-coated implants. Previous studies on BIC found similar results using the same animal model, coating technique, and implantation time [36,38]. Furthermore, there is no difference in BIC between HA coatings and uncoated implants according to a recent review by Surmenev (2012) on plasma-assisted CaP coatings fabrication methods [3]. Only one study has shown higher BIC for crystalline HA coated implants 6 weeks after implantation in femoral bone in rabbits compared to non-coated control implants [37]. To date, no studies have reported on TTCP-sputtered coatings upon *in vivo* implantation. The absence of an effect of the various CaP coatings

CALCIUM PHOSPHATE CERAMICS FOR BONE REGENERATION

on BIC can be due to the chosen implantation time. After 6 weeks of implantation, bone healing in a rabbit will be almost completed. Therefore, it is recommended to include shorter implantation times in future studies to allow for the observation of a possible effect during the initial stage of implant-bone healing. On the other hand, the results of this study showed differences in peri-implant BV formation in the inner 0-300 μm compared to middle 300-600 μm for the HAH and TTCPH coatings. Furthermore, there is an apparent increase in TRAP-positive staining percentage, which represents the presence of osteoclast-like cells, with decreasing coating stability. These results on BV formation and TRAP-positive staining indicate that variation in coating chemistry influences bone remodeling process directly adjacent to the implant surface.

Chemical composition and structural properties have been related with the osteoinductive capacity of CaP bulk ceramics in literature. The chemical composition is often the first coating parameter to be modified in studies. In a recent study, functionalized nanotopographic geometries on the surface of HA coated titanium implants were placed in heterotopic sites⁴⁷. Induction of bone formation and regulation of gene products were observed to be functions of substrate topography, which dictated biological patterns [47]. Ripamonti et al. [47] conducted their study in heterotopic intramuscular sites, while CaP coatings were implanted in bone tissue in the current study. The difference in implant location between the current study and Ripamonti et al. [47] makes direct comparison inappropriate. However, the results of the current study

suggest that varying CaP stoichiometry gives different degrees of bone remodeling. In view of the results of Ripamonti et al. [47], surface topography appears hierarchically superior to CaP stoichiometry for osteoinductive capacity of CaP-based ceramic coatings. However, supplementary chemical composition seems to represent a small but important approach to further influence peri-implant osteogenic processes.

5 . Conclusion

This study has shown that differences in Ca/P ratio in sputter targets influence dissolution and precipitate formation of the resulting CaP coatings when tested *in vitro*. The *in vivo* study showed that neither peri-implant BV nor BIC were significantly affected in relation to different CaP coatings. However, the presence of TRAP-positive staining in the peri-implant region suggests increased bone remodeling around CaP-based coatings with lower stability (i.e., TTCPH > TCPH > HAH > non-coated controls). Future research should focus on combining critical surface parameters, e.g. coating composition and surface topography, to optimize surface properties for bone implants.

Acknowledgments

The authors would like to thank Mr. Vincent Cuijpers and Mr. Jan Mulder for their kind assistance in micro-CT 3D image reconstructions and statistical analyses, respectively.

CALCIUM PHOSPHATE CERAMICS FOR BONE REGENERATION

This research forms part of the Project P2.04 BONE-IP of the research program of the BioMedical Materials institute, co-funded by the Dutch Ministry of Economic Affairs, Agriculture and Innovation.

References

1. Dorozhkin SV, Epple M. *Biological and medical significance of calcium phosphates. Angew Chem Int Ed Engl* 2002;41(17):3130-46.
2. Dorozhkin SV. *Biphasic, triphasic and multiphasic calcium orthophosphates. Acta Biomaterialia* 2012;8(3):963-977.
3. Surmenev RA. *A review of plasma-assisted methods for calcium phosphate-based coatings fabrication. Surface and Coatings Technology* 2012;206(8–9):2035-2056.
4. Yuan H, Fernandes H, Habibovic P, de Boer J, Barradas AM, de Ruiter A, Walsh WR, van Blitterswijk CA, de Bruijn JD. *Osteoinductive ceramics as a synthetic alternative to autologous bone grafting. Proc Natl Acad Sci U S A* 2010;107(31):13614-9.
5. Shadanbaz S, Dias GJ. *Calcium phosphate coatings on magnesium alloys for biomedical applications: A review. Acta Biomaterialia* 2012;8(1):20-30.
6. Kim KH, Ramaswamy N. *Electrochemical surface modification of titanium in dentistry. Dent Mater J* 2009;28(1):20-36.
7. Voigt JD, Mosier M. *Hydroxyapatite (HA) coating appears to be of benefit for implant durability of tibial components in primary total knee arthroplasty. Acta Orthop* 2011;82(4):448-59.

CALCIUM PHOSPHATE CERAMICS FOR BONE REGENERATION

8. Singh TP, Singh H, Singh H. Characterization of thermal sprayed hydroxyapatite coatings on some biomedical implant materials. *J Appl Biomater Funct Mater* 2012;0.
9. Suarez-Gonzalez D, Lee JS, Lan Levengood SK, Vanderby R, Jr., Murphy WL. Mineral coatings modulate beta-TCP stability and enable growth factor binding and release. *Acta Biomater* 2012;8(3):1117-24.
10. Roy M, Bandyopadhyay A, Bose S. In vitro antimicrobial and biological properties of laser assisted tricalcium phosphate coating. *Mater Sci Eng C Mater Biol Appl* 2009;29(6):1965-1968.
11. Tang R, Wu W, Haas M, Nancollas GH. Kinetics of Dissolution of β -Tricalcium Phosphate. *Langmuir* 2001;17(11):3480-3485.
12. Moseke C, Gbureck U. Tetracalcium phosphate: Synthesis, properties and biomedical applications. *Acta Biomater* 2010;6(10):3815-23.
13. de Bruijn JD, Bovell YP, van Blitterswijk CA. Structural arrangements at the interface between plasma sprayed calcium phosphates and bone. *Biomaterials* 1994;15(7):543-50.
14. Klein CP, Patka P, Wolke JG, de Blicck-Hogervorst JM, de Groot K. Long-term in vivo study of plasma-sprayed coatings on titanium alloys of tetracalcium phosphate, hydroxyapatite and alpha-tricalcium phosphate. *Biomaterials* 1994;15(2):146-50.
15. de Groot K, Geesink R, Klein CP, Serekian P. Plasma sprayed coatings of hydroxylapatite. *J Biomed Mater Res* 1987;21(12):1375-81.

16. Sun L, Berndt CC, Gross KA, Kucuk A. *Material fundamentals and clinical performance of plasma-sprayed hydroxyapatite coatings: a review. J Biomed Mater Res* 2001;58(5):570-92.
17. Kurzweg H, Heimann RB, Troczynski T, Wayman ML. *Development of plasma-sprayed bioceramic coatings with bond coats based on titania and zirconia. Biomaterials* 1998;19(16):1507-11.
18. Wolke JG, van Dijk K, Schaeken HG, de Groot K, Jansen JA. *Study of the surface characteristics of magnetron-sputter calcium phosphate coatings. J Biomed Mater Res* 1994;28(12):1477-84.
19. Ozeki K, Fukui Y, Aoki H. *Influence of the calcium phosphate content of the target on the phase composition and deposition rate of sputtered films. Applied Surface Science* 2007;253(11):5040-5044.
20. Jansen JA, Wolke JG, Swann S, Van der Waerden JP, de Groot K. *Application of magnetron sputtering for producing ceramic coatings on implant materials. Clin Oral Implants Res* 1993;4(1):28-34.
21. Shi JZ, Chen CZ, Yu HJ, Zhang SJ. *Application of magnetron sputtering for producing bioactive ceramic coatings on implant materials. Bulletin of Materials Science* 2008;31(6):877-884.
22. Yoshinari M, Hayakawa T, Wolke JG, Nemoto K, Jansen JA. *Influence of rapid heating with infrared radiation on RF magnetron-sputtered calcium phosphate coatings. J Biomed Mater Res* 1997;37(1):60-7.
23. Kokubo T, Takadama H. *How useful is SBF in predicting in vivo bone bioactivity? Biomaterials* 2006;27(15):2907-2915.

CALCIUM PHOSPHATE CERAMICS FOR BONE REGENERATION

24. *van der Lubbe HB, Klein CP, de Groot K. A simple method for preparing thin (10 microM) histological sections of undecalcified plastic embedded bone with implants. Stain Technol 1988;63(3):171-6.*
25. *Piattelli A, Trisi P, Passi P, Piattelli M, Cordioli GP. Histochemical and confocal laser scanning microscopy study of the bone-titanium interface: an experimental study in rabbits. Biomaterials 1994;15(3):194-200.*
26. *Thian ES, Huang J, Best SM, Barber ZH, Bonfield W. Silicon-substituted hydroxyapatite thin films: effect of annealing temperature on coating stability and bioactivity. J Biomed Mater Res A 2006;78(1):121-8.*
27. *Yang Y, Agrawal CM, Kim KH, Martin H, Schulz K, Bumgardner ID, Ong JL. Characterization and dissolution behavior of sputtered calcium phosphate coatings after different postdeposition heat treatment temperatures. J Oral Implantol 2003;29(6):270-7.*
28. *Yang Y, Kim KH, Mauli Agrawal C, Ong JL. Effect of post-deposition heating temperature and the presence of water vapor during heat treatment on crystallinity of calcium phosphate coatings. Biomaterials 2003;24(28):5131-7.*
29. *Toque JA, Hamdi M, Ide-Ektessabi A, Sopyan I. Effect of the precrossing parameters on the integrity of calcium phosphate coatings*

- produced by RF-magnetron sputtering. *International Journal of Modern Physics B* 2009;23(31):5811-5818.
30. Ievlev VM, Kostyuchenko AV, Belonogov EK, Barinov SM. Hardness and the nature of microplasticity of hydroxyapatite. *Inorganic Materials* 2013;49(4):416-422.
 31. Feddes B, Wolke JG, Vredenberg AM, Jansen JA. Initial deposition of calcium phosphate ceramic on polyethylene and polydimethylsiloxane by rf magnetron sputtering deposition: the interface chemistry. *Biomaterials* 2004;25(4):633-9.
 32. Wolke JG, de Groot K, Jansen JA. Subperiosteal implantation of various RF magnetron sputtered Ca-P coatings in goats. *J Biomed Mater Res* 1998;43(3):270-6.
 33. Kim H, Camata RP, Vohra YK, Lacefield WR. Control of phase composition in hydroxyapatite/tetracalcium phosphate biphasic thin coatings for biomedical applications. *J Mater Sci Mater Med* 2005;16(10):961-6.
 34. Klein CP, de Bleeck-Hogervorst JM, Wolke JG, de Groot K. Studies of the solubility of different calcium phosphate ceramic particles in vitro. *Biomaterials* 1990;11(7):509-12.
 35. Lu X, Leng Y. Theoretical analysis of calcium phosphate precipitation in simulated body fluid. *Biomaterials* 2005;26(10):1097-108.
 36. Hulshoff JE, van Dijk K, van der Waerden JP, Wolke JG, Kalk W, Jansen JA. Evaluation of plasma-spray and magnetron-sputter Ca-P-

CALCIUM PHOSPHATE CERAMICS FOR BONE REGENERATION

- coated implants: an in vivo experiment using rabbits. J Biomed Mater Res 1996;31(3):329-37.*
37. Mohammadi S, Esposito M, Hall J, Emanuelsson L, Krozer A, Thomsen P. Short-term bone response to titanium implants coated with thin radiofrequent magnetron-sputtered hydroxyapatite in rabbits. *Clin Implant Dent Relat Res* 2003;5(4):241-53.
38. Kyosuke Ueda YK, Takayuki Narushima, Takashi Goto, Jun Kurihara, Hironobu Nakagawa, Hiroshi Kawamura and Masayuki Taira. Calcium Phosphate Films with/without Heat Treatments Fabricated Using RF Magnetron Sputtering. *Journal of Biomechanical Science and Engineering* 2009.
39. Vercaigne S, Wolke JG, Naert I, Jansen JA. A histological evaluation of TiO₂-gritblasted and Ca-P magnetron sputter coated implants placed into the trabecular bone of the goat: Part 2. *Clin Oral Implants Res* 2000;11(4):314-24.
40. Hulshoff JE, Jansen JA. Initial interfacial healing events around calcium phosphate (Ca-P) coated oral implants. *Clin Oral Implants Res* 1997;8(5):393-400.
41. Ueda K, Narushima T, Goto T, Taira M, Katsube T. Fabrication of calcium phosphate films for coating on titanium substrates heated up to 773 K by RF magnetron sputtering and their evaluations. *Biomed Mater* 2007;2(3):S160-6.

42. Ong JL, Bessho K, Cavin R, Carnes DL. Bone response to radio frequency sputtered calcium phosphate implants and titanium implants in vivo. *J Biomed Mater Res* 2002;59(1):184-90.
43. Ozeki K, Yuhta T, Aoki H, Nishimura I, Fukui Y. Push-out strength of hydroxyapatite coated by sputtering technique in bone. *Biomed Mater Eng* 2001;11(1):63-8.
44. Kyosuke Ueda TN, Takashi Goto, Tomoyuki Katsube,, Hironobu Nakagawa HKaMT. Evaluation of Calcium Phosphate Coating Films on Titanium Fabricated Using RF Magnetron Sputtering. *Materials Transactions* 2007;48:307 to 312.
45. Alghamdi HS, Bosco R, van den Beucken JJ, Walboomers XF, Jansen JA. Osteogenicity of titanium implants coated with calcium phosphate or collagen type-I in osteoporotic rats. *Biomaterials* 2013;34(15):3747-57.
46. Fugl A, Ulm C, Tangl S, Vasak C, Gruber R, Watzek G. Long-term effects of magnetron-sputtered calcium phosphate coating on osseointegration of dental implants in non-human primates. *Clin Oral Implants Res* 2009;20(2):183-8.
47. Ripamonti U, Roden LC, Renton LF. Osteoinductive hydroxyapatite-coated titanium implants. *Biomaterials* 2012;33(15):3813-3823.

CALCIUM PHOSPHATE CERAMICS FOR BONE REGENERATION

4

RESIDUAL STRESS EVALUATION WITHIN HYDROXYAPATITE COATINGS OF DIFFERENT MICROMETER THICKNESSES

1. Introduction

Calcium phosphate (CaP) ceramic materials have large compositional similarity to the bone mineral phase and are known to allow direct physicochemical bonding with bone and to enhance bone tissue formation [1]. In view of their favorable biological performance, CaP ceramics are used as coatings on mechanically strong bioinert or biotolerant implants for load bearing applications (e.g. metallic joint prostheses and dental implants). Hydroxyapatite (HA; $\text{Ca}_{10}(\text{PO}_4)_6(\text{OH})_2$) is the main CaP crystal used for surface-engineering in the form of a coating on metallic implants due to its low solubility in combination with the aforementioned biological properties [2-4].

The CaP ceramic itself as well as the coating deposition process strongly determine the coating properties [5-8]. Plasma-spraying is the most commonly used technique for the deposition of CaP ceramic coatings [9, 10]. Despite the simplicity and versatility of plasma-spray deposition, its poor control over physicochemical parameters, lack of coating thickness uniformity, and poor coating adhesion [10-12] have limited its range of applications. Consequently, alternative coating deposition methods have been explored.

Radio frequency (RF) magnetron sputtering is an alternative coating deposition technique, which can generate dense, uniform, and well-adherent coatings on different substrate materials [13, 14]. For the deposition of CaP-coatings, RF magnetron sputtering is based on the bombardment of a CaP target material with high energetic ions (accelerated by high voltage from an RF

source). Subsequently, atoms or small clusters of atoms of the CaP target material are ejected at a very high speed toward the substrate surface depositing a thin coating that is chemically bonded with the substrate [15]. The formation of the coating starts when arriving atoms and/or clusters diffuse across the surface, resulting in the formation of a continuously growing film with time on the substrate surface. Furthermore, RF magnetron sputtering provides strong CaP coating adhesion and control over coating thickness, composition, and, to some extent, coating structure.

In view of the mismatch between material properties of the substrate versus coating, deposited CaP coatings usually show residual stress [16-18]. Residual stress may increase severely with increase in coating thickness. From an application perspective, high residual stress is related to increased dissolution, promotion of peeling or flaking of the coating, and reduced adhesive properties, all of which compromises long-term durability and reliability of HA coatings [19, 20]. In order to achieve high coating integrity, the residual stress should be controlled with processing methods such as heat treatment.

This study aimed to evaluate the residual stress within an HA-coating deposited using RF magnetron sputtering via two different analyses, based on either the Stoney formula (i.e. based on curvature measurements of the substrate [21]) or the $\sin^2 \psi$ method (i.e. based on X-ray diffraction patterns of the coating [22]). Additionally, the effect of HA-coating thickness (i.e. 1 or 4 μm) on residual stress and surface topography were addressed. We

CALCIUM PHOSPHATE CERAMICS FOR BONE REGENERATION

hypothesized that (i) both methods to determine residual stress would show similar results, and that (ii) thick coatings would increase residual stress compared to thin coatings.

2. Materials and Methods

2.1. Materials

Silicon wafers (100) with 75 mm diameter were used as substrates for coating deposition; prior to deposition, silicon wafers were ultrasonically cleaned in acetone and ethanol.

The target material used in the deposition process was hydroxyapatite (HA; $\text{Ca}_{10}(\text{PO}_4)_6(\text{OH})_2$) granulate with a diameter of 0.5-1.0 mm (CAMCERAM[®], CAM Bioceramics, Leiden, The Netherlands).

2.2. Coating deposition technique

Coatings were deposited using a commercially available RF magnetron sputter system (Edwards High Vacuum ESM 100 system, Crawford, England) [13, 15]. Wafers were mounted on a rotating and water cooled substrate holder. The distance between target and wafers was 80 mm. During deposition, argon pressure was kept at 5×10^{-3} mbar and a sputter power of 400 W was used. Coatings with two thicknesses were prepared, i.e. 1 and 4 μm thickness. The as-deposited coating thickness was confirmed using strips cut from a silicon wafer

into pieces of 1 cm² and placed right next to the wafers and analyzed with a Universal Surface Tester (UST, Innowep[®], Würzburg, Germany).

After deposition, all coated wafers were subjected to an additional heat treatment for 2 hours at 650 °C at a temperature ramp of 100 °C per hour (Quad Ellipse Chamber, Model E4- 10-P, Research Inc, Minnesota, United States).

2.3. X-ray diffraction

The crystallographic structure of the HA target material was determined by X-ray diffraction (XRD, Philips, PW3710, Eindhoven, The Netherlands) using CuK α -radiation (PW 3710, 40 kV, 30 mA), the diffraction scans were recorded between 20-36° 2 θ with a step size of 0.02° 2 θ and a sample time of 2 s/step. The deposited coatings were analyzed by fixing the coated substrates at a position of 2.5° and scanning the detector between 20-70° 2 θ with a step size of 0.02° 2 θ and a sample time of 2 s/step.

2.4. Atomic force microscopy

Surface topography and surface roughness measurement of the coatings were examined using Atomic Force Spectroscopy (AFM, Nanoscope IIIa, Bruker, Santa Barbara, CA, USA). The silicon wafers were scanned under ambient conditions and the AFM probe (RTESPA, Bruker) was made out of phosphorus doped Si and the tip had a pyramidal geometry with an end radius of 8 nm. The cantilever had a spring constant of 40 Nm⁻¹ and a resonant

CALCIUM PHOSPHATE CERAMICS FOR BONE REGENERATION

frequency of 338 KHz. The topographic measurements were done in tapping mode at three different locations for each sample. Nanoscope analysis software (version 1.4, Bruker) was used to analyze the root mean square surface roughness (R_q) and the arithmetic average roughness (R_a) values of the deposited coatings. The average roughness measurements were based on $3\mu\text{m} \times 3\mu\text{m}$ AFM images of the nanostructure CaP coatings.

2.5. Stress measurements

2.5.1. Substrate curvature technique

The stress of the CaP coatings was evaluated by a substrate curvature technique; a detailed description of the apparatus used for this study is contained in a previous publication [23, 24].

In summary, the technique is based on observations made from wafer curvature radii measurements using two-laser beam setup. From this information the wafer curvature shift ($1/R$) can be calculated. Substrate curvature measurements were determined before coating deposition, as-deposited and after heat treatment for $n=3$ substrates; these measurements showed the change of curvature of the wafer due stress in the coating. Subsequently, the average residual stress σ through the entire coating thickness was calculated using Stoney's formula:

$$\sigma = \frac{1}{6R} \frac{E}{(1-\nu)} \frac{D^2}{d}$$

where E is the Young modulus of the substrate, ν the Poisson's ratio for the substrate, D the substrate thickness, d the coating thickness (assuming that $d < D$) and R the radius of curvature of the initial flat substrate after deposition of the coating [for Silicon (100) $E/(1-\nu)$ equals 180.5 GPa].

2.5.2. X-ray diffraction stress analysis

In addition to substrate curvature measurements, the residual stress of the CaP deposited coatings was analyzed by the X-ray diffraction method. A Philips diffractometer with Cu $K\alpha$ radiation, angle of incidence $\theta = 0.25^\circ$ and a scan of $2\theta = 20-70^\circ$ was used to obtain the XRD patterns. An internal standard of silicon powder was dispersed onto the sputtered films to correct the observed diffraction angles for errors caused by small sample displacement.

Residual stress was determined by measuring the interplanar spacing (d_{obs}), which is the distance between two parallel planes of atoms in a crystalline material, of a given reflection along several different directions in the sample. Knowing the unstressed interplanar spacing (d_0) of the CaP powders, the measured lattice spacing can be converted to strain components in the coating and the stress can be calculated. A modification of the $\sin 2\Phi$ method [25], assuming a Poisson ratio (ν) of 1/3 gives the $\cos 2\Phi$ method were a suitable value for the Young's modulus (E) was assumed. The results are

CALCIUM PHOSPHATE CERAMICS FOR BONE REGENERATION

shown as a straight line fitted to the lattice strain $(d_{\text{obs}}-d_0)/d_0$ data points plotted as a function of $\cos 2\Phi$.

2.6. Statistical analysis

All statistical analyses were performed with GraphPad Instat[®] 3.05 software (GraphPad Software Inc, San Diego, CA, USA), using Student's t-tests. Results were considered significant at $p < 0.05$.

3. Results

3.1. CaP target material

The XRD pattern of the commercial HA powder is shown in **Figure 1**. Minimal line broadening was observed with the four largest crystal planes in the XRD pattern for the 002, 211, 112 and 300 reflections corresponding to 25.99° , 31.89° , 32.29° and 33.03° 2θ , respectively. This diffractogram fully matched with the diffraction data of standard synthetic hydroxyapatite reported in the International Centre for Diffraction Data (ICDD), file 24-0033 (HA).

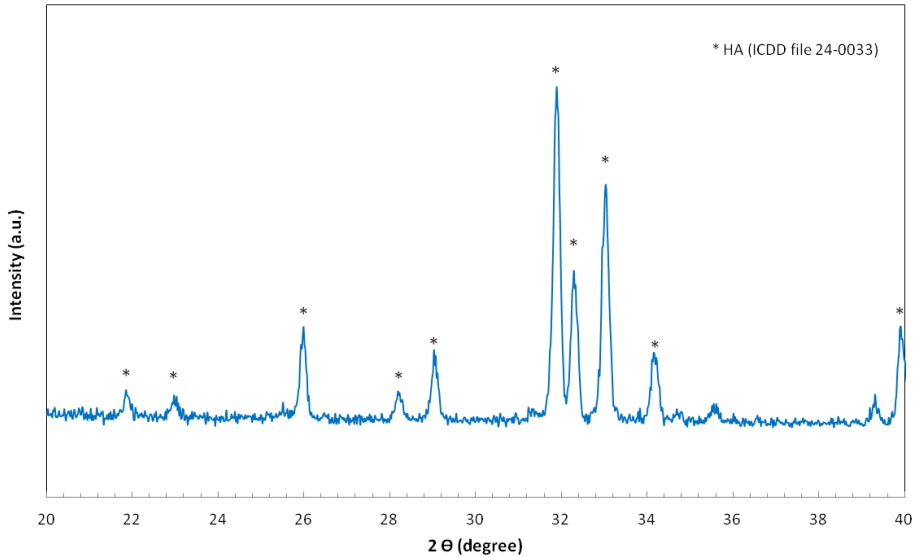


Figure 1. Diffraction pattern obtained using XRD for HA target material.

3.2. CaP coatings structural and morphological characteristics

XRD patterns of the as-deposited CaP coatings showed a crystalline structure with a preferred (002) crystallographic orientation, showing reflections peaks of 002, 102, 112 and 202 corresponding to 25.73°, 28.04°, 31.93° and 33.83° 2θ , respectively (**Figure 2**; insert). Heat treatment at 650 °C hardly altered the crystallographic structure with the main reflection peaks at 25.87°, 32.14° and 34.00° (**Figure 2**). With increasing coating thickness, higher relative peak intensities of the main diffraction peaks were observed.

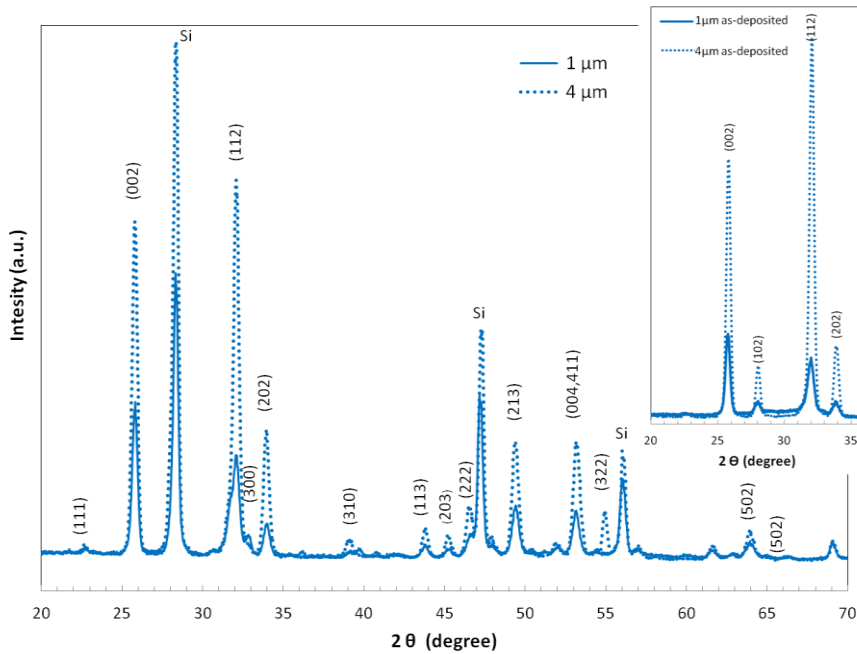


Figure 2. XRD pattern of the as-deposited (insert) and heat treated HA coatings, with 1 and 4 μm thicknesses.

Atomic force microscopy (AFM) was used to analyze surface morphology and surface roughness of the HA coatings. AFM results (**Figure 3**) showed that the surface morphology of HA coatings was different for coatings with different thicknesses. Thin 1 μm coatings presented a surface morphology characterized by relatively large globular elevations (~2-4 μm diameter) with a μm-scale spacing, whereas thick 4 μm coatings presented substantially smaller and sharper elevation (sub-μm scale) with sub-μm scale spacing. The roughness of both HA coatings (**Table 1**) was in the nm-scale with Rq-values of 64.4 and 32.2 nm, and Ra-values of 52.1 and 26.6 nm for coatings with a thickness of 1 μm and 4 μm coatings, respectively.

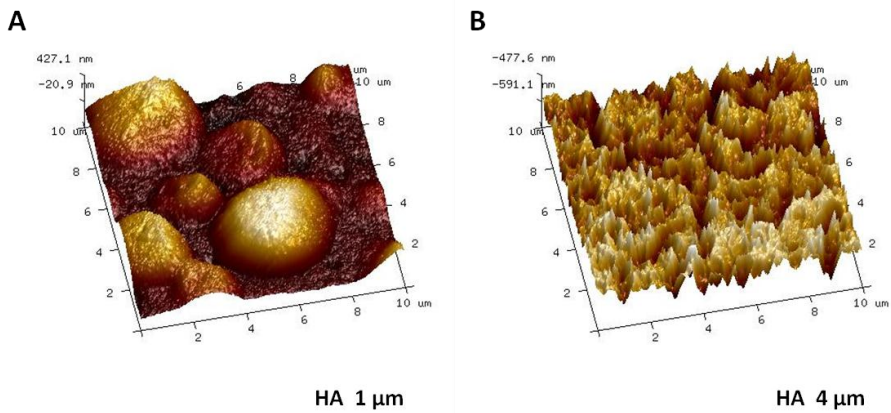


Figure 3. Reconstructed 3-dimensional AFM images of HA coatings with a thickness of (A) 1 μm and (B) 4 μm after heat treatment at 650 $^{\circ}\text{C}$.

Material	Area	Thickness (μm)	Rq* (nm)	Ra** (nm)
HA	3 x 3 μm	1	64.4 \pm 22	52.1 \pm 34
		4	32.2 \pm 4	26.6 \pm 3

*root mean square roughness

**arithmetic average roughness

Table 1. Surface roughness data measured by atomic force microscopy over a fixed scan area of 3 x 3 μm for the HA coatings after heat treatment at 650 $^{\circ}\text{C}$.

3.3. Residual stress measurements

Substrate curvature measurements were used to evaluate residual stress of the HA coatings after deposition and after heat treatment (**Figure 4**). Tensile stress was observed for the 1 μm as-deposited HA coating (76.5 \pm 8.4 MPa),

CALCIUM PHOSPHATE CERAMICS FOR BONE REGENERATION

whereas for 4 μm thick as-deposited HA coating the residual stress was compressive (-63.4 ± 6.3 MPa). Heat treated HA coatings of either 1 or 4 μm thickness both showed a tensile residual stress (i.e. 65.2 ± 5.4 MPa, 14.0 ± 10.3 MPa, respectively).

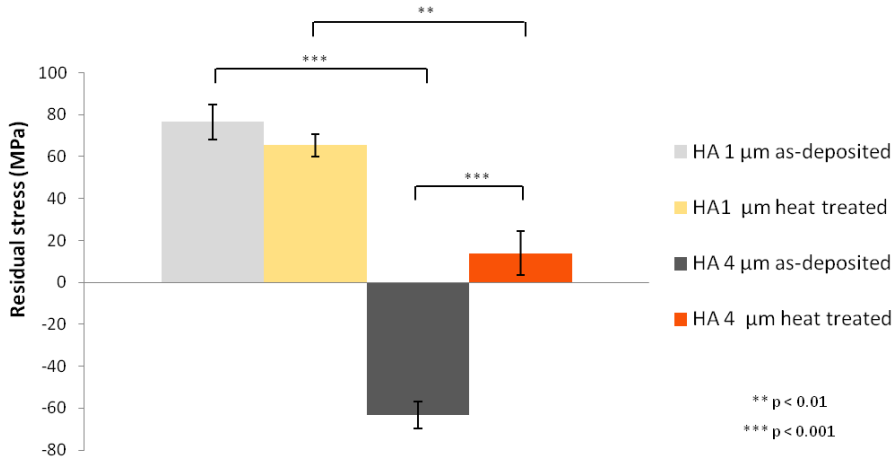


Figure 4. Residual stress for as-deposited and heat treated 1 and 4 μm HA coatings. Data represent mean \pm SD ($n=3$). Statistically significant differences (Student's *t*-test) are indicated (asterisks represent significance levels; ** $p < 0.01$, *** $p < 0.001$).

As an alternative, residual stress was determined using X-ray diffraction data using $(d_{\text{obs}}-d_0)/d_0$ vs. $\cos 2\Phi$ for the HA coatings with 1 and 4 μm thickness (**Figure 5**). The fit of the reflection data demonstrated the presence of compressive stress for as-sputtered HA coatings of both 1 and 4 μm . After heat treatment, the fit showed a decrease in compressive residual stress for HA coatings of both 1 and 4 μm .

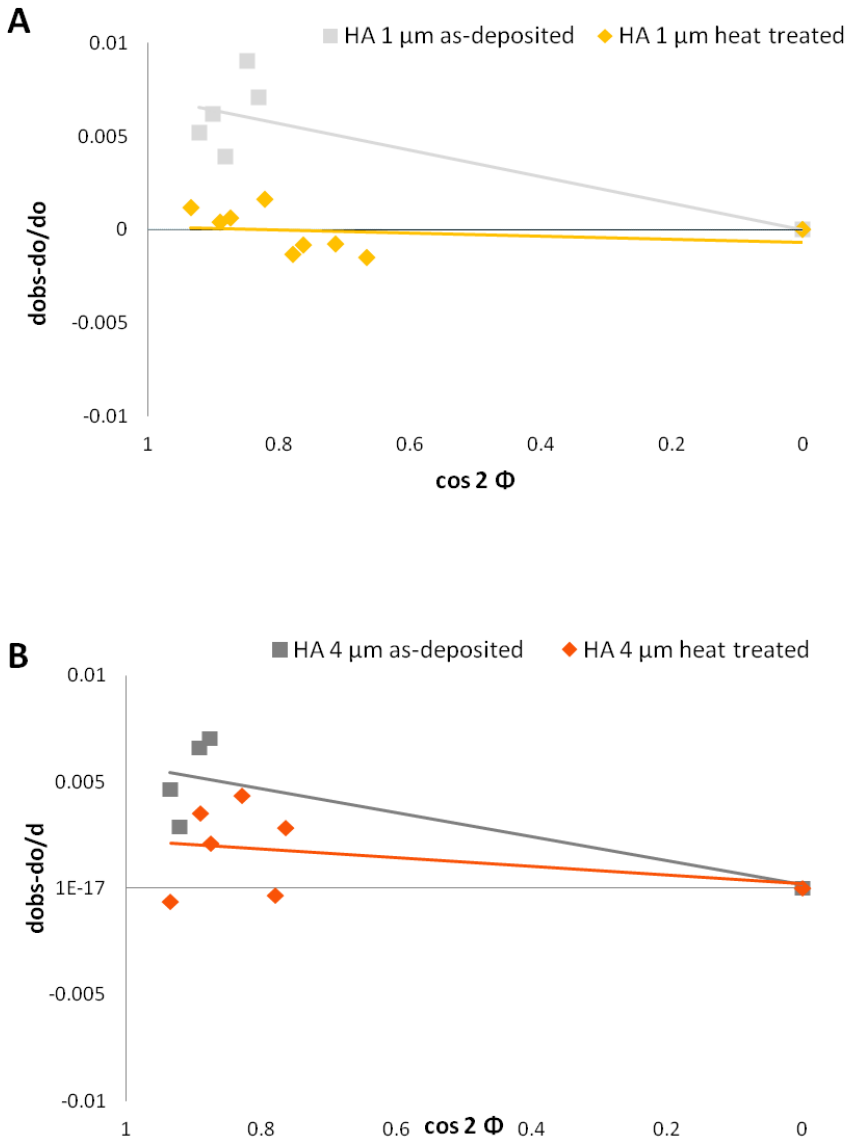


Figure 5. Plot of $(d_{obs}-d_o)/d_o$ as a function of $\cos^2 \Phi$ for the deposited HA coatings and after heat treatments at 650°C. A) HA-coating with 1 μm thickness, B) HA-coating with 4 μm thickness.

4. Discussion

The aim of this study was to evaluate the residual stress within an HA-coating deposited using RF magnetron sputtering via two different analyses, based on either curvature measurements of the substrate or alterations in the X-ray diffraction patterns of the coating. Additionally, the effect of HA-coating thickness (i.e. 1 or 4 μm) on residual stress and surface topography were addressed. We hypothesized that: (i) both methods to determine residual stress would show similar results, and (ii) thick coatings would increase residual stress compared to thin coatings. The main findings showed agreement of both residual stress measurement methods on the relaxation effect of heat treatment on residual stress for HA coatings. However, controversial results were obtained for as-deposited and heat treated HA coatings, for which residual stress determined via diffraction pattern alterations showed compressive residual stress for all coatings, whereas curvature measurements indicated tensile residual stress for all but the as-deposited 4 μm thick HA coating.

Techniques to determine residual stress within coatings can be categorized into techniques based on (i) curvature measurements, (ii) crystallographic lattice parameters, and (iii) strain measurements after layer removal [22]. Evidently, all of these different techniques have their specific pros and cons. In terms of accuracy, lattice-based and layer removal techniques are generally considered superior to substrate curvature measurement techniques. Other differences relate to sample preparation and instrumentation, for which

accounts that time consumption and costs vary considerably for different techniques. For reasons of accuracy and availability, this study utilized a curvature measurement technique and a lattice-based technique. In view of the former, it is imperative to realize that the measurement is based on the distribution and magnitude of stresses within the coating-substrate couple, whereas the latter depends fully on the crystallographic characteristics of only the coating. Additionally, it needs to be emphasized that total stress within a coatings is the result of three separate contributing factors: external stress (due to potential external loading), thermally-induced stress (due to a mismatch in thermal expansion coefficients of substrate and coating material), and intrinsic stress (related to coating microstructure and the coating growth process) [26].

The build-up of a polycrystalline coating is known to be accompanied by different stages of stress within this coating [27]. Although this study did not utilize continuous *in situ* measurements for residual stress analysis, the differences in residual stress for HA coatings with a thickness of 1 and 4 μm clearly showed an effect of coating thickness on the type and magnitude of residual stress. Expectedly, residual stress analysis based on curvature measurements showed the largest differences related to thickness, with tensile residual stress for 1 μm as-deposited HA coatings and compressive residual stress for 4 μm as-deposited HA coatings. This difference can be explained by the differences in the increased sputtering time and the consequent increase of the bombardment of argon- and calcium phosphate ions on the growing HA film. This effect is known as ion shot peening, which induces defects, leading

CALCIUM PHOSPHATE CERAMICS FOR BONE REGENERATION

to large compressive stresses [28, 29]. Remarkably, lattice-based determination of residual stress showed compressive residual stress for as-deposited HA coatings, irrespective of coating thickness. Although the nature of this discrepancy remains unclear, a likely explanation is the setup of the X-ray diffraction method with an angle of incidence of 2.5° . This low angle results in a precise analysis of the top-layer of the deposited HA coating, without measuring the substrate underneath. Consequently, the residual stress will be influenced by the contribution of above mentioned ion shot peening effect of the HA film and result in a different outcome compared to the curvature measurement. Further, our residual stress measurements showed values between 80 to -60 MPa, which can be considered as low values.

As RF magnetron sputter deposition of HA coatings is performed at relatively low temperatures (i.e. $<150^\circ\text{C}$), the normal procedure for HA coatings deposited using RF magnetron sputtering is to utilize heat treatment for post-deposition annealing [30, 31]. The use of silicon wafers apparently makes that already as-deposited HA coatings have a highly crystalline lattice structure, whereas as-deposited HA coatings on titanium substrates generally show an amorphous apatitic structure. This difference is likely explained by differences in the thermal conductivity (λ , in $\text{W}\cdot\text{m}^{-1}\cdot\text{K}^{-1}$) of substrate materials and their thickness (silicon substrate, $\lambda = 149 \text{ W}\cdot\text{m}^{-1}\cdot\text{K}^{-1}$, thickness = 0.36 mm; titanium substrate, $\lambda = 21.9 \text{ W}\cdot\text{m}^{-1}\cdot\text{K}^{-1}$, thickness = 2 mm). Still, to comply with the regular procedure for HA coatings aimed for biomedical application, this study included a heat treatment at 650°C . The effect of this (integral) heat

treatment induced relaxation of the residual stress within the coatings, for which substrate curvature measurement and lattice-based techniques to determine residual stress showed consistency. Additionally, our observations corroborate previously reported data on residual stress within HA coatings deposited using RF magnetron sputtering and the decreasing effects of heat treatment on this residual stress [32].

Surface morphology was clearly influenced by HA coating thickness, as an obvious change in surface morphology was observed with increasing coating thickness. These differences in surface morphology were demonstrated by a higher surface roughness for 1 μm HA coatings compared to 4 μm HA coatings. The presence of large globular particles on the 1 μm HA coating surface could be due to collision by high energy ions and melting of clusters or aggregates instead of atoms from the powder material to the silicon wafer. With an increase in coating thickness, and therefore sputtering time, the particles deposited would have more time to grow, coalesce, and become sharper producing a more homogeneous coating. In view of the already crystalline nature of as-deposited HA coatings on the silicon wafer, this increased exposure to peri-annealing temperatures might alter surface morphology toward smaller elevations at regular intervals, as was observed previously by Ong and co-workers [16].

From a translational perspective with in mind the biomedical application of 3-dimensionally HA coated bone implants, several issues related to coating adhesion and residual stress are important. Firstly, the deposition of HA

CALCIUM PHOSPHATE CERAMICS FOR BONE REGENERATION

coatings on extremely smooth silicon wafers is incomparable and adhesive properties thereof are completely different for deposition on rough, grit-blasted titanium implants. Aside from the difference in thermal expansion coefficient (α) for both substrate materials (silicon, $\alpha = 2.6 \times 10^{-6} \text{ K}^{-1}$; titanium, $\alpha = 8.6 \times 10^{-6} \text{ K}^{-1}$) compared to HA ($\alpha = 17.1 \times 10^{-6} \text{ K}^{-1}$), presenting a 6.6-fold mismatch for silicon versus a 2-fold mismatch for titanium, the effect of surface roughness might even be more pronounced. The stability of an HA coating within the body (or simulating environments) is known to be affected by intrinsic properties (e.g. crystallinity) [33], but also by external conditions including the presence of aqueous liquids [33] and loading [32]. An increased surface roughness (e.g. resulting from grit-blasting) will particularly benefit HA coating stability under the latter external conditions for reasons of increased interfacial surface area for interaction between substrate and coating as well as mechanical interlocking. Finally, the fact that heat treatment reduces the residual stress within HA coatings contributes to the prevention of potential chipping of or crack formation within the coating.

5. Conclusion

HA coatings deposited using RF magnetron sputtering show residual stress within the coating, which can be reduced by a post-deposition heat treatment. Coating thickness variation in the micrometer scale showed no major effects on residual stress magnitude. For reasons of accuracy and similarity to

the actual conditions, determination of residual stress via lattice-based techniques is preferable.

Acknowledgments

This research forms part of the Project P2.04 BONE-IP of the research program of the BioMedical Materials institute, co-funded by the Dutch Ministry of Economic Affairs, Agriculture and Innovation.

CALCIUM PHOSPHATE CERAMICS FOR BONE REGENERATION

References

1. R.Z. LeGeros, *Chemical reviews*, 108 (2008) 4742-4753.
2. L. Meirelles, A. Arvidsson, M. Andersson, P. Kjellin, T. Albrektsson, A. Wennerberg, *Journal of biomedical materials research. Part A*, 87 (2008) 299-307.
3. R.S. Faeda, R. Spin-Neto, E. Marcantonio, A.C. Guastaldi, E. Marcantonio. *Microscopy research and technique*, 75 (2012) 940-948.
4. T.G. Eom, G.R. Jeon, C.M. Jeong, Y.K. Kim, S.G. Kim, I.H. Cho, Y.S. Cho, J.S. Oh, *Oral surgery, oral medicine, oral pathology and oral radiology*, 114 (2012) 411-418.
5. J. Huang, S.N. Jayasinghe, S.M. Best, M.J. Edirisinghe, R.A. Brooks, N. Rushton, W. Bonfield, *Journal of materials science. Materials in medicine*, 16 (2005) 1137-1142.
6. N. Hijon, M. Victoria Cabanas, J. Pena, M. Vallet-Regi, *Acta biomaterialia*, 2 (2006) 567-574.
7. J.W. Hwang, E.U. Lee, J.S. Lee, U.W. Jung, I.S. Lee, S.H. Choi, *Journal of periodontal & implant science*, 43 (2013) 291-300.
8. A. Rabiei, B. Thomas, C. Jin, R. Narayan, J. Cuomo, Y. Yang, J.L. Ong, *Surface and Coatings Technology*, 200 (2006) 6111-6116.
9. P.S. Gomes, C. Botelho, M.A. Lopes, J.D. Santos, M.H. Fernandes, *Journal of biomedical materials research. Part B, Applied biomaterials*, 94 (2010) 337-346.

10. F.J. Xiao, L. Peng, Y. Zhang, L.J. Yun, *Journal of materials science. Materials in medicine*, 20 (2009) 1653-1658.
11. R.A. Surmenev, *Surface and Coatings Technology*, 206 (2012) 2035-2056.
12. L. Sun, C.C. Berndt, K.A. Gross, A. Kucuk, *Journal of biomedical materials research*, 58 (2001) 570-592.
13. J.G. Wolke, K. van Dijk, H.G. Schaeken, K. de Groot, J.A. Jansen, *Journal of biomedical materials research*, 28 (1994) 1477-1484.
14. B. Feddes, J.G. Wolke, A.M. Vredenberg, J.A. Jansen, *Biomaterials*, 25 (2004) 633-639.
15. J.A. Jansen, J.G. Wolke, S. Swann, J.P. Van der Waerden, K. de Groot, *Clinical oral implants research*, 4 (1993) 28-34.
16. Y. Yang, K.-H. Kim, J.L. Ong, *Biomaterials*, 26 (2005) 327-337.
17. D.J. Curran, T.J. Fleming, M.R. Towler, S. Hampshire, *Journal of materials science. Materials in medicine*, 21 (2010) 1109-1120.
18. B. Cofino, P. Fogarassy, P. Millet, A. Lodini, *Journal of biomedical materials research. Part A*, 70 (2004) 20-27.
19. Y. Han, K. Xu, J. Lu, *Journal of biomedical materials research*, 55 (2001) 596-602.
20. Y.C. Yang, E. Chang, *Biomaterials*, 22 (2001) 1827-1836.
21. G.G. Stoney, *The Tension of Metallic Films Deposited by Electrolysis*, 1909.

CALCIUM PHOSPHATE CERAMICS FOR BONE REGENERATION

22. T.C. Totemeier, J.K. Wright, *Surface and Coatings Technology*, 200 (2006) 3955-3962.
23. G.C.A.M. Janssen, *Thin Solid Films*, 515 (2007) 6654-6664.
24. G.C.A.M. Janssen, M.M. Abdalla, F. van Keulen, B.R. Pujada, B. van Venrooy, *Thin Solid Films*, 517 (2009) 1858-1867.
25. E.L. Haase, *The Determination of Lattice Parameters and Strains in Stressed Thin Films Using X-Ray Diffraction: Extensions*, in: J. Hašek (Ed.) *X-Ray and Neutron Structure Analysis in Materials Science*, Springer US, 1989, pp. 191-198.
26. I.A. Alhomoudi, G. Newaz, *Thin Solid Films*, 517 (2009) 4372-4378.
27. E. Chason, *Thin Solid Films*, 526 (2012) 1-14.
28. G.C.A.M. Janssen, J.D. Kamminga, *Applied Physics Letters*, 85 (2004) 3086-3088.
29. G.C.A.M. Janssen, F.D. Tichelaar, C.C.G. Visser, *Journal of Applied Physics*, 100 (2006) -.
30. K. van Dijk, H.G. Schaeken, J.G. Wolke, J.A. Jansen, *Biomaterials*, 17 (1996) 405-410.
31. Y. Yonggang, J.G. Wolke, L. Yubao, J.A. Jansen, *Journal of materials science. Materials in medicine*, 18 (2007) 1061-1069.
32. J.G. Wolke, J.P. van der Waerden, K. de Groot, J.A. Jansen, *Biomaterials*, 18 (1997) 483-488.
33. J.G. Wolke, K. de Groot, J.A. Jansen, *Journal of biomedical materials research*, 39 (1998) 524-530.

5

SUBSTRATE GEOMETRY DIRECTS THE IN VITRO MINERALIZATION OF CALCIUM PHOSPHATE CERAMICS

1. Introduction

Commonly employed biomaterials in bone tissue engineering and regenerative medicine include bioactive ceramics and glasses, natural and synthetic polymers and composites thereof [1]. In particular, calcium orthophosphates (CaPs) are the most widely investigated materials for the substitution of lost or damaged hard tissue due to their similarity to the inorganic phase of bone as well as excellent biocompatibility and bioactivity [2-4]. Noticeably, several CaPs recently were demonstrated to exhibit osteoinductive capacity, i.e. the ability to induce bone tissue formation at an ectopic location which in turn requires the differentiation of osteoprogenitor cells into bone-forming osteoblasts [5-7].

CaPs are available in a number of chemical compositions and crystalline phases, among which hydroxyapatite (HA), β -tricalcium phosphate (β -TCP) and biphasic HA/TCP ceramics are the most common for bone replacement. The bioactivity of these CaPs is strongly related to their solubility in the physiological environment, which increases with increasing amount of β -TCP (i.e. β -TCP > biphasic CaP > HA) [2]. In addition to compositional effects, surface morphologies have been shown to affect biological performance [8, 9]. It is now clear that micro- and nanoscale morphologies of the CaP surface can strongly influence osteoblast and stem cell adhesion, proliferation and differentiation [10-12]. During the last decades, Ripamonti and co-workers extensively investigated the osteogenic effect of repetitive

surface concavities on either bulk ceramics [13] or CaP-coated titanium implants [14]. The starting hypothesis for these studies was that concavities, by resembling the hemi-osteon trench observable at different stages of osteoclastogenesis, are able to initiate the ripple-like cascade of bone induction and morphogenesis [15]. Actually, Ripamonti and co-workers found that the presence of concavities (diameter 800-1600 μm , depth 400-800 μm) strongly affected the osteoinductive capacity, noteworthy without the need for exogenous osteogenic soluble molecules [13]. More recently, Scarano et al. showed that 500 x 500 μm hemi-spherical concavities prepared at the surface of CaP-coated titanium implants inserted into the tibia of rabbits, led to a significant increase in bone formation inside the concavities compared to the convex areas [16].

Despite this increasing number of *in vivo* studies demonstrating a positive effect of concavities on osteogenesis, no attempts have been carried out in order to rationalize the mineralization process through *in vitro* tests. Consequently, the aim of the current study was to evaluate the role of concavities on the *in vitro* mineralization of different bioceramic materials. To this end, HA and β -TCP disks sintered at 1100 $^{\circ}\text{C}$ or 1200 $^{\circ}\text{C}$ were prepared with concavities of hemi-spherical shape with different diameters. Mineralization at the surface of these bioceramic disks upon immersion in simulated body fluid (SBF) for up to 28 days was assessed by means of scanning electron microscopy (SEM), Energy Dispersive Spectroscopy (EDS), X-ray Diffraction (XRD) and calcium quantification assays. Our starting

CALCIUM PHOSPHATE CERAMICS FOR BONE REGENERATION

hypotheses were that (i) concavities prepared at the surface of bioceramic disks could effectively guide the surface mineralization process in vitro, and (ii) that concavity dimension represents a key parameter for controlling the extent of surface mineralization in vitro.

2. Materials and Methods

2.1 Fabrication of heat-treated calcium phosphate disks

Ceramic disks were prepared from hydroxyapatite (HA, Merck, Germany) or β -tricalcium phosphate (β -TCP, CAM Bioceramics BV, The Netherlands) powder source materials. Powders were uniaxially pressed at 103 MPa (15000 lb/psi) for 10 min in a cylindrical steel mold (internal diameter ~ 21 mm). Subsequently, cylindrical HA and β -TCP green ceramics were heat-treated in a furnace at 800°C for 6h (1.67°C/min) to provide suitable strength to the ceramic to withstand the stresses applied during the machining process. Subsequently, heat-treated HA and β -TCP cylinders were cut into disks (thickness ~4 mm, diameter ~21 mm).

2.2. Role of composition and sintering temperature on mineralization onset

For a preliminary evaluation of the role of chemical composition and sintering temperature on the onset of the mineralization process, drill tips with different diameter sizes (2.1, 1 and 0.5 mm, Horico, Germany) were used to prepare the hemi-spherical concavities (4 of each diameter) at the surface of

heat-treated HA and β -TCP disks (**Table 1** and **Figure 1a**) of the following diameters: 1.8 mm (large concavities), 0.8 mm (medium concavities) and 0.4 mm (small concavities). The center-to-center distance between similar concavities was set at twice the concavity diameter in order to display the maximum number of concavities on the same disk while minimizing possible mutual effects on the deposition of calcium phosphate. Subsequently, the disks were sintered in a furnace for 6h (1.67°C/min) at either 1100°C (HA11_LMS and TCP11_LMS; LMS: large, medium and small concavities) or 1200°C (HA12_LMS and TCP12_LMS). Freshly prepared, filter-sterilized simulated body fluid (SBF; pH 7.4, ionic composition: 142.0 mM Na⁺, 5.0 mM K⁺, 1.5 mM Mg²⁺, 2.5 mM Ca²⁺, 147.8 mM Cl⁻, 4.2 mM CO₃²⁻, 1.0 mM HPO₄²⁻ and 0.5 mM SO₄²⁻) was used to assess the surface mineralization capacity of the experimental CaP disks [17]. HA and β -TCP disks (n = 3 for each experimental group) were transferred into 6-well plates and immersed in SBF solution (10 ml/well) for 7, 14, 21 and 28 days. The plate was kept at 37 °C while shaking moderately (1 Hz). Additionally, controls (n = 3) consisting of empty wells filled with only SBF were used for each time point in order to detect any homogeneous nucleation in the solution or heterogeneous nucleation on the walls of well plates. The SBF was changed daily, and the supernatant was collected to determine calcium levels using the ortho-cresolphthalein complexone (OCPC, Sigma-Aldrich) method. To this end, 100 μ l of the supernatant was mixed with 100 μ l of 1N acetic acid (Boom BV, Meppel, The Netherlands) and incubated overnight on a shaking table. Calcium

CALCIUM PHOSPHATE CERAMICS FOR BONE REGENERATION

concentrations were calculated with respect to the controls (empty wells) and averaged for three samples per group. At 7, 14, 21 and 28 days, disks were removed from the SBF, gently washed with distilled water and dried at 40 °C for 24 hours.

Study	CaP ceramics investigated	Concavity dimension investigated	Nº of concavities on each disk	Distribution of concavities on each disk	Sintering T	Sample acronym
Role of chemical composition and sintering T on mineralization process	HA, β -TCP	Large (1.8 mm)	12	4L + 4M + 4S	1100 °C 1200 °C	HA11-LMS
		Medium (0.8 mm)				TCP11-LMS
		Small (0.4 mm)				HA12-LMS
						TCP12-LMS
Role of concavity size on mineralization process content	HA		12	12L or 12M or 12S	1200 °C	HA12-L HA12-M HA12-S

Table 1. Overview of the experimental setup

2.3. Role of concavity dimension on mineralization process

For the quantitative evaluation of the effect of concavity size on the mineralization process, a different surface geometry was adopted: 12 concavities of either 1.8 mm, 0.8 mm, or 0.4 mm in diameter were prepared onto the surface of HA green ceramic disks heat-treated at 800 °C (**Table 1** and **Figure 1b**). The center-to-center distance was set at 4 mm in order to maximize the distance between adjacent concavities. Finally, disks were sintered for 6h at 1200°C (1.67°C/min). For surface mineralization experiments, 2 HA12 disks containing 12 surface concavities of large (HA12_L), medium (HA12_M) or

small diameters (HA12_S) were immersed in SBF for 14 days according to the protocol as described above. Additionally, the disks were weighed before and at the end of the experiment, after being gently washed with distilled water and dried at 40 °C for 24 h.

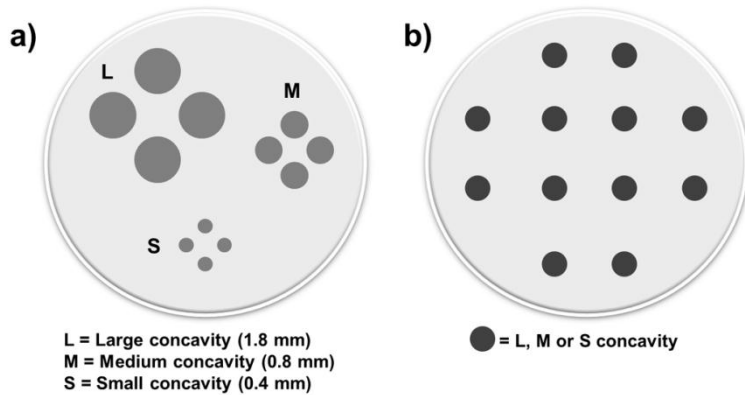


Figure 1. Schematic representation of disks surface geometry employed in the current study. (a) Schematic distribution of the concavities at the surface of the disks for the preliminary experiment on the effect of chemical composition and sintering temperature on the mineralization process *in vitro*. For each size, 4 concavities were prepared onto the surface of the disks: 1.8 mm (large concavity, L), 0.8 mm (medium concavity, M) and 0.4 mm (small concavity, S); the center to center distance was kept at twice the concavity diameter. (b) Scheme of the distribution of the concavities at the surface of the disks for the experiment on the effect of concavity size on mineralization process *in vitro*. Disks were machined with 12 concavities of the same size (L, M or S).

2.4 Disk characterization

The mineralization process on the surface of the CaP disks was followed through SEM, EDS and XRD analyses. Surface morphology and microstructure of the specimens were observed using a scanning electron microscope (JSM6310, JEOL, Japan operating at a accelerating voltage of 10

CALCIUM PHOSPHATE CERAMICS FOR BONE REGENERATION

kV and a current ~ 10 mA) after coating the samples with a thin gold layer (5-10 nm). The elemental analysis was carried out using a Scanning Electron Microscope (Philips XL30, the Netherlands) equipped with an Energy Dispersive Spectrometer (EDS, EDAX, AMETEK Materials Analysis Division, USA) at an accelerating voltage of 10 kV, a working distance of 10 mm and different magnifications. To improve the surface conductivity of the samples, a thin gold layer was deposited on the samples using a common sputtering instrument, which did not affect the measurement of the phosphorus content using EDS. The crystal phase composition of the specimens was characterized by means of a PW3710 X-Ray Diffractometer (Philips, The Netherlands, thin film configuration (fixed angle of incidence of 2.5 °), Cu K_α radiation, voltage 40 kV, current 30 mA, step-size 0.02° 2θ, scanning speed 0.005 ° 2θ/s and a sample time of 4s/step).

2.5 Statistical analysis

All quantitative data were expressed as mean ± SD and statistical analyses were performed with GraphPad® InStat 3.05 software (GraphPad Software Inc, San Diego, CA, USA), using one-way analysis of variance (ANOVA) with Tukey Kramer Multiple Comparison's post-hoc tests. Results were considered significant at $p < 0.05$.

3. Results

3.1 Role of chemical composition and sintering temperature

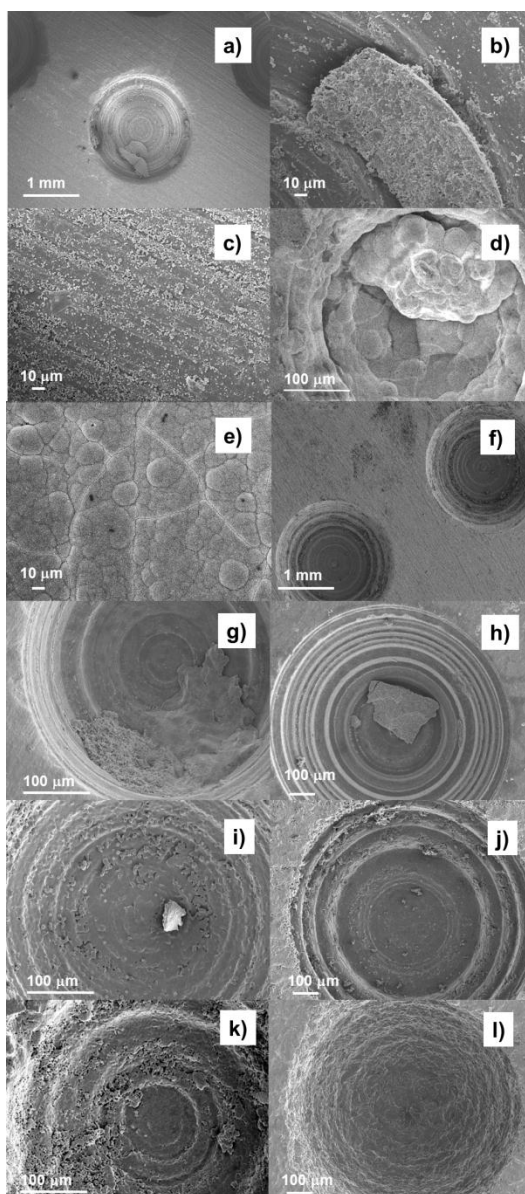
The effect of sintering temperature on crystallite size in base materials and sintered disks is presented in **Table 2**.

Material	Temperature (°C)	2 θ	Crystallite size (nm)
HA powder	-	25.888	44.3
β -TCP powder	-	25.822	46.6
HA	1100	25.920	140.6
HA	1200	25.885	151
β -TCP	1100	25.801	140.5
β -TCP	1200	25.856	262.9

Table 2. Crystallite size of the ceramics used, obtained via de Scherrer equation.

Initial evaluations focused on the effect of disk chemical composition and sintering temperature on the mineralization process in vitro. SEM images of the surface of HA and β -TCP disks containing four large, four medium and four small (LMS) concavities on their surface at different experimental time points are depicted in **Fig. 2**. After the first week of soaking in SBF, large CaP aggregates up to several hundred micrometers long were observed only within the concavities of HA12_LMS disks and not on the planar surface (**Fig. 2a** and **b**). In contrast, only small isolated CaP particles of about 1-5 μm were detected on the planar surface of HA12_LMS disks (outside concavities; **Fig. 2c**). From the second to the third week of immersion in SBF, a globular CaP layer was formed inside concavities (**Fig. 2d**), while the planar surface between HA12_LMS disks was homogeneously covered with CaP after three weeks of soaking (**Fig. 2e**), which finally dissolved during the fourth week (**Fig. 2f**).

Figure 2. SEM evaluation of the mineralization process on HA and β -TCP disks sintered at 1100 °C and 1200 °C at different experimental time points. (a) low magnification image of the surface of HA12_LMS after week 1 showing macroscopic CaP aggregates inside a large concavity; (b) detail of a CaP aggregate inside a large concavity of HA12_LMS after week 1; (c) planar surface between concavities at the surface of HA12_LMS after week 1; (d) small concavity at the surface of HA12_LMS completely filled by CaP between week 2 and 3; (e) planar surface between concavities at the surface of HA12_LMS after week 3; (f) low magnification image of the surface of HA12_LMS after week 4; (g) CaP aggregate inside small concavity at the surface of HA11_LMS after week 1; (h) CaP aggregate inside medium concavity at the surface of HA11_LMS after week 3; (i) small CaP aggregate inside small concavity at the surface of TCP12_LMS after week 1; (j) medium concavity surface of TCP12_LMS after week 3; (k) small concavity surface of TCP11_LMS after week 1; (l) medium concavity surface of TCP11_LMS after week 3.



Analysis of the HA11 samples revealed no formation of such globular layer, but only the presence of CaP aggregates inside large, medium and small concavities and not at the planar surface at any of the experimental time points (**Fig. 2g,h**). Less and smaller aggregates were found inside concavities of TCP12_LMS (**Fig. 2i,j**), whereas hardly any CaP aggregates were detected within the concavities of TCP11_LMS disks (**Fig. 2k,l**). Further, the surface of TCP11_LMS showed partial degradation after three weeks of soaking in SBF, as evidenced by the decreased intensity of machining features inside concavities, whereas the surface of TCP12_LMS was only slightly changed and the surfaces of HA11_LMS and HA12_LMS retained their original appearance.

Calcium quantification analysis revealed that all experimental disks induced calcium uptake during immersion in SBF (**Fig. 3**). Similar calcium uptake profiles were observed for TCP11_LMS and TCP12_LMS; a significantly ($p < 0.001$) higher calcium uptake was observed for HA11_LMS compared to the calcium uptake of the β -TCP disks, whereas the largest calcium uptake was observed for HA12_LMS. From the second week onward, a significant difference ($p < 0.001$) between the calcium uptake of HA12_LMS and HA11_LMS was observed. The final cumulative calcium uptake for HA12_LMS was 2-fold higher compared to the uptake for HA11_LMS and 4.6- and 5.4-fold higher compared to the uptake for TCP12_LMS and TCP11_LMS ($p < 0.001$). Due to the observed superior ability to induce surface mineralization for HA12_LMS, further studies were carried out using

CALCIUM PHOSPHATE CERAMICS FOR BONE REGENERATION

HA12_LMS disks in order to rationalize the mineralization process and the effect of concavity size on CaP mineralization at the surface.

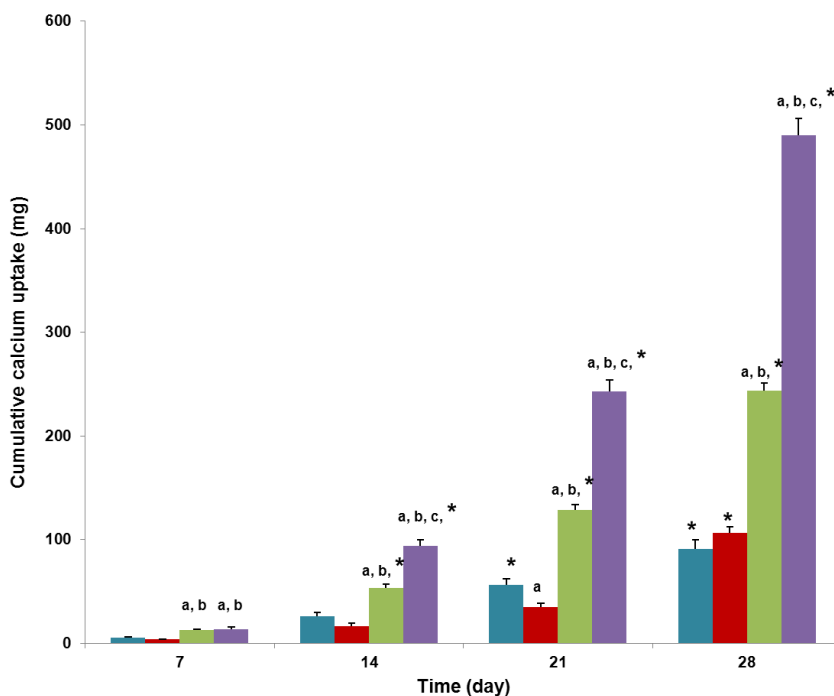


Figure 3. Calcium uptake of TCP11_LMS, TCP12_LMS, HA11_LMS and HA12_LMS disks during SBF immersion. Each data point represents the average and standard deviation of values obtained from three disks (n=3): (a) significantly different compared to TCP11_LMS within the same experimental time; (b) significantly different compared to TCP12_LMS within the same experimental time; (c) significantly different compared to HA11_LMS within the same experimental time; (*) significantly different compared to the same group (same disk type) between one experimental time and the previous one.

3.2 Mineralization process

SEM and XRD analyses were performed to follow the onset of the mineralization process. SEM images of CaP deposition onto HA12_LMS disks after different immersion times in SBF are presented in **Fig. 4**. The large aggregates found within concavities after the first week of immersion were composed of micron-sized CaP spherical-like cohesive particles (**Fig. 4a**).

EDS analysis (**Fig. 5a**) revealed a molar ratio of calcium to phosphorus (Ca/P) of 1.9-2.0 for these CaP spherical-like particles. At two weeks immersion in SBF, a globular CaP deposition layer grew within the concavities that gradually covered the underlying spherical-like CaP particles (**Fig. 4b** and **c**). This globular CaP deposition layer was composed of ~ 50 nm thick crystals (**Fig. 4d**) with a Ca/P ratio of 1.4-1.5 arranged into a reticular porous structure. EDS analysis (**Fig. 5b**) revealed a slightly higher atomic % of carbon (C; ~ 15%) compared to spherical-like particles (9–10%), next to small amounts of sodium (Na; 1-1.5%) and magnesium (Mg; 1-1.1%) and traces of potassium (K; < 1%) and chlorine (Cl; <1%). SEM images presented in **Fig. 4e** and **4f**, show two small concavities on the same HA12_LMS disk after a 2-week incubation period in SBF completely filled by the globular CaP. Specifically, in **Fig. 4e** initial outgrowth of CaP from the concavity can be detected (black arrows), while in **Fig. 4f** the globular CaP was already spread over the planar surface close to the concavity (black head arrows show the directions of the CaP outgrowth).

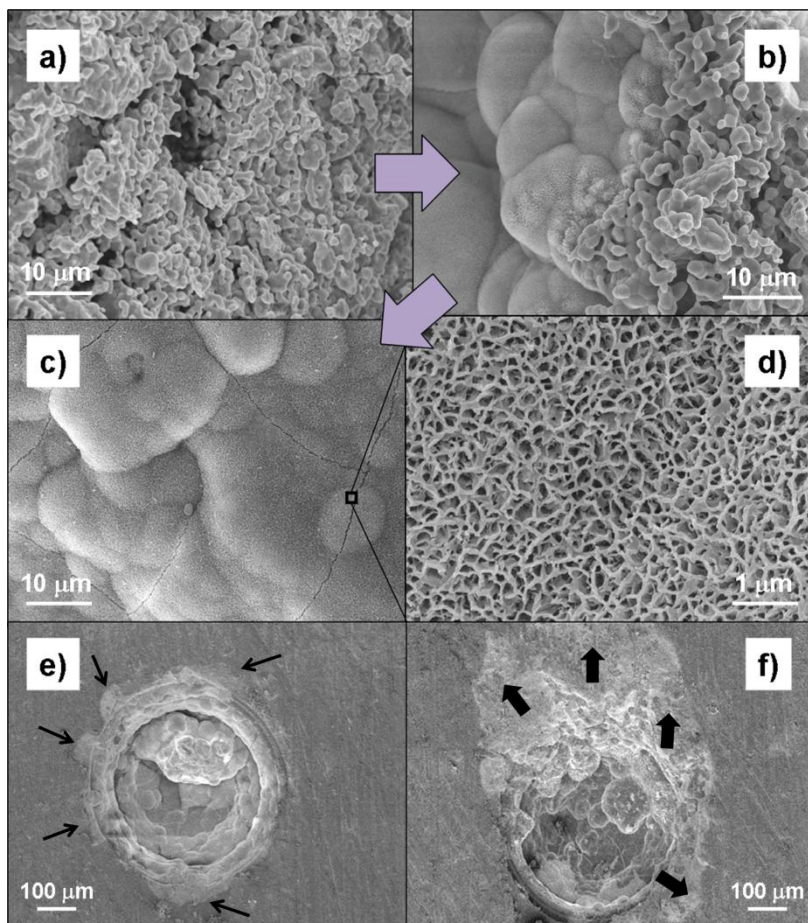


Figure 4. SEM images of different morphologies of CaP deposits on HAI2_LMS disks observed during SBF immersion. (a) Detail of the spherical-like structure of a CaP aggregate (large concavity, week 1); (b) Transition phase between the spherical-like and the globular macro-porous structure (medium concavity, week 3); (c) globular CaP deposits (medium concavity, week 3); (d) detail of globular CaP deposits (medium concavity, week 3); (e) small concavity completely filled by globular CaP deposit (week 3); arrows indicated the initial outgrowth of CaP outside the concavity; (f) spreading of CaP deposits outside a small concavity onto the planar surface (week 3, same disk of (e)); arrowheads indicate the outgrowth direction of the CaP outside the concavity on the planar surface.

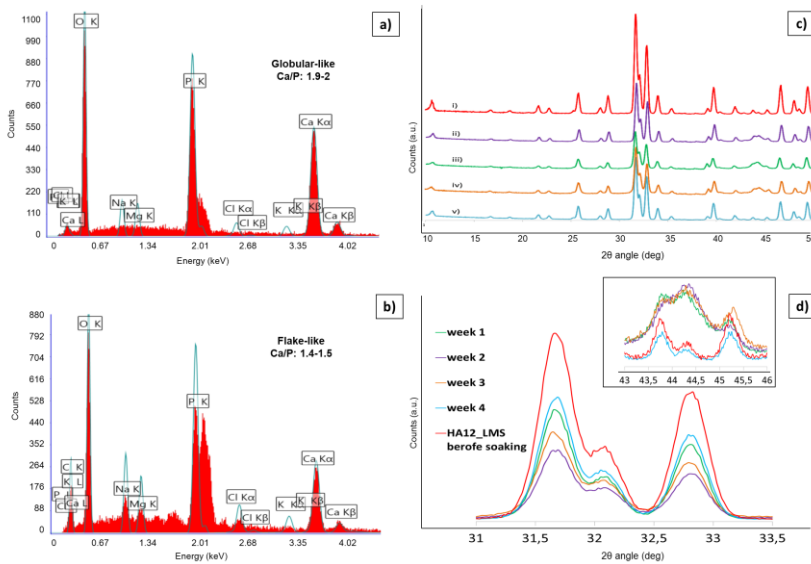


Figure 5. EDS and XRD spectra of HA12_LMS. (a) EDS spectrum of spherical-like CaP deposits; (b) EDS spectrum of globular CaP deposits; (c) XRD spectra diffractograms of HA12_LMS at different SBF soaking times: 0 (i), 7 (ii), 14 (iii), 21 (iv) and 28 (v) days; (d) detail of the XRD diffractograms spectra of (c) between 31 and 33.5 °.

XRD diffractograms of HA12_LMS after different SBF immersion times are presented in **Fig. 5c**. The intensity of all main reflection peaks of the diffractogram of HA12_LMS virgin disks decreased from week 0 (before soaking) to week 1, until a minimum was reached at 2 and 3 weeks. After a 4-week SBF immersion period, the spectrum showed an increase in intensity again. **Fig. 5d** shows the HA12_LMS diffractograms between 31°-33° 2θ ((211), (112) and (300) crystal planes), where the main hydroxyapatite peaks can be found, in order to observe the above-mentioned behavior in more detail. Several secondary reflection peaks were observed between 43 °- 46 ° 2θ ((113),

CALCIUM PHOSPHATE CERAMICS FOR BONE REGENERATION

(400) and (203) crystal planes) corresponding to the CaP deposited on the disks. The intensity of these peaks corresponding to the deposited CaP increased from week 0 to week 3, followed by a decrease at week 4.

3.3 Role of concavity dimension on SBF mineralization

In order to quantify the effect of concavity dimension on CaP nucleation in vitro, HA12_L, HA12_M and HA12_S disks were soaked in SBF at 37 °C for 14 days and characterized for morphology, crystal phase and calcium uptake. The final time point of 14 days was selected in order to study the mineralization process before the spreading of CaP deposits over the planar surface of the disks. **Fig. 6** displays representative SEM images of the concavities of HA12_L, HA12_M and HA12_S after a 2-week immersion period in SBF. From detailed SEM investigation, it was observed that nearly all (23 out of 24, 96 %) of the concavities at the surface of HA12_S disks were filled with spherical-like CaP. In contrast, filling of concavities at the surface of HA12_M and HA12_L disks were only partially or scarcely filled with CaP deposits, respectively. Similar to the results described above, substantial CaP aggregates were only observed inside concavities and not at the planar surface. This absence of a planar surface CaP layer was confirmed by XRD spectra of HA12_L, HA12_M, and HA12_S, which did not show differences between the various experimental disks or as compared to the non-soaked HA12 control samples (data not shown).

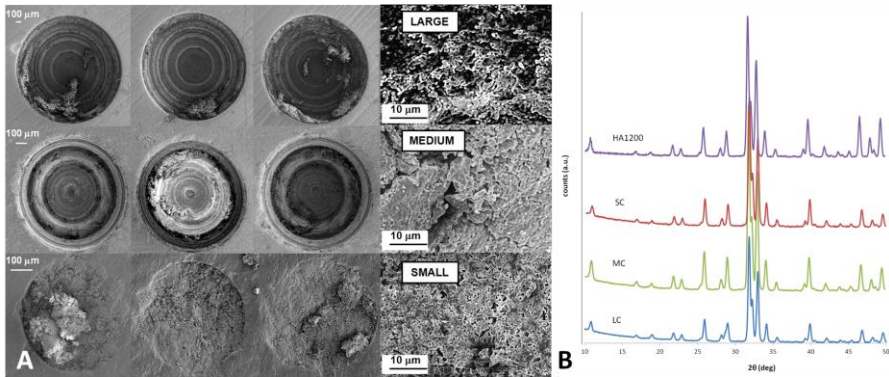


Figure 6. SEM images of large, medium and small concavities at the surface of HA12 disks after 14 days immersion in SBF. Top view SEM images of large cavities (top), medium cavities (middle) and small cavities (bottom) on HA12_L, HA12_M and HA12_S respectively, after 14 days of immersion in SBF at 37°C. Representative concavities for each dimension are displayed. Panels on the right show magnifications of the mineralization inside the concavities.

Differences in the extent of calcium uptake by HA12_L, HA12_M, and HA12_S revealed a clear effect of the concavity dimension on the extent of mineralization (**Fig. 7a**). Calculated amounts of calcium uptake relative to the concavity volume are presented in **Table 3**. The total calcium uptake of HA12_S was ~ 1.7- and ~ 1.8-fold higher compared to HA12_M and HA12_L, respectively. Direct weight measurements of the disks before and after the SBF immersion experiment revealed a weight increase (ΔW) of 0.36 % for HA12_S, a weight increase of 0.33 % for HA12_M, and a weight increase of 0.24 % for HA12_L. The total calcium uptake per volume unit (Ca/mm^3 , calculated by assuming that all CaP was deposited in the concavities) of the concavities of HA12_S (**Fig. 7b**) was ~ 123- and ~ 10-fold higher compared to HA12_L (S/L)

and HA12_MC (S/M), respectively, whereas ΔW per volume unit of the concavities (mg mm^3) of HA12_S was ~ 109 - and ~ 7 -fold higher compared to HA12_L (S/L) and HA12_MC (S/M), respectively.

4. Discussion

The aim of this study was to evaluate the effect of surface concavities on the surface mineralization of different CaP ceramics *in vitro*. Our hypothesis was that concavities prepared at the surface of bioceramic disks (i) could induce surface mineralization *in vitro*, as surface concavities have been previously demonstrated to induce bone formation at ectopic locations *in vivo* [13], and (ii) that concavity dimensions affect the extent of surface mineralization. The results of this study clearly demonstrated a strong effect of both disk chemical composition (HA > β -TCP) and sintering temperature ($1200\text{ }^\circ\text{C}$ > $1100\text{ }^\circ\text{C}$) on CaP deposition from SBF. Further, it was shown that CaP deposition was initiated exclusively within concavities and not on the planar surface of the disks. Finally, concavity dimensions showed a strong effect on surface mineralization with a 4-fold reduction of concavity dimensions resulting in a ~ 123 -fold increase of calcium uptake.

The results of the present study showed that only HA disks sintered at $1200\text{ }^\circ\text{C}$ supported abundant CaP deposition. Sintering has a strong effect on the density, grain size, porosity, crystalline phases and surface charge of ceramics [18, 19]. HA sintered at lower temperature is known to be composed

of grains of smaller size, thus exhibiting a higher porosity and lower crystallinity compared to HA sintered at higher temperature [19]. Consequently, it can be envisaged that dissolution rates were higher for HA11_LMS compared to HA12_LMS, which in turn limited the extent of nucleation and growth of stable CaP aggregates for HA11_LMS compared to HA12_LMS. Similarly, the faster dissolution of β -TCP surface compared to HA most likely prevented nucleation of stable CaP nuclei, despite locally (i.e. at the surface) increased ionic concentrations of calcium and phosphate ions. β -TCP disks sintered at lower temperature were even more unstable, as partial degradation of the surface without CaP nucleation on the surface was observed for these disks, corroborating previously reported results [20].

The results of the present study suggest the occurrence of a two-step mineralization process on the HA disks heat treated at 1200 °C, represented by an initial aggregation of spherical-like CaP particles within the concavities (no large aggregates were found on the planar surface of the disks), which were subsequently replaced by a globular-like CaP phase consisting of crystals arranged into a reticular macro-porous structure, exhibiting a chemical composition which resembled the the inorganic phase in bone tissue more closely [21]. At this stage of complete filling of small concavities, globular CaP started to spread out from the concavities, ultimately coverage the planar surface of the disks completely, as suggested by SEM images like Figs. 4e and 4f. The formation and subsequent dissolution of the globular CaP coating on the HA12 disk surface could also be monitored by XRD analysis: specifically,

CALCIUM PHOSPHATE CERAMICS FOR BONE REGENERATION

the intensity of the main peaks of the HA substrate decreased with soaking time, indicating the establishment of a layer of lower crystallinity on the surface of the disks that limited x-ray diffraction from the more crystalline underlying substrate; after week 4, peak intensity increased again toward the starting conditions, which most likely suggests a partial re-dissolution of the globular CaP layer.

Concavities resemble the hemi-osteonic trenches (from few to several hundreds of micrometers) generated during osteoclastogenesis [22, 23]. The effect of concavities on bone growth in ectopic extra-skeletal sites in vivo has been already well-documented [24], whereas no study attempted to rationalize this phenomenon in vitro.

The results of the current study evidenced a very strong templating effect of surface concavities on CaP surface mineralization, whereas no significant CaP deposition occurred on planar surface. Although no solid explanation could be found yet to account for this intriguing phenomenon, we speculate that supersaturation with respect to calcium and phosphate ions increased with decreasing curvature of the concavity according to the Thompson-Freundlich equations [25]. In addition, flow rates of the incubation media were lower within concavities compared to the planar surface, thereby allowing for a further local up-concentration of Ca^{2+} and PO_4^{3-} ions within the concavities.

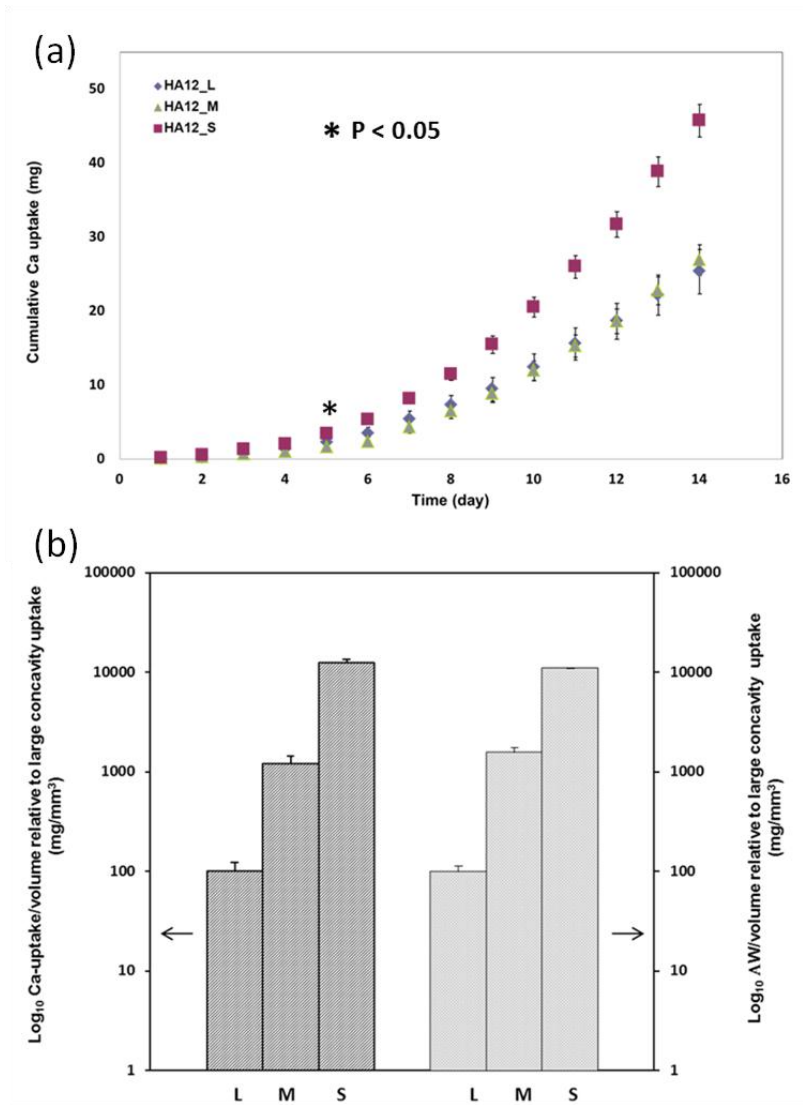


Figure 7. Quantification of the mineralization process at the surface of HA12 disks after 14 days immersion in SBF. (a) Cumulative calcium uptake for HA12_L (rhombus), HA12_M (triangle) and HA12_S (square) after 14 days immersion in SBF. (b) Graph showing the calcium uptake per concavity volume unit of the disks normalized to the uptake of HA12_L (left bars, log scale) and the weight variation for concavity volume unit of the disks normalized to the uptake of HA12_L (right bars, log scale).

CALCIUM PHOSPHATE CERAMICS FOR BONE REGENERATION

	Concavity diameter (mm)	Mean disk surface area (mm ²)	SBF vol. to surf. area (ml/mm ²)	Vol. of 1 concavity (mm ³)	Vol. of 12 concavities (mm ³)	Total Ca uptake (mg)	Ca uptake per concavity vol. (mg/mm ³)	ΔW (mg)	ΔW per concavity vol. (mg/mm ³)
LC	1.79 ± 0.03	376 ± 39	0.027 ± 0.003	1.5 ± 0.1	18 ± 2	25 ± 3	1.4 ± 0.3	5.0 ± 0.2	0.28 ± 0.04
MC	0.80 ± 0.02	352 ± 35	0.028 ± 0.003	0.13 ± 0.01	1.6 ± 0.1	27 ± 2	17 ± 3	7.1 ± 0.2	4.4 ± 0.5
SC	0.44 ± 0.01	348 ± 34	0.029 ± 0.003	0.022 ± 0.001	0.27 ± 0.01	46 ± 2	172 ± 14	8.1 ± 0.2	30.5 ± 0.09

LC = Large concavity; MC = Medium concavity; SC = Small concavity; ΔW = (Weight)_{final} – (Weight)_{initial}

Table 3. Quantification of the *in vitro* mineralization process.

Accordingly, smaller concavities were able to induce more mineralization than larger concavities also due to the more static microenvironment of the concavities, which in turn lead to an accelerated increase of local ionic concentrations of Ca²⁺ and PO₄³⁻ compared to larger concavities, where higher flow rates are expected due to the larger size. Finally, since mineralization is a unique process involved in bone tissue formation, the herein presented data represent a first attempt to link mineralization to osteoinduction, which by itself is a completely novel approach.

5. Conclusions

The results of the present study showed that the *in vitro* surface mineralization process of CaP ceramics with surface concavities starts

preferentially within the concavities and not on the planar surface of the ceramics, indicating a strong templating effect of the concavities on CaP surface mineralization. Further, concavity dimensions revealed to be an extremely effective parameter for controlling the extent of in vitro surface mineralization with small concavity dimensions resulting in considerably increased surface mineralization.

Acknowledgments

This research forms part of the Project P2.04 BONE-IP of the research program of the BioMedical Materials institute, co-funded by the Dutch Ministry of Economic Affairs, Agriculture and Innovation.

References

1. Rezwan K, Chen QZ, Blaker JJ, Boccaccini AR. *Biodegradable and bioactive porous polymer/inorganic composite scaffolds for bone tissue engineering. Biomaterials.* 2006;27(18):3413-31.
2. Dorozhkin SV. *Bioceramics of calcium orthophosphates. Biomaterials.* 2010;31(7):1465-85.
3. Tampieri A, Sprio S, Sandri M, Valentini F. *Mimicking natural biomineralization processes: A new tool for osteochondral scaffold development. Trends Biotechnol.* 2011;29(10):526-35.
4. Chai YC, Carlier A, Bolander J, Roberts SJ, Geris L, Schrooten J, et al. *Current views on calcium phosphate osteogenicity and the translation into effective bone regeneration strategies. Acta Biomater.* 2012;8(11):3876-87.
5. Ozdemir T, Higgins AM, Brown JL. *Osteoinductive biomaterial geometries for bone regenerative engineering. Current pharmaceutical design.* 2013;19(19):3446-55.
6. Yuan HP, Fernandes H, Habibovic P, de Boer J, Barradas AMC, de Ruiter A, et al. *Osteoinductive ceramics as a synthetic alternative to autologous bone grafting. P Natl Acad Sci USA.* 2010;107(31):13614-9.
7. Habibovic P, Sees TM, van den Doel MA, van Blitterswijk CA, de Groot K. *Osteoinduction by biomaterials - Physicochemical and*

- structural influences. J Biomed Mater Res Part A. 2006;77A(4):747-62.*
8. *Tampieri A, Celotti G, Landi E. From biomimetic apatites to biologically inspired composites. Analytical and Bioanalytical Chemistry. 2005;381(3):568-76.*
 9. *Schouten C, Meijer GJ, van den Beucken J, Spauwen PHM, Jansen JA. Effects of implant geometry, surface properties, and TGF-beta 1 on peri-implant bone response: an experimental study in goats. Clinical Oral Implants Research. 2009;20(4):421-9.*
 10. *Li B, Liao XL, Zheng L, Zhu XD, Wang Z, Fan HS, et al. Effect of nanostructure on osteoinduction of porous biphasic calcium phosphate ceramics. Acta Biomater. 2012;8(10):3794-804.*
 11. *Prodanov L, Lamers E, Domanski M, Luttge R, Jansen JA, Walboomers XF. The effect of nanometric surface texture on bone contact to titanium implants in rabbit tibia. Biomaterials. 2013;34(12):2920-7.*
 12. *Graziano A, d'Aquino R, Cusella-De Angelis MG, Laino G, Piattelli A, Pacifici M, et al. Concave Pit-Containing Scaffold Surfaces Improve Stem Cell-Derived Osteoblast Performance and Lead to Significant Bone Tissue Formation. Plos One. 2007;2(6).*
 13. *Ripamonti U, Roden LC, Ferretti C, Klar RM. Biomimetic Matrices Self-Initiating the Induction of Bone Formation. Journal of Craniofacial Surgery. 2011;22(5):1859-70.*

CALCIUM PHOSPHATE CERAMICS FOR BONE REGENERATION

14. Ripamonti U, Roden LC, Renton LF. Osteoinductive hydroxyapatite-coated titanium implants. *Biomaterials*. 2012;33(15):3813-23.
15. Ripamonti U. Biomimetism, biomimetic matrices and the induction of bone formation. *Journal of Cellular and Molecular Medicine*. 2009;13(9B):2953-72.
16. Scarano A, Degidi M, Perrotti V, Degidi D, Piattelli A, Iezzi G. Experimental Evaluation in Rabbits of the Effects of Thread Concavities in Bone Formation with Different Titanium Implant Surfaces. *Clinical Implant Dentistry and Related Research*. 2013:n/a-n/a.
17. Kokubo T, Takadama H. How useful is SBF in predicting in vivo bone bioactivity? *Biomaterials*. 2006;27(15):2907-15.
18. Kim HM, Himeno T, Kokubo T, Nakamura T. Process and kinetics of bonelike apatite formation on sintered hydroxyapatite in a simulated body fluid. *Biomaterials*. 2005;26(21):4366-73.
19. Mezahi FZ, Oudadesse H, Harabi A, Lucas-Girot A, Le Gal Y, Chaair H, et al. Dissolution kinetic and structural behaviour of natural hydroxyapatite vs. thermal treatment. *Journal of Thermal Analysis and Calorimetry*. 2009;95(1):21-9.
20. Xin RL, Leng Y, Chen JY, Zhang QY. A comparative study of calcium phosphate formation on bioceramics in vitro and in vivo. *Biomaterials*. 2005;26(33):6477-86.

21. Landi E, Tampieri A, Celotti G, Langenati R, Sandri M, Sprio S. Nucleation of biomimetic apatite in synthetic body fluids: dense and porous scaffold development. *Biomaterials*. 2005;26(16):2835-45.
22. Ripamonti U, Crooks J, Kirkbride AN. Sintered porous hydroxyapatites with intrinsic osteoinductive activity: geometric induction of bone formation. *South African Journal of Science*. 1999;95(8):335-43.
23. Parfitt AM, Mundy GR, Roodman GD, Hughes DE, Boyce BF. A new model for the regulation of bone resorption, with particular reference to the effects of bisphosphonates. *J Bone Miner Res*. 1996;11(2):150-9.
24. Ripamonti U, Tsiridis E, Ferretti C, Kerawala CJ, Mantalaris A, Heliotis M. Perspectives in regenerative medicine and tissue engineering of bone. *British Journal of Oral & Maxillofacial Surgery*. 2011;49(7):507-9.

CALCIUM PHOSPHATE CERAMICS FOR BONE REGENERATION

6

**INFLUENCE OF CERAMIC
DISK MATERIAL,
SURFACE HEMISPHERES,
AND SBF VOLUME ON IN
VITRO MINERALIZATION**

1. Introduction

Calcium phosphate (CaP) ceramics closely resemble the inorganic component of bone and teeth and hence have been extensively investigated synthetic materials for bone regenerative applications. As a major asset, surfaces of synthetic CaP implants have the capacity to chemically bond with surrounding osseous tissue [1,2]. Biological properties of CaP materials upon implantation in bone tissue, such as osteoconductivity [3] (i.e. the process by which bone conforms to a material's surface) and bioactivity [4-6] (i.e. the ability to stimulate bone tissue formation and directly bond to bone without an intervening soft tissue layer), are related to their physicochemical properties, for which both CaP chemistry and crystallinity are key factors.

Bioactive behavior of a material surface is generally tested predictively *in vitro* using Simulated Body Fluid (SBF) [7-9]. During such a test, partial dissolution of CaP materials with subsequent nucleation and re-precipitation on the surface can occur, which is suggested to be predictive for actual *in vivo* bioactive behavior and bone bonding ability [10]. Additionally, it is known that the formed carbonate apatite layer creates an ideal environment for cellular attachment and subsequent new bone formation that has strong bonding to the material surface [11,12].

Although the use of SBF as an *in vitro* test for examining bone bonding potential is widely accepted, some researchers have argued its predictive validity [13] and efforts have been made to improve the current

protocol [14]. According to Bohner et al., the protocol needs to have a simple SBF preparation procedure able to mimic the main features of blood serum and results of *in vivo* and *in vitro* test must correspond [14]. Furthermore, Bohner et al. claimed that a change of volume or sample size is expected to modify the rate of apatite formation [14]. Kokubo et al. [15] suggested to calculate the volume of SBF following the equation $V_s = S_a / 10$, (where V_s is the volume of SBF in ml and S_a is the apparent surface area of the specimen). However, the optimal SBF volume ratio remains unclear and variations in experimental set-up could provoke changes in results.

In a previous study, we assessed the surface mineralization process through an *in vitro* test in SBF and surface concavities were used as additional parameter to CaP chemistry and crystallinity [16]. The study showed that mineralization started preferentially within concavities in hydroxyapatite (HA) disks sintered at 1200 °C and that concavity size controlled the extent of mineralization. In the current study, we focused on how SBF volume variations (i.e., material liquid/ratio) influence the rate of apatite formation. Using titanium (Ti) disks, we anticipated to be able to differentiate between effects of material chemistry (initiation of nucleation due to release of Ca^{2+} and PO_4^{3-} ions from the material) and surface geometry and nucleation induced by concavity roughness.

In the current study, four different materials (i.e., HA, β -tricalcium phosphate [β -TCP], biphasic calcium phosphate [BCP] and titanium [Ti]) were used in which hemispherical surface concavities were created. Nucleation and

CALCIUM PHOSPHATE CERAMICS FOR BONE REGENERATION

crystal growth was assessed after immersion of the samples in SBF up to 14 days by means of calcium assay and scanning electron microscopy (SEM). It is known that CaP disks, immersed in SBF, release calcium and phosphate ions into the medium at a rate dependent on the solubility and Ca/P ratio of the ceramic. In view of this, we hypothesized that smaller SBF volumes would more rapidly increase the concentration of ionic species within the SBF solution compared to larger volumes, thus accelerating nucleation and re-precipitation on the CaP material surface compared to a titanium surface.

2. Materials and Methods

Materials

HA (Ca/P molar ratio 1.67; Merck, Darmstadt, Germany) and β -TCP (Ca/P molar ratio 1.50; CAM Bioceramics b.v., Leiden, the Netherlands) commercial powders were used in this study (**Table 1**).

Nomenclature	Abbreviation	Chemical Formula	Theoretical Ca/P ratio	Solubility $-\log(K_s)^a$
Hydroxyapatite	HA	$\text{Ca}_{10}(\text{PO}_4)_6(\text{OH})_2$	1.67	116.8
β -Tricalcium phosphate	β -TCP	$\text{Ca}_3(\text{PO}_4)_2$	1.50	28.9

^a The solubility at 25°C in water is given as the logarithm of the ion product of the given formulas with concentrations in mol/l³¹.

Table 1. Chemical composition, Ca/P molar ratio and solubility in aqueous solutions of the calcium phosphate powder materials

Also, custom-made commercially pure titanium disks (16 mm diameter, 3 mm height; Machinefabriek G Janssen, Valkenswaard, the Netherlands) with twelve hemispheres (400 μm diameter x 200 μm height) arranged over the surface were used for the study.

Preparation of ceramic disks

HA and β -TCP powders were solid state mixed with a weight ratio of 50:50 to obtain biphasic calcium phosphate (BCP) powder (composition of the experimental groups is shown in **Table 2**).

	HA (wt %)	TCP (wt %)
HA	100	0
β -TCP	0	100
BCP	50	50
Ti	0	0

Table 2. *Composition of prepared disks.*

Ceramic powders (HA, β -TCP and BCP) were uniaxially pressed at 103 MPa (15,000 psi) for 10 min in a cylindrical steel mold (internal diameter ~21 mm). After pressing, the blocks were heat treated in a furnace at 800°C for 6 h (1.67°C min⁻¹) to provide suitable strength to the ceramic to withstand the stresses applied during machining. Subsequently, heat-treated blocks were cut into disks (21 x 4 mm). A drill tip with a diameter size of 500 μm (Horico, Berlin, Germany) was used to create twelve hemispherical concavities across

CALCIUM PHOSPHATE CERAMICS FOR BONE REGENERATION

the surface of the disks with a center-to-center distance of 4 mm between hemispheres (**Figure 1**). Subsequently, disks were sintered in a furnace for 6 h ($1.67^{\circ}\text{C min}^{-1}$) at 1200°C , resulting in reduced disk dimensions (16 mm diameter, 3 mm height) as well as reduced hemisphere sizes (400 μm diameter x 200 μm height).

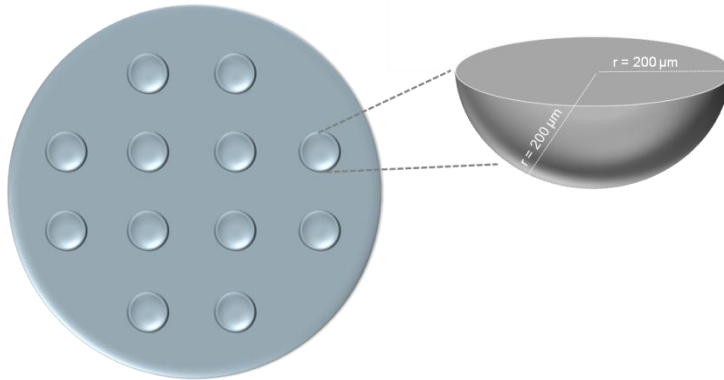


Figure 1. Schematic representation of disk surface geometries employed in the current study. Twelve hemispherical concavities were made on the surface of the disk with a hemisphere radius value of 200 μm .

X-ray diffraction

The crystallographic structure of the CaP ceramics was studied by thin-film X-ray diffraction (XRD, Philips, PW3710, Eindhoven, the Netherlands) using $\text{CuK}\alpha$ -radiation (PW 3710, 40 kV, 30 mA). The phase composition of the powder materials was determined by X-ray diffraction (XRD), diffraction scans were recorded between $10^{\circ} 2\theta$ to $50^{\circ} 2\theta$ with a step size of $0.02^{\circ} 2\theta$ and a sample time of 6 s/step. The crystal structure of the disks after sintering at 1200°C was analyzed and diffractograms were collected for 20

values between 10° and 50° with a step size of $0.02^\circ 2\theta$ and a sample time of 2 s/step.

Scanning electron microscopy

The surface morphology and microstructure of the ceramic and Ti disks were observed using a scanning electron microscope (SEM, Jeol, SEM6310, Tokyo, Japan) with an electron accelerating voltage of 10 kV and a current of ~ 10 mA. All SEM samples were sputter-coated with a thin, gold layer (5-10 nm) to minimize negative charge accumulation from the electron beam during scanning. A working distance of 10 mm was used for the scans.

SBF studies and assessment of the mineralization process

Freshly prepared filter-sterilized simulated body fluid (SBF) [15] was used throughout the study to determine the surface nucleation and crystal growth of the experimental disks. All disks (**Table 2**; $n = 3$ for each experimental group), with the side containing the hemispherical concavities facing up, were incubated for 14 days into 50 ml sterile conical centrifuge tubes (one disk per tube) (Greiner Bio-One, Berlin, Germany) filled with SBF solution (5, 10 or 20 ml per tube). The tubes were tightly closed with a tube cap to minimize evaporation during incubation and kept at 37°C on a shaking table (1 Hz). Additionally, controls ($n = 3$) consisting of empty tubes filled with only SBF were used for each time point in order to detect any homogeneous

CALCIUM PHOSPHATE CERAMICS FOR BONE REGENERATION

nucleation in the solution or heterogeneous nucleation on the walls of well plates. The SBF was daily refreshed, and the supernatant was collected to determine calcium levels using the ortho-cresolphthalein complexone (Sigma–Aldrich, St. Louis, MO, USA) method. To this end, 100 µl of the supernatant was mixed with 100 µl of 1 N acetic acid (Boom BV, Meppel, the Netherlands) and incubated overnight on a shaking table. The amount of calcium uptake by the disk was calculated with respect to the controls (SBF in empty tubes) and averaged for three samples per group. At 14 days, disks were removed from the tubes, gently washed with distilled water and dried at 40°C for 24 h. Subsequently, the surface of the studied disks was observed using SEM analysis.

Statistical analysis

All statistical analyses were performed with GraphPad Instat[®] 3.05 software (GraphPad Software Inc, San Diego, CA, USA), using analysis of variance (ANOVA) combined with a post-hoc Tukey-Kramer Multiple Comparisons Test. Results were considered significant at $p < 0.05$.

3. Results

Characterization of starting powders

The starting HA and β -TCP ceramic powder materials were characterized using XRD in order to confirm their phase composition before disk preparation. **Figure 2** shows peak position and relative peak intensities for the HA and β -TCP powders that correspond closely to those indicated in the International Center for Diffraction Data (ICDD) data file no. 09-0432 (HA) and no. 70-2065 (β -TCP). The main characteristic peaks associated with HA were assigned to the 002, 102, 210, 211, 112, 300 and 202 reflections corresponding to 25.9°, 28.1°, 28.9°, 31.9°, 32.2°, 33.0° and 34.1° 2 θ values. For β -TCP, a series of sharp characteristic diffraction peaks were observed at 25.7°, 27.7°, 31.0°, and 34.3° 2 θ values, corresponding to the crystal planes of 1010, 214, 0210 and 220 respectively.

CALCIUM PHOSPHATE CERAMICS FOR BONE REGENERATION

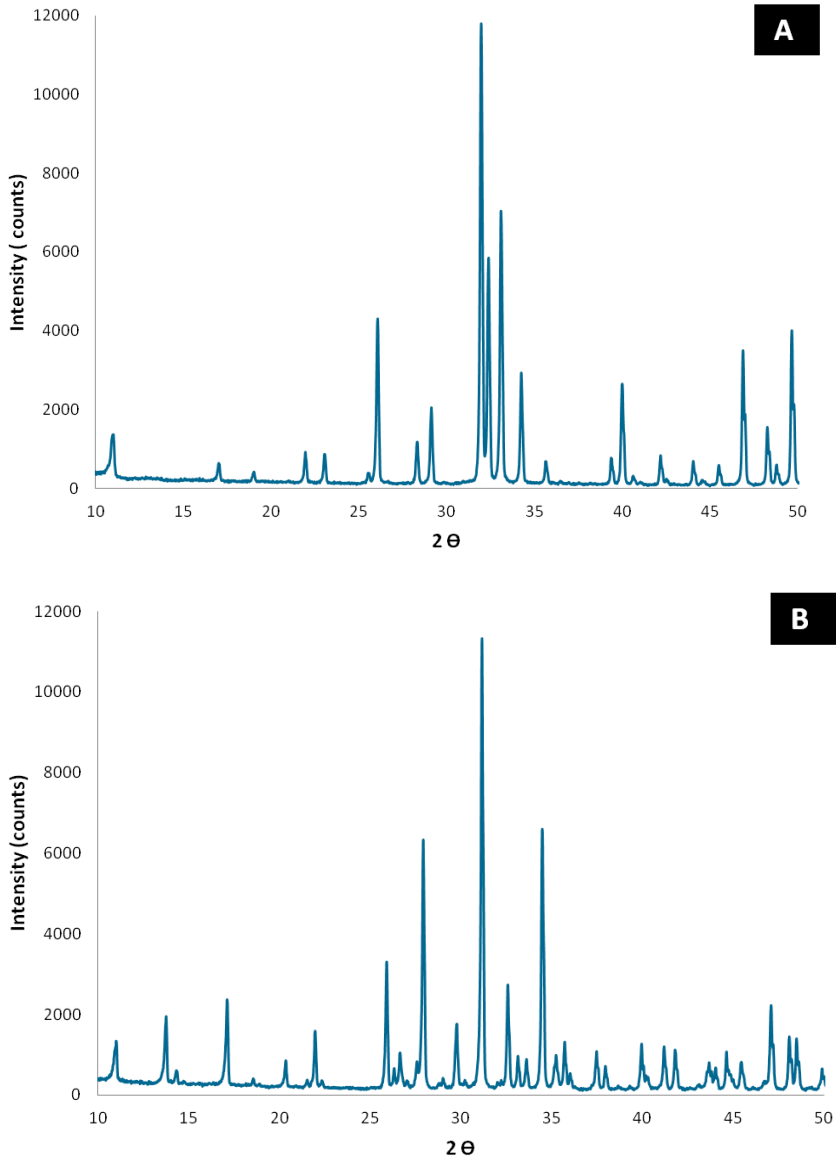


Figure 2. Diffraction patterns obtained using XRD for calcium phosphate starting ceramic powder materials. A) HA powder with main characteristic peaks assigned to the 002, 211, 112 and 300 reflections. B) β -TCP powder with main characteristic peaks assigned to the 1010, 214, 0210 and 220 reflections.

Characterization of prepared CaP disks

The apatitic nature of prepared CaP disks was revealed by XRD analysis. HA disks showed an XRD pattern with main reflection peaks at 25.9° , 31.9° , 32.4° and 33.2° 2θ corresponding to the 002, 211, 112 and 300 reflections, respectively (**Fig. 3a**). β -TCP disks showed a strong reflection at 2θ values of 27.7° , 31.0° and 34.2° corresponding to 214, 210 and 220 reflections for β -TCP, respectively. BCP ceramic disks had a biphasic structure consisting of HA and β -TCP, illustrated by main diffraction peaks at 25.9° , 28.9° , 31.9° , 32.4° and 33.2° 2θ corresponding to the 002, 210, 211, 112 and 110 reflections for HA, respectively, and diffraction peaks at 2θ values of 27.7° , 31.1° and 34.2° corresponding to 214, 0210 and 220 reflections for β -TCP, respectively.

CALCIUM PHOSPHATE CERAMICS FOR BONE REGENERATION

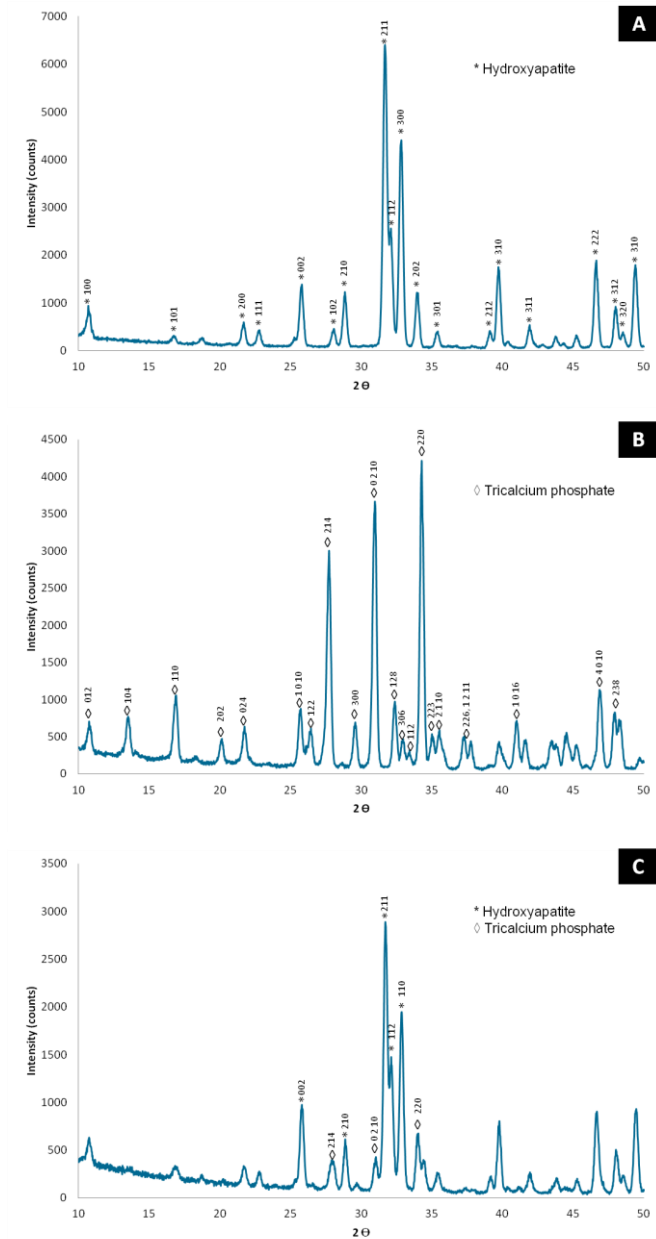


Figure 3. XRD pattern of the sintered ceramic disks produced from the ceramic powder materials. A) HA disk sintered at 1200 °C B) β -TCP disk sintered at 1200 °C and C) BCP disk sintered at 1200 °C.

Influence of SBF volume on mineralization

The surface area of the disks used in this study was 202.9 mm². Each disk had 12 hemispherical concavities at its surface (one side only). The volume of SBF was calculated following Kokubo's equation [15]:

$$V_s = S_a / 10$$

where V_s is the volume of SBF (ml) and S_a is the apparent surface area of the specimen (mm²). Using Kokubo's equation, an approximate value of 20 ml of SBF per disk is required. In the current study, 5, 10, and 20 ml were selected for the experiments based on our initial hypothesis.

All disks were immersed in parallel in different SBF volumes (i.e., 5, 10, or 20 ml) at 37°C for 14 days (**Figure 4**). Ti and CaP disks immersed in either 5 or 20 ml of SBF showed very low calcium deposition on their disks surfaces. Calcium amounts deposited on the disks reached 4.3 ± 2.5 , 1.1 ± 0.7 , 0.6 ± 0.5 and 0.3 ± 0.8 mg for HA, TCP, BCP and Ti, respectively, for 5 ml volumes after 14 days immersion in SBF. Significantly higher calcium deposition was observed for HA vs. Ti disks ($p < 0.05$), TCP vs. Ti ($p < 0.01$) and BCP vs. Ti ($p < 0.05$). Calcium uptake deposited on the disks reached 5.9 ± 2.5 , 9.2 ± 2.6 , 8.8 ± 1.6 and 3.3 ± 2.0 mg for HA, TCP, BCP and Ti, respectively, for 20 ml volume after 14 days immersion in SBF.

Significantly higher calcium deposition was observed for TCP vs. Ti disks ($p < 0.05$). In contrast, the cumulative calcium uptake after a 14 days

CALCIUM PHOSPHATE CERAMICS FOR BONE REGENERATION

immersion period in 10 ml of SBF reached 41.6 ± 1.8 mg for HA disks, whereas 11.0 ± 1.8 , 3.2 ± 0.6 and 1.2 ± 0.6 mg was reached for TCP, BCP and Ti disks, respectively. Significantly higher calcium deposition was observed for HA vs. TCP disks ($p < 0.001$), HA vs. Ti ($p < 0.001$) and TCP vs. Ti ($p < 0.001$).

Figure 5 shows representative SEM images of HA disks in different SBF volumes after 14 days SBF soaking experiments. Hemispherical concavities of HA disks immersed in either 5 or 20 ml SBF were scarcely populated with CaP nanoparticles.

The amount of CaP deposited within the concavities observed for 5 and 20 ml SBF was in contrast with the results of concavities of HA disks immersed in 10 ml SBF volume, the latter for which nearly all concavities were filled with an agglomeration of CaP deposited material.

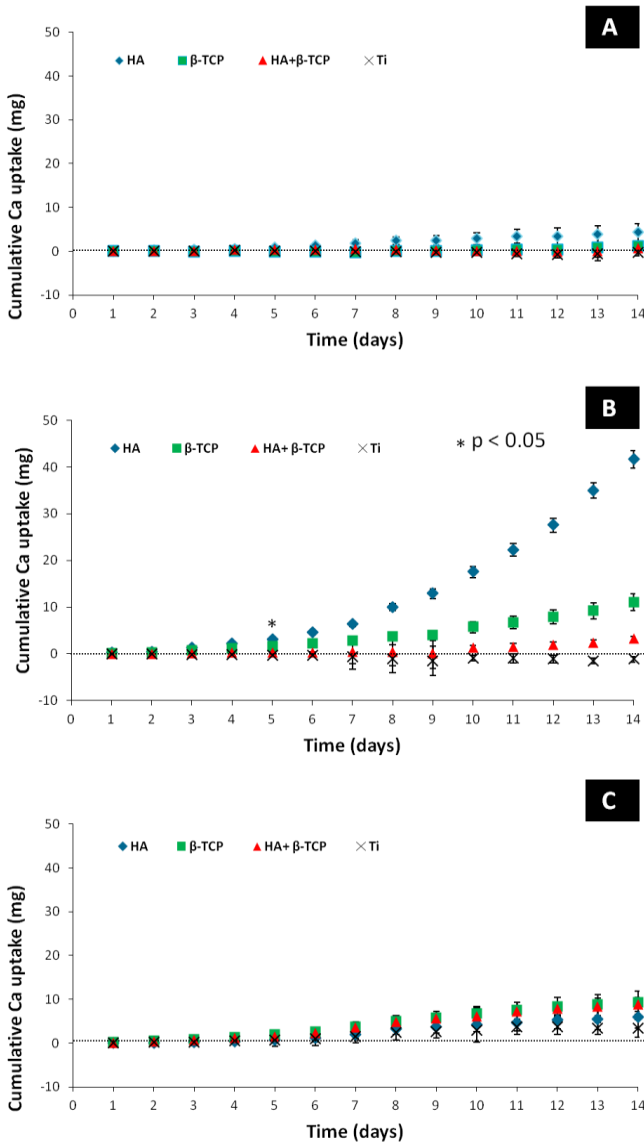


Figure 4. Cumulative calcium uptake by experimental disks Ti, HA, β-TCP and BCP after 14 days SBF soaking experiment. A) Disks immersed in 5 ml of SBF. B) Disks immersed in 10 ml of SBF. C) Disks immersed in 20 ml of SBF. Each data point represents the average and standard deviation of values obtained from three different disks (n=3).

CALCIUM PHOSPHATE CERAMICS FOR BONE REGENERATION

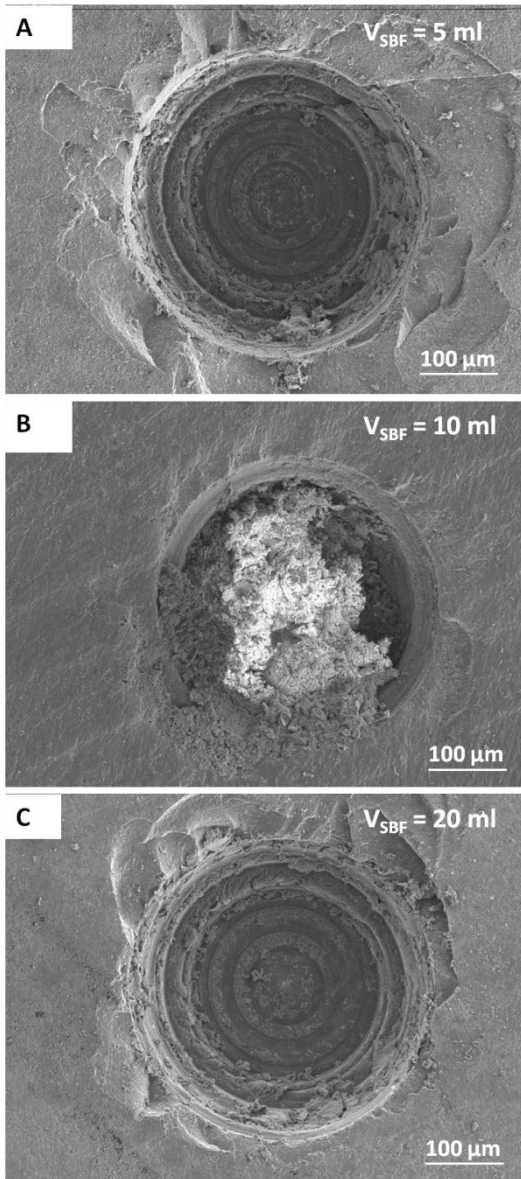


Figure 5. SEM images of hemispherical concavities on the surface of HA disks when using either 5, 10 or 20 ml of SBF after 14 days immersion.

Influence of disk material and surface hemispheres on mineralization

An apparent effect of disk material on mineralization occurred in 10 ml SBF volume. Therefore, experimental substrate disks were immersed in 10 ml of SBF for 14 days at 37°C. Ti disks showed no calcium deposition during the 14 days of immersion in SBF (**Figure 4b**). However, all CaP disks showed calcium deposition after immersion in SBF for 14 days. From day 5, HA disks showed a continuous significant ($p < 0.05$) temporal increase in calcium deposition compared to β -TCP and BCP ceramic disks. The cumulative calcium deposition reached 41.6 ± 1.8 mg for HA disks, whereas 11.0 ± 1.8 and 3.2 ± 0.6 was reached for β -TCP and BCP, respectively.

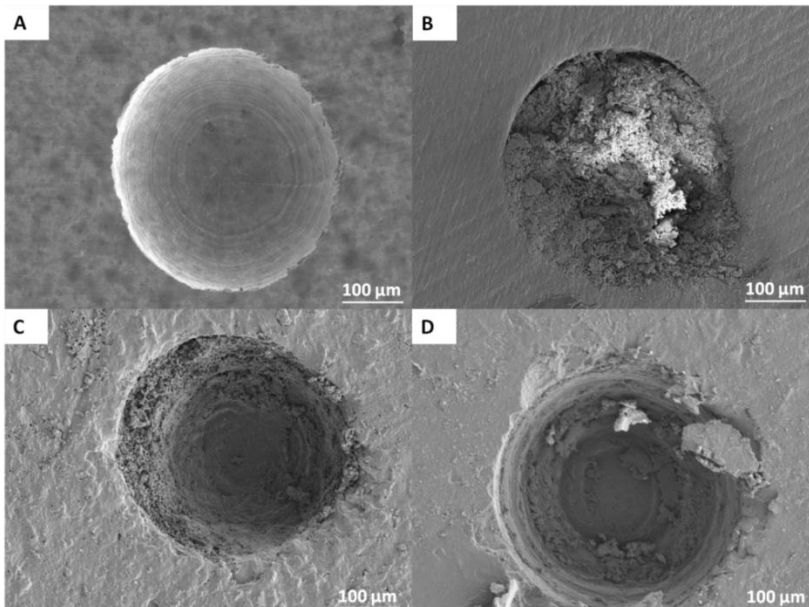


Figure 6. SEM images of hemispherical concavities after 14 days immersion in SBF. A) Ti disks, B) HA disks, C) β -TCP disks and D) BCP disks.

CALCIUM PHOSPHATE CERAMICS FOR BONE REGENERATION

Figure 6 shows representative SEM images of disk concavities for different groups after 14 days SBF soaking experiments. While no difference was observed between the Ti disk at days 0 and 14, for which the disks surface remained unaltered during the 14 days soaking in SBF (**Figure 6a**), a clear growth of mineralized structures was observed for HA disks (**Figure 6b**). β -TCP and BCP disks (**Figure 6c** and **d** respectively) showed few aggregates of CaP deposits inside of the hemispherical concavities after 14 days of immersion.

4. Discussion

The aim of this study was to investigate the effect of disk material, surface geometry, and simulated body fluid (SBF) volume on the in vitro surface mineralization capacity. We hypothesized that smaller SBF volumes would lead to more rapidly increased concentrations of ionic species within SBF solution compared to larger volumes, thus accelerating nucleation and re-precipitation of calcium phosphate. Disk material was also included as a factor in the study to investigate the effect on mineral deposition. This study showed that different SBF volumes have different effects on mineralization, with an optimum SBF volume of 10 ml. Additionally, at this volume, apparent differences based on disk material became obvious. Finally, also surface hemispherical concavities acted as initiator areas for nucleation and crystal growth.

In agreement with previous observations [16], nucleation and re-precipitation started preferentially within the concavities, rather than on the planar surface of the disks. However, in contrast to our initial hypothesis, our results showed that higher surface mineralization was achieved when half of the volume suggested by Kokubo's protocol was used [15]. According to Kokubo's protocol and the surface area of our disks, SBF volume should be around 20 ml per disk. Although we can reason that effects of (partial) dissolution on CaP disks on the concentration of SBF will be lower with larger volumes (i.e. 20 ml), our results demonstrate the presence of an optimal volume for nucleation and re-precipitation in SBF. Our finding is remarkable, and the reason for an optimal calcium deposition at the intermediate volume of 10 ml remains unclear. Nevertheless, based on our findings we recommend an optimal material/liquid ratio of 5 ml SBF per cm^2 .

Significant CaP mineralization on HA disks was observed within 14 days of immersion in SBF compared to low and insignificant mineralization on β -TCP, BCP, and Ti disks. Surface mineralization depends on factors including calcium phosphate composition and solubility (i.e., β -TCP > BCP > HA [17,18]). Bioactive materials require a certain chemical solubility to allow the necessary reactions to take place between the SBF solution and the material surface [19]. The adsorption of Ca^{2+} and PO_4^{3-} ions from the SBF combined with low flow inside the hemispherical concavity most likely increases the local ionic concentration and initiates nucleation of CaP nuclei within these microenvironments. CaP nucleation and subsequent crystal growth by

CALCIUM PHOSPHATE CERAMICS FOR BONE REGENERATION

aggregation form a stable crystalline apatitic phase on the surface of HA disks [20]. However, in the case of β -tricalcium phosphate (β -TCP) disks, the continued dissolution of Ca^{2+} and PO_4^{3-} ions from the disks followed by re-precipitation during SBF immersion limited the formation of a stable carbonate apatite layer, impeding with the mineralization process. The fact that β -TCP sintered ceramics show a poor ability for apatite formation *in vitro* in SBF has been previously reported [21-23]. Although β -TCP ceramic is widely considered to be bioactive *in vivo* [24,25], the lack of *in vitro* apatite-forming ability confirms the potentially limited validity of the SBF test to predict *in vivo* bone bonding.

Biphasic calcium phosphate (BCP) ceramic disks are made of intimate mixtures of HA and β -TCP (50:50), for which we expected to have and intermediate dissolution behavior. However, our results showed higher calcium deposition for β -TCP disks compared to BCP disks. Lower calcium deposition by BCP disks can be attributed to the selected mixture ratio of the two CaP ceramics, which exhibited a negative interaction effect of BCP on Ca^{2+} and PO_4^{3-} ion dissolution. Comparing CaP ceramics with Ti disks, we observed no mineralization on Ti, although all disk types had rough concavity surfaces, indicating no interference of concavity roughness on the initiation of surface nucleation.

The rate and ability of CaP ceramics to form apatite is dependent on the SBF type used. More particularly, the presence of other species (e.g. buffers, such as Tris (tris-hydroxymethyl-aminomethane)-HCl or Hepes (2-(4-

(2-hydroxyethyl)-1-piperaziny)ethane sulphonic acid-NaOH) and other concentrations of calcium and phosphate ions in the SBF influence the rate of apatite formation. In recent years, several studies have used high ionic concentrations of SBF, often referred to as supersaturated calcification solutions (SCSs). Concentrations of calcium and phosphate in SCSs of 1.5, 2, 5 and 10 times higher than blood serum values have been used to accelerate the SBF precipitation process [26-30]. The idea of using SCS is to enhance the kinetics of apatite formation in order to increase the utility of SBF and to reduce the immersion period. Although SCSs are suitable for use with materials that have fast degradation rates (e.g. polymers), conventional SBF is recommendable to mimic *in vivo* reactions in a more optimal manner. Since conventional SBF has similar ion concentrations to human blood plasma, rates of apatite formation can more accurately be estimated with SBF than with SCS.

5. Conclusion

This work suggests an optimal material/liquid ratio of 5 ml SBF per cm^2 disk surface to observe mineralization. HA disks showed considerable mineralization capacity in contrast to β -TCP and BCP ceramic disks, for which little mineralization was observed. Mineralization preferentially started within the hemispherical concavities, which acted as initiator areas for nucleation and crystal growth.

Acknowledgments

This research forms part of the Project P2.04 BONE-IP of the research program of the BioMedical Materials institute, co-funded by the Dutch Ministry of Economic Affairs, Agriculture and Innovation.

References

1. Ducheyne P, Qiu Q. Bioactive ceramics: the effect of surface reactivity on bone formation and bone cell function. *Biomaterials* 1999;20(23-24):2287-303.
2. LeGeros RZ. Calcium phosphate-based osteoinductive materials. *Chem Rev* 2008;108(11):4742-53.
3. Albrektsson T, Johansson C. Osteoinduction, osteoconduction and osseointegration. *Eur Spine J* 2001;10 Suppl 2:S96-101.
4. Lee KY, Park M, Kim HM, Lim YJ, Chun HJ, Kim H, Moon SH. Ceramic bioactivity: progresses, challenges and perspectives. *Biomed Mater* 2006;1(2):R31-7.
5. LeGeros RZ. Biodegradation and bioresorption of calcium phosphate ceramics. *Clin Mater* 1993;14(1):65-88.
6. El-Ghannam A. Bone reconstruction: from bioceramics to tissue engineering. *Expert Rev Med Devices* 2005;2(1):87-101.
7. Filgueiras MR, LaTorre G, Hench LL. Solution effects on the surface reactions of three bioactive glass compositions. *J Biomed Mater Res* 1993;27(12):1485-93.
8. Jonasova L, Muller FA, Helebrant A, Strnad J, Greil P. Hydroxyapatite formation on alkali-treated titanium with different content of Na⁺ in the surface layer. *Biomaterials* 2002;23(15):3095-101.

CALCIUM PHOSPHATE CERAMICS FOR BONE REGENERATION

9. Czikó M, Bogya E-S, Barabás R, Bizo L, Stefan R. *In vitro biological activity comparison of some hydroxyapatite-based composite materials using simulated body fluid. Central European Journal of Chemistry* 2013;11(10):1583-1598.
10. Lu X, Leng Y. *Theoretical analysis of calcium phosphate precipitation in simulated body fluid. Biomaterials* 2005;26(10):1097-108.
11. Hench LL, Thompson I. *Twenty-first century challenges for biomaterials. Journal of The Royal Society Interface* 2010;7(Suppl 4):S379-S391.
12. Hench LL. *Bioceramics. Journal of the American Ceramic Society* 1998;81(7):1705-1728.
13. Pan H, Zhao X, Darvell BW, Lu WW. *Apatite-formation ability – Predictor of “bioactivity”?* *Acta Biomater* 2010;6(11):4181-4188.
14. Bohner M, Lemaître J. *Can bioactivity be tested in vitro with SBF solution?* *Biomaterials* 2009;30(12):2175-2179.
15. Kokubo T, Takadama H. *How useful is SBF in predicting in vivo bone bioactivity?* *Biomaterials* 2006;27(15):2907-15.
16. Bianchi M, Urquia Edreira ER, Wolke JG, Birgani ZT, Habibovic P, Jansen JA, Tampieri A, Marcacci M, Leeuwenburgh SC, van den Beucken JJ. *Substrate geometry directs the in vitro mineralization of calcium phosphate ceramics. Acta Biomater* 2014;10(2):661-9.
17. Yuan H, Fernandes H, Habibovic P, de Boer J, Barradas AM, de Ruiter A, Walsh WR, van Blitterswijk CA, de Bruijn JD.

- Osteoinductive ceramics as a synthetic alternative to autologous bone grafting. Proc Natl Acad Sci U S A 2010;107(31):13614-9.*
18. *Kwon S-H, Jun Y-K, Hong S-H, Kim H-E. Synthesis and dissolution behavior of β -TCP and HA/ β -TCP composite powders. Journal of the European Ceramic Society 2003;23(7):1039-1045.*
 19. *Kokubo T. Surface chemistry of bioactive glass-ceramics. Journal of Non-Crystalline Solids 1990;120(1-3):138-151.*
 20. *Wang L, Nancollas GH. Calcium orthophosphates: crystallization and dissolution. Chem Rev 2008;108(11):4628-69.*
 21. *Xin R, Leng Y, Chen J, Zhang Q. A comparative study of calcium phosphate formation on bioceramics in vitro and in vivo. Biomaterials 2005;26(33):6477-6486.*
 22. *Driessens F.C.M. VRME. Relation between physico-chemical solubility and biodegradability of calcium phosphates. Amsterdam: Elsevier Science Publishers 1988.*
 23. *Driessens FC, Verbeeck RM, van Dijk JW, Borggreven JM. Degree of saturation of blood plasma in vertebrates with octocalcium phosphate. Z Naturforsch C 1988;43(1-2):74-6.*
 24. *Ohtsuki C, Kokubo, T., Neo, M., Kotani, S., Yamamuro, T., Nakamura, T. & Bando, Y. Bone-bonding mechanism of sintered β -3 CaO P₂O₅. Phosphorus Res. Bull. 1991;1:191-196.*

CALCIUM PHOSPHATE CERAMICS FOR BONE REGENERATION

25. Kotani S, Fujita Y, Kitsugi T, Nakamura T, Yamamuro T, Ohtsuki C, Kokubo T. Bone bonding mechanism of beta-tricalcium phosphate. *J Biomed Mater Res* 1991;25(10):1303-15.
26. Li Y, Liu J, Shi F, Tang N, Yu L. [Preparation of hydroxyapatite coating in concentrated simulated body fluid by accelerated biomimetic synthesis]. *Sheng Wu Yi Xue Gong Cheng Xue Za Zhi* 2007;24(6):1314-8.
27. Jayasuriya AC, Shah C, Ebraheim NA, Jayatissa AH. Acceleration of biomimetic mineralization to apply in bone regeneration. *Biomed Mater* 2008;3(1):015003.
28. Chen Y, Mak AF, Li J, Wang M, Shum AW. Formation of apatite on poly(alpha-hydroxy acid) in an accelerated biomimetic process. *J Biomed Mater Res B Appl Biomater* 2005;73(1):68-76.
29. Barrere F, van BC, de GK, Layrolle P. Nucleation of biomimetic Ca-P coatings on ti6Al4V from a SBF x 5 solution: influence of magnesium. *Biomaterials* 2002;23(10):2211-20.
30. Tas AC, Bhaduri SB. Rapid coating of Ti6Al4V at room temperature with a calcium phosphate solution similar to 10× simulated body fluid. *Journal of Materials Research* 2004;19(09):2742-2749.
31. Chow LC. Next generation calcium phosphate-based biomaterials. *Dent Mater J* 2009;28(1):1-10.

7

EFFECT OF CALCIUM PHOSPHATE CERAMIC SUBSTRATE GEOMETRY ON MSC ORGANIZATION AND OSTEOGENIC DIFFERENTIATION

1. Introduction

One of the most challenging aspects in tissue regenerative research is to find an appropriate material for bone regeneration therapy. Because of high osteoinductive and osteoconductive capacities, autologous bone graft still is the most frequently applied material for bone regeneration [1]. However, bone grafting is an invasive procedure, associated with high morbidity due to a second surgery site and the amount of grafted bone is rather limited [2]. In view of this, it has become a scientific challenge to find effective alternatives for autologous bone graft.

Calcium phosphate (CaP) based biomaterials are the most frequently used synthetic alternatives in bone regenerative research, because their chemical composition resembles the inorganic part of bone [3] and these materials possess a high bioactive and osteoconductive capacity [4]. It has been demonstrated that an implant surface, coated with a layer of CaP, favors bone healing resulting in firm fixation between bone and implant [5]. For this biological osseointegration process, surface topography is known to play a crucial role [6]. Even more interestingly, Ripamonti et al. have extensively investigated the osteoinductive effect of (repetitive) surface concavities of bulk CaP ceramics and CaP-coated titanium implants [7-9]. These studies have demonstrated that the presence of surface concavities provides osteoinductive capacity without loading any osteogenic factors or osteogenic cells on the CaP

ceramics. Evidently, CaP ceramics in combination with implant surface geometry can have a strong effect on the final biological performance [7].

The concept of mineralization within the concavities was studied recently, and it was shown that concavity dimensions can control cell-free mineralization process in simulated body fluid [10]. Among the concavities in different CaP ceramic materials, the mineralization process started preferentially in small concavities (~440 μm hemispheres) on hydroxyapatite (HA) disks sintered at 1200 $^{\circ}\text{C}$, where the mineralization was increased 124- and 10-fold in the small concavities compared to large (~1800 μm hemispheres) and medium (~800 μm hemispheres) concavities respectively [10].

From a cellular perspective, it is known that CaP ceramics (e.g. hydroxyapatite, HA, and tricalciumphosphate, TCP) can promote proliferation and osteogenic differentiation of cells [11, 12]. Several studies indicated that micro- and nano-scale surface morphology of CaP ceramics strongly influence cell adhesion, proliferation and differentiation [13-15]. However, little is known about the effect of such surface concavities on the cell behavior of MSCs [16].

To evaluate the effect of surface concavities on CaP ceramics on the cellular behavior of MSCs, human adipose tissue derived mesenchymal stromal cells (AT-MSCs) were cultured on CaP ceramic scaffolds with different surface concavity sizes. The outcome parameters included analyses on cellular organization, cell proliferation, and osteogenic differentiation. We hypothesized that compared to planar control surfaces, the pronounced 3D microenvironment

CALCIUM PHOSPHATE CERAMICS FOR BONE REGENERATION

of surface concavities promotes proliferation, organization as well as osteogenic differentiation of cells, resulting in mineral (CaP) nucleation in the concavities [10]. Additionally, we hypothesized that the proliferation and differentiation of cells increases with smaller concavity size due to a lower flow rate and more rapidly occurring 3D cell–cell interactions and subsequent molecular cross-talk.

2. Materials and methods

Substrate preparation and geometrical characteristics of disks

HA powder (Merck, Darmstadt, Germany) with a Ca/P molar ratio of 1.67 was used in this study. The powder was uniaxially pressed at 103 MPa (15,000 psi) for 10 min in a cylindrical steel mold (internal diameter ~21 mm). Subsequently, cylindrical HA ceramics were heat-treated in a furnace at 800°C for 6 h ($1.67\text{ }^{\circ}\text{C min}^{-1}$) to provide suitable strength to the ceramic to withstand the stresses applied during the machining process. Thereafter, heat-treated HA cylinders were cut into disks (thickness 4 mm, diameter 21 mm). Drill tips with different diameter sizes (2.1, 1.0 and 0.5 mm; Horico Dental, Berlin, Germany) were used to prepare hemispherical concavities at the disk surfaces. Subsequently, the disks were sintered in a furnace for 6 h ($1.67\text{ }^{\circ}\text{C min}^{-1}$) at 1200°C, by which disk dimensions were reduced to 3 mm thickness and 16 mm diameter and cavities sizes to diameters of 440 μm (small concavity; SC), 800

μm (medium concavity; MC) and $1800 \mu\text{m}$ (large concavity; LC). Afterwards, the disks were prepared based on the experimental setup.

For imaging methods, the heat-treated HA disks were divided (without cutting) in three different regions, each containing a specific cavity size/diameter (SC $\rightarrow 440 \mu\text{m}$, MS $\rightarrow 800 \mu\text{m}$ or LC $\rightarrow 1800 \mu\text{m}$) with a total 6 cavities for each size. The flat surface in the centre of the disk was considered as a control surface (**Figure 1a**).

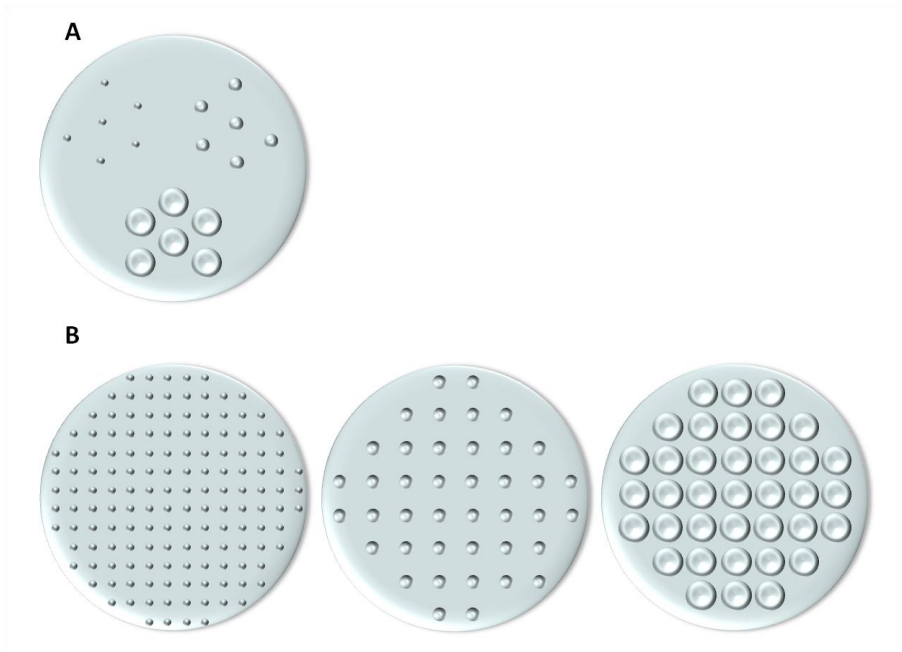


Figure 1. Schematic representation of disk surface geometry employed in the study. (A) Schematic distribution of the concavities at the surface of the disks for confocal microscopy; 6 concavities of each size (small cavity (SC) $\rightarrow 440 \mu\text{m}$, medium cavity (MC) $\rightarrow 800 \mu\text{m}$; and large cavity (LC) $\rightarrow 1800 \mu\text{m}$) were prepared on the surface of the disks, and the center to center distance was kept the same (SC=2.1, MC=2.5, LC=2.8 mm). The planar surface in the centre of the disk was considered as a control planar surface (PS). (B) Schematic distribution of the concavities at the surface of the disks for biochemical assays.

CALCIUM PHOSPHATE CERAMICS FOR BONE REGENERATION

Disks were completely covered with each size of concavities (SC, MC, LC) and the center to center distance was kept the same (SC=0.6, MC=1.2, LC=2.7 mm).

For the evaluation of cellular behavior and gene expression, the heat-treated HA disks were covered completely with the same type of concavities i.e. only SC, MS or LC. The total number of hemispherical concavities in each disk was 148 for SC, 42 for MC, and 36 for LC, resulting in a total surface area respectively 2.23 cm² (SC), 2.22 cm² (MC) and 2.92 cm² (LC). As a control group, disks with planar surface (PS) were used with a total surface area of 2,01 cm² (**Figure 1b**). Each disk was cut into four equal parts (n=4). Before cell seeding, disks were sterilized by autoclavation.

AT-MSc isolation, expansion and characterization

AT-MSCs were isolated from fat tissue of healthy donors via the Department of Plastic Surgery (Radboudumc, Nijmegen, the Netherlands) after written informed consent, following a previously described AT-MSCs isolation procedure [17, 18]. Harvested cells were cultured in proliferation media, consisting of alpha Minimal Essential Medium (α -MEM; Gibco[®], Life Technologies, Grand Island, USA) supplemented with 5% platelet lysate (PL, Sanquin Blood Bank, Nijmegen, the Netherlands), 100 U/ml penicillin (Gibco[®]), 10 μ g/ml streptomycin (Gibco[®]), and 10 U/ml heparin (LEO Pharma, Amsterdam, the Netherlands) at 37°C in a humid atmosphere with 5% CO₂.

Medium was changed twice a week. Cells were passaged upon reaching ~80% confluency using 0.25% w/v trypsin/0.02% EDTA (Gibco®).

Biochemical assays for cellular behavior

AT-MSCs were cultured in osteogenic media with 10,000 cells/cm² seeding density (relative to planar surface), consisting of α -MEM supplemented with 5% PL (Sanquin), 100 U/ml penicillin (Gibco®), 10 μ g/ml streptomycin (Gibco®), 10 U/ml heparin (LEO Pharma), 0.2 mM L-ascorbic acid-2-phosphate (Sigma-Aldrich, St. Louis, MO, USA), 2mM L-glutamine (Gibco®), 10⁻⁸M dexamethasone (Sigma-Aldrich) and 0.01 M β -glycerophosphate, at 37°C in a humid atmosphere with 5% CO₂. Cell proliferation was evaluated with a DNA assay and osteogenic differentiation was evaluated with an ALP-activity assay. Samples were collected at 3 time points relative to cell seeding (i.e. day 3, 14, 28). The same samples were used for DNA and ALP assay.

Cellular DNA content

The cellular DNA content was measured using a QuantiFluor® dsDNA System Kit (Promega, the Netherlands). For the standard curve, serial dilutions of dsDNA stock (range: 0-2000 ng/ml) were prepared. Next, 100 μ l of either sample of standard solution was added into the wells, followed by 100 μ l of working solution. The plate was incubated at room temperature for 5 min, and then the absorbance of samples/standards was measured at 450 nm using a fluorescence microplate reader (FL600, BioTek, Canada).

CALCIUM PHOSPHATE CERAMICS FOR BONE REGENERATION

Alkaline phosphatase (ALP) activity

ALP activity was measured using a 5 nM p-nitrophenyl phosphate (4-NP) colorimetric assay (Sigma Aldrich). According to the manufacture instructions, 80 μ l of sample solution (the same samples used for the measurement of cellular DNA content) was combined with 20 μ l of buffer (0.5 M 2-amino-2methyl-1-propanol). For the standard curve, serial dilutions of 4-NP (range: 0-25 nmol) were used. Next, 100 μ l substrate solution (5 nM p-nitrophenyl phosphate) was added to the samples/standards and the plates were incubated for 60 min at 37°C. The reaction was stopped by adding 50 μ l 0.3M NaOH. The absorbance of samples was measured at 405 nm using an ELISA microplate reader (EL800, BioTek, Abcoude, the Netherlands). The ALP content was normalized using the corresponding cellular dsDNA amount.

Immunofluorescence and quantitative cell measurements

For the immunofluorescence and quantitative cell measurements, the seeding density was 10.000 cells/cm² (relative to planar surface). At selected time points (3, 14, 21 and 28 days), cells were washed 2x in phosphate buffered saline (PBS, Gibco®), fixed in 2% paraformaldehyde (PFA, Sigma-Aldrich) for 20 min, permeabilized by 0.25% Triton X100 (Koch, Light-Laboratories, Colebrook, UK) in PBS for 10 min, washed again 2x in PBS and blocked in 1% BSA (Sigma Aldrich) for 1 hour. Thereafter, cells were washed 2x in PBS and stained as follows:

1. For the visualization of dsDNA in nucleus, cells were stained with blue fluorescent DAPI (Invitrogen, Molecular probes) for 1 min, in a dilution of 1:2500. Afterwards, cells were washed 2 x 5 min in PBS;
2. For the visualization of cytoskeletal morphology, the filamentous F-actin was stained with Alexa Flour[®] 568 phalloidin (Invitrogen, Molecular probes, Eugene-Oregon, USA) for 2 hours, in a dilution of 1:250. Afterwards cells were washed 2 x 5 min in PBS;
3. For visualization of the osteogenic marker osteocalcin, cells were stained with a monoclonal osteocalcin antibody, labeled with Alexa Flour[®] 488 (Novus Biologicals, Cambridge, UK) for 2 hours in a dilution of 1:1000. Afterwards, cells were washed 2 x 5 min in PBS.

Subsequently, the samples were mounted with Mowiol[®] 4.88 solution (Merk Millipore, Darmstadt, Germany), covered with cover-glasses, and stored at +4°C for immunofluorescence analysis.

For visualization of calcium crystals at the same time points (3, 7, 14, and 28 days), separate samples were stained in 2% (2g in 100ml) Alizarin Red S 598 (ScienCell Research Laboratories, Carlsbad CA, USA) for 15 min. Subsequently, samples were washed 5x with PBS for 1 min and stained with blue fluorescent DAPI for 1min in a dilution 1:2500. Afterwards, the samples were mounted with Mowiol[®] 4.88 solution (Merk Millipore, Darmstadt,

CALCIUM PHOSPHATE CERAMICS FOR BONE REGENERATION

Germany), covered with coverglasses, and stored at +4°C for immunofluorescence analysis.

In order to visualize the presence of cells on the scaffold surface and the presence of molecules of interest, after each staining, the samples were analyzed first with a fluorescence microscope (Axio Imager Microscope Z1, Carl Zeiss Micro imaging, Gottingen, Germany). The excitation and emission wavelength for a filamentous F-actin was 568 and 603 nm respectively, for dsDNA (DAPI) was 405 and 428 nm, for osteocalcin was 495 and 519 nm, and for alizarin red staining was 590 and 617 nm, respectively. The images were captured with 20x/0.75 objective.

To obtain high-resolution 3D images for analysis of cellular organization within concavities, the samples were analyzed using confocal laser scanning microscopy (CLSM; Olympus FV1000, Olympus, Center Valley PA, USA). The images were captured with 20x/0.75 objective. In order to obtain qualitative and quantitative data on concavity volumes, the images were analyzed with Image J software (Centre for Information Technology, National institutes of Health, Bethesda MD, USA). Cell nuclei were quantified with 3D object counter plugin from image J, prior to analysis the number of object's voxels and threshold were set on the images [19].

Statistical analysis

Data are presented as mean \pm standard deviation. Statistical analysis was performed with Graphpad Prism[®] 5.03 software (Graphpad Software Inc,

San Diego, CA, USA). Quantitative results were analyzed using a one-way ANOVA with a posthoc Tukey Multiple Comparisons Test. A probability (p) value <0.05 was considered statistically significant.

3. Results

Cellular behavior

According to results of DNA content, in the first 14 days, the highest cell proliferation was observed on the PS disks, where the proliferation of SC disk showed the lowest cell proliferation. However, after 28 days of culture, an increase of cell proliferation was observed on the SC and MC disks compared with the PS disks at the same time point (**Figure 2a**). Because of the differences between the available surface area of the disks (PS $\rightarrow 2.01 \text{ cm}^2$, SC $\rightarrow 2.23 \text{ cm}^2$, MC $\rightarrow 2.22 \text{ cm}^2$ and LC $\rightarrow 2.92 \text{ cm}^2$), the results of DNA content were normalized for surface area (**Figure 2b**). After normalization, the pattern of the cell proliferation in each group remained similar, showing at day 14 significantly lower DNA-content values for SC ($p < 0.001$), MC ($p < 0.001$), and LC ($p < 0.05$), and at day 28 significantly higher DNA-content values for SC ($p < 0.01$) and MC ($p < 0.01$) compared to PS. Additionally, DNA-content values showed a tendency to decrease with smaller surface concavity size at day 14, and to increase with smaller surface concavity at day 28.

CALCIUM PHOSPHATE CERAMICS FOR BONE REGENERATION

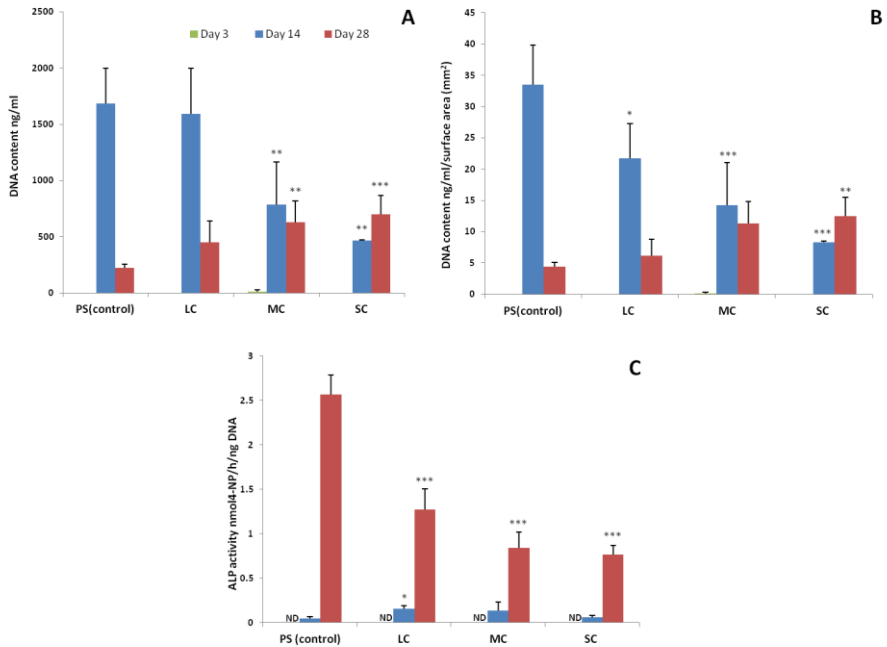


Figure 2. (A) Cellular DNA content (ng/ml)/proliferation level during 28 days of culture. (B) Cellular DNA content normalized for surface area of the disks. (C) ALP-activity during 28 days of culture. Cellular behavior within different concavity sizes. P-values (* $p < 0.05$, (** $p < 0.01$, (***) $p < 0.001$) indicate significant differences compared to PS at the same time point. ND means not determined.

At day 28, ALP-activity was significantly lower ($p < 0.001$) for SC, MC, and LC compared to PS. Similar as for DNA-content values, a tendency to decreasing ALP-activity values with decreasing surface concavity size was observed at day 28.

Cellular organization

Analysis of Immunofluorescence measurement

The samples for immunofluorescence measurements were stained with 3 different dyes, i.e. DAPI (in blue) for nuclear visualization, actin (in red) for visualization of the cytoskeleton, and osteocalcin (in green) for the identification of this late stage marker of osteogenic differentiation.

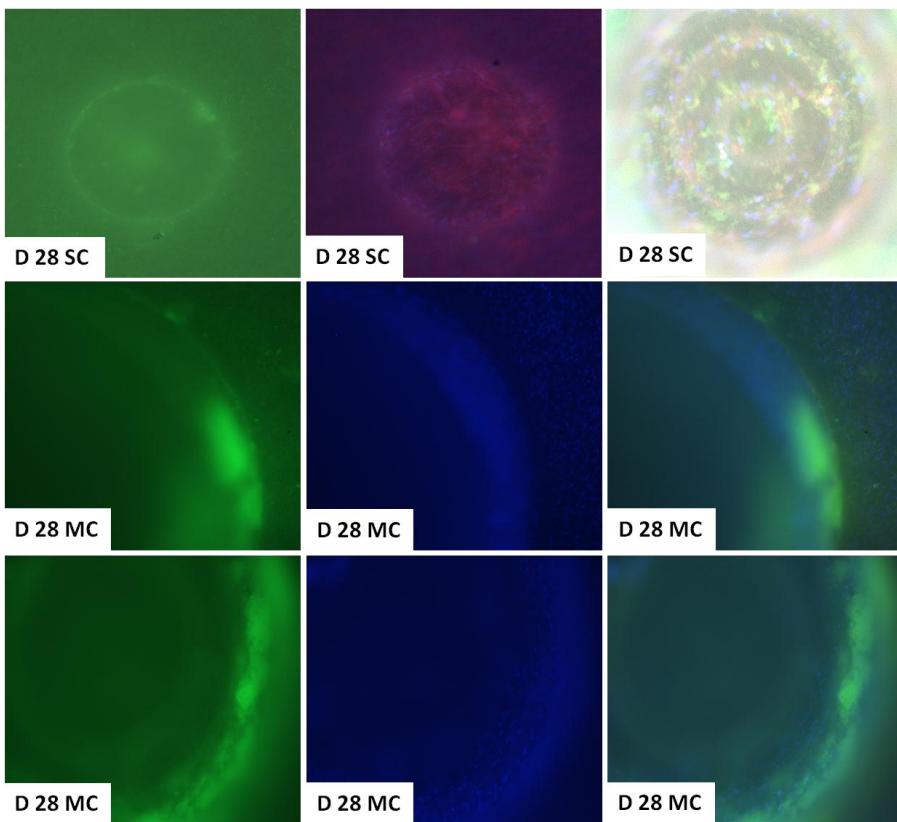


Figure 3. Fluorescence microscopy images. For visualization of dsDNA in nuclei, cells were stained with fluorescent DAPI (in blue); for cytoskeletal structure visualizations, filamentous F-actin (in cells) was stained with Alexa Flour[®] 568 phalloidin (in red); for visualization of osteocalcin, cells were

CALCIUM PHOSPHATE CERAMICS FOR BONE REGENERATION

stained with a monoclonal osteocalcin antibody, labeled with Alexa Flour[®] 488 (in green).

After each staining, samples were checked with fluorescence microscopy (Figure 3). The simultaneous visualization of the 3 stainings was possible only for the 28 day samples, as osteocalcin staining was not detectable at earlier time points. According to the fluorescence microscopy results, osteocalcin was detectable in SC and MC concavities. In SC, the green color was distributed within the entire concavity volume, while in MC osteocalcin was detected only on the edges of the concavities (**Figure 3**).

To analyze the mineralization pattern of AT-MSCs, samples were stained with Alizarin Red S 598 (**Figure 4**). During 28 days of culture a gradual increase of calcium crystals (stained in red) was observed on the surface of experimental scaffolds onto which cells had been cultured. The negative control at day 28 showed no positive Alizarin staining.



Figure 4. *Qualitative evaluation of calcium deposition during 28 days of culture. Samples were stained with Alizarin Red S 598 (in red).*

Qualitative analysis of confocal microscopy results

In the confocal microscopy images after 3 days of culture, only few cells were observed for all concavity sizes (**Figure 5a**). However, several differences in cellular organization, i.e. cell distribution in the different concavity sizes, were detectable. In the SC and MC, cells were distributed already in a 3D volume, where in LC cells generally covered the concavity walls (**Figure 5a**).

After 14 days of culture, a high increase in the number of cell nuclei was observed for all concavity sizes. In SC and MC, cells created an apparent multilayered cell sheet, covering the surface area of concavity walls, and in SC cells started to fill the entire concavity volume (3D cellular organization). The planar surface area between concavities was also covered with a cellular multilayer. In contrast to SC and MC, the cellular organization in LC was different, where cell populations were localized in two levels on the concavity walls close to planar surface area of the disk and at the bottom of the concavities. At day 14, still a gap between these two cell populations in LC was observed (**Figure 5b**).

After 21 days of culture, very densely distributed cell nuclei were observed in SC and MC. In SC, cells were homogeneously distributed the entire concavity volume. In MC, the cellular organization was different from SC with a less dense cell population in the concavity center compared to the edges of the concavities. The cellular organization in LC at day 21 was similar to the LC at day 14 with a separation in two cell populations (on the concavity walls close to

CALCIUM PHOSPHATE CERAMICS FOR BONE REGENERATION

surface area of the disk and at the bottom of the concavities), and still a gap between those populations (**Figure 5c**).

After 28 days of culture, cells in SC and MS were homogenously distributed within the entire concavity volumes. At day 28, cells also reached the highest deepness within the concavities in SC and MC. However, in LC the cellular organization was still different from SC and MC, with still the existence of two separated cell populations, but the distance between those populations was smaller compared to day 21 (**Figure 5d**).

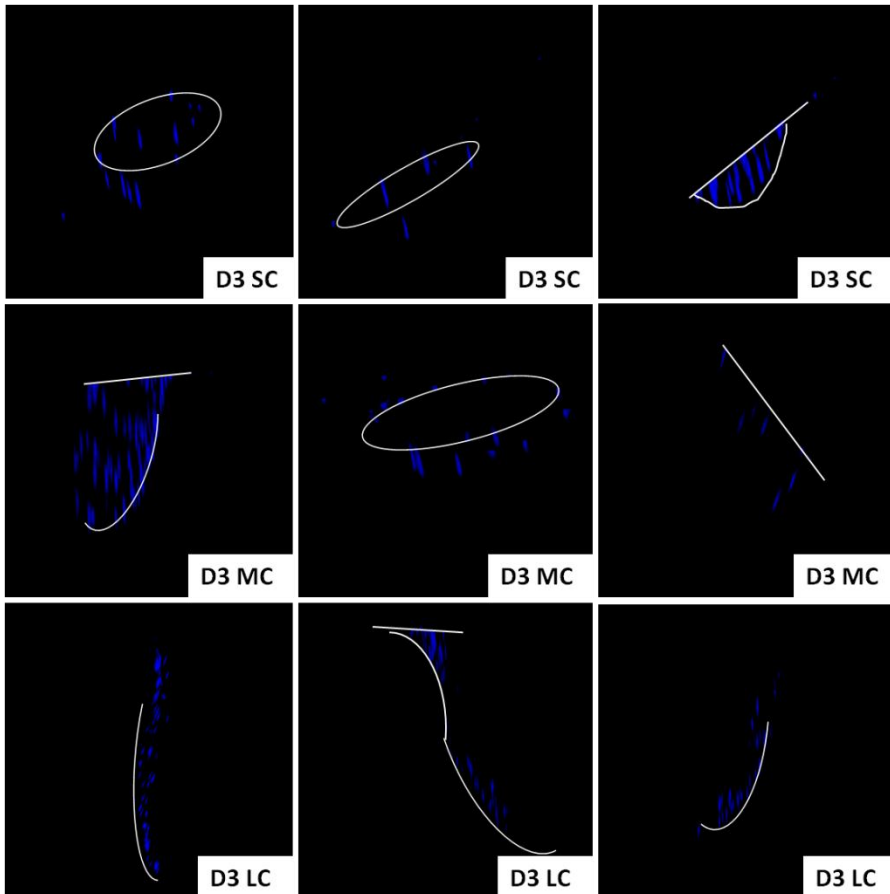
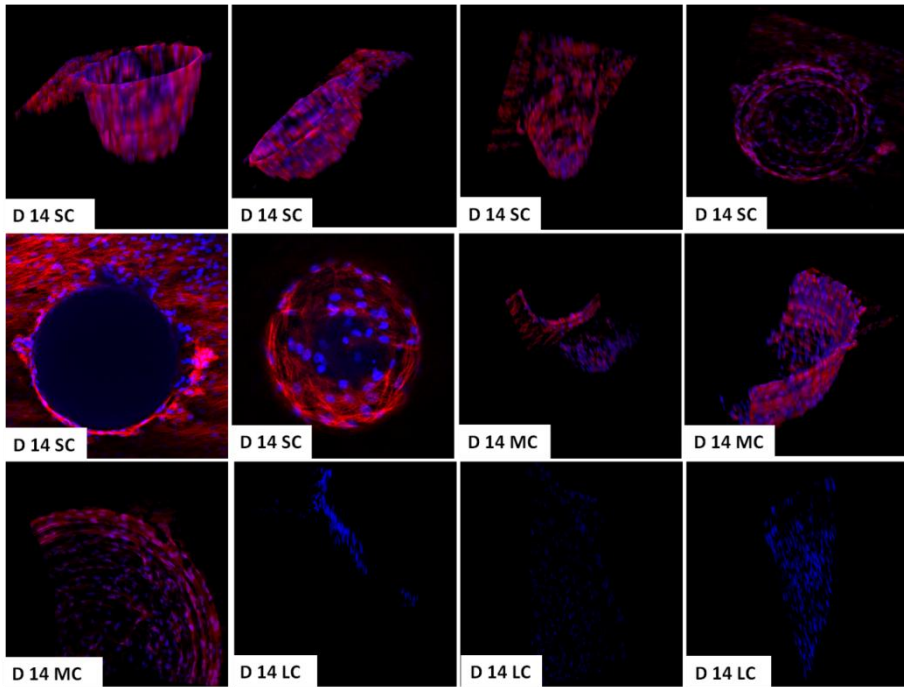
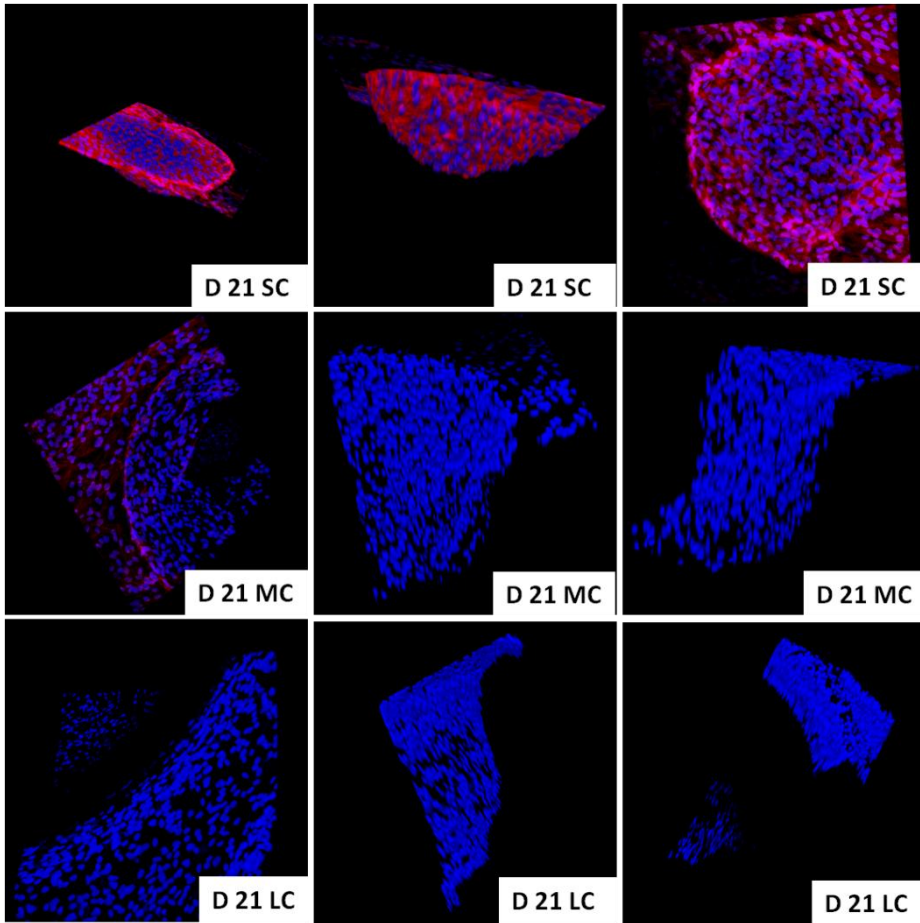


Figure 5. Confocal microscopy images with 3D reconstruction of SC, MC and LC. Cell nuclei were stained with fluorescent DAPI (in blue); filamentous F-actin (in cells) was stained with Alexa Flour[®] 568 phalloidin (in red). (a) Samples with different concavity sizes after 3 days of culture.

CALCIUM PHOSPHATE CERAMICS FOR BONE REGENERATION

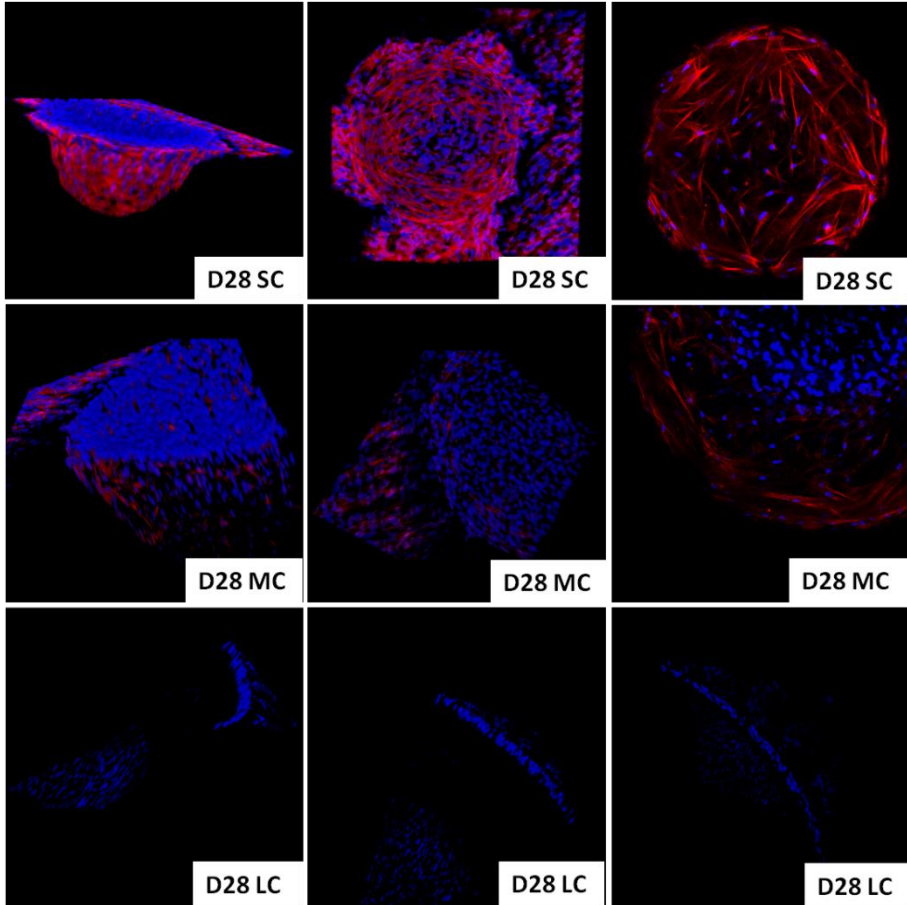


(b) Samples with different concavity sizes after 14 days of culture



(c) Samples with different concavity sizes after 21 days of culture.

CALCIUM PHOSPHATE CERAMICS FOR BONE REGENERATION



(d) Samples with different concavity sizes after 28 days of culture.

Quantitative analysis of cellular organization

The cell nuclei were quantified in SC, MC and LC at all time points. For SC and MC, a gradual increase of cell nuclei was observed until day 28. The number of the nuclei was normalized for concavity volume (**Figure 6**). In the first 3 days, the average number of cell nuclei per mm^3 (based on $n=3$) in SC was 793 ± 181 , in MC 464 ± 529 and in LC 497 ± 46 . After 14 days, an increase of cell nuclei was observed for all groups, where the average (based on $n=3$) number of nuclei per

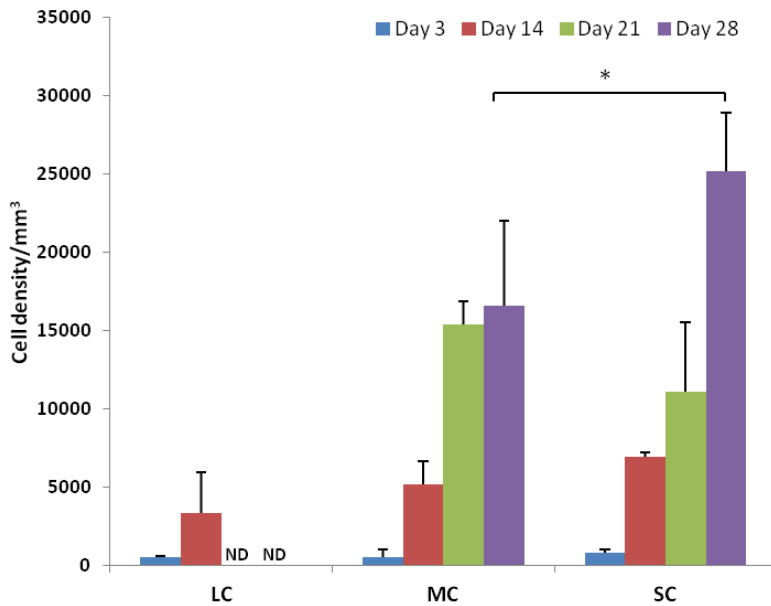


Figure 6. Results of quantitative analysis of the number of cell nuclei within the concavities normalized for concavity volume. *P*-values (* $p < 0.05$, ** $p < 0.01$, *** $p < 0.001$) indicate significant differences compared to PS at the same time point. ND means not determined.

CALCIUM PHOSPHATE CERAMICS FOR BONE REGENERATION

mm³ in SC was 6939 ± 247 , in MC 5138 ± 1481 , and in LC 3310 ± 2585 . Then, at day 21 even higher cell densities were observed with per mm³ in SC 11096 ± 4416 nuclei and in MC 15412 ± 1481 nuclei. Cell nuclei counts in LC at days 21 and 28 were not possible due to large data information and limited capability of the software (Image J). Finally, at day 28 a significantly higher cell density ($p=0.0329$) was observed in SC with an average number of nuclei per mm³ of 25153 ± 3736 compared to MC with 16601 ± 1476 nuclei.

4. Discussion and conclusion

The aim of this study was to evaluate the effect of surface concavities in CaP ceramic scaffolds on cellular organization, cell proliferation, and osteogenic differentiation. We hypothesized that compared to planar control surfaces, the pronounced 3D microenvironment of surface concavities promotes proliferation, organization as well as osteogenic differentiation of cells, resulting in mineral (CaP) nucleation in the concavities [10]. Additionally, we hypothesized that the proliferation and differentiation of cells increases with smaller concavity size due to a lower flow rate and more rapidly occurring 3D cell–cell interactions and subsequent molecular cross-talk. The main findings of this study were that surface concavities evoked cell proliferation pattern, which was dependent of concavity sizes. The small size concavities increased cell proliferation to a larger extent compared to medium and large concavities. Additionally, concavity size influenced cellular organization within concavities,

and their distribution in 2D or 3D. Finally, concavity size influenced osteogenic differentiation of cells, based on results of osteocalcin expression only in small (440 μm) and medium (800 μm) surface concavities.

Our study indicated that surface concavities affect cell proliferation, which was proven by quantitative analysis of cell nuclei within the concavities. In addition, the proliferation pattern promoted by different concavity sizes was altered. The small concavities increased cell proliferation to a larger extent, because at day 28 the highest cell number (nuclei) was found in small concavities. The quantitative analysis of cell nuclei showed that concavities can affect on cell proliferation and that proliferation potential of cells increases with smaller concavity size, possibly due to the cell proximity, because the distance between cells have shown to influence cellular communication [20]. The cell-cell interaction and cellular communication is based on molecular exchange, which activates appropriate signals in cells. This phenomenon is called sense of smell [21, 22]. In addition, cells are able to adhere to the surface and recognize its geometrical properties, and they sense and respond to geometrical stimuli [23, 24]. This adhesion-mediated signaling provides cells with information about their microenvironment, including geometrical and chemical characteristics of substrate [25]. Our results indicate that cells were able to recognize the geometrical properties of surface, based on proliferation and differentiation results in different concavity sizes.

The fact that CaP based biomaterials with specific surface geometry can promote bone formation *in vivo*, was proven by several studies [26-29].

CALCIUM PHOSPHATE CERAMICS FOR BONE REGENERATION

However, little is known about the influence of CaP based biomaterials combined with geometrical properties (size, shape) on cellular organization and cell differentiation [14]. In this study, we found that concavity size can influence cellular organization, because already at day 3 in small and medium concavities cells were distributed in a 3D manner in contrast to large concavities, in which cells were distributed still at a 2D level. This observation can be explained by the fact that cells recognize geometrical properties of the surface and respond differently to their cellular organization [23, 24].

Next, the results of mineralization of cells on the surface of experimental scaffolds (covered with different size concavities) showed a gradual increase of Ca deposition, which indicates that cells can proliferate as well as differentiate on the surface of CaP based biomaterials. However, the method to visualize Ca deposition (Alizarin Red S staining) was not selective for the quantification of mineralization level in different concavity sizes. Therefore, for the analysis of osteogenic differentiation/mineralization within the concavities, the secretion of osteocalcin (osteogenic differentiation marker) was analyzed. We observed that concavity size influences osteogenic differentiation of MSCs, because osteocalcin was found in small and medium concavities, but not in large concavities. This is an indication that extracellular stimulation factors (e.g. geometrical properties, cell-cell communication, and local calcium nucleation) can provide specific signal activation and osteogenic differentiation of MSCs.

In conclusion, CaP disks covered with different surface concavities (in size) were able to affect MSCs behavior in terms of proliferation and osteogenic differentiation. The results of this study suggest a correlation between concavity size, cell proliferation, cellular organization and osteogenic differentiation of cells within surface concavities. Finally, in order to develop advanced scaffolds able to mimic the natural bone microenvironment, it is critical to understand how cells interact with 3D matrices, recognize their surface properties (e.g. at geometrical, physical, and chemical levels), and use intracellular signaling pathways responsible for that interaction and subsequent behavior [30].

References

1. Barradas, A.M., et al., Secondary author, *Molecular mechanisms of biomaterial-driven osteogenic differentiation in human mesenchymal stromal cells. Integrative Biology*, 2013. 5(7): p. 920-931.
2. Arrington, E.D., et al., Secondary author, *Complications of iliac crest bone graft harvesting. Clinical orthopaedics and related research*, 1996. 329: p. 300-309.
3. Giannoudis, P.V., H. Dinopoulos, and E. Tsiridis, Secondary author, *Bone substitutes: an update. Injury*, 2005. 36(3): p. S20-S27.
4. LeGeros, R.Z., Secondary author, *Calcium phosphate-based osteoinductive materials. Chemical reviews*, 2008. 108(11): p. 4742-4753.
5. Le Guéhennec, L., et al., Secondary author, *Surface treatments of titanium dental implants for rapid osseointegration. Dental materials*, 2007. 23(7): p. 844-854.
6. Cooper, L.F., Secondary author, *A role for surface topography in creating and maintaining bone at titanium endosseous implants. The Journal of prosthetic dentistry*, 2000. 84(5): p. 522-534.
7. Ripamonti, U., L.C. Roden, and L.F. Renton, Secondary author, *Osteoinductive hydroxyapatite-coated titanium implants. Biomaterials*, 2012. 33(15): p. 3813-3823.

8. *Lee, B.L.-P., et al., Secondary author, Femtosecond laser ablation enhances cell infiltration into three-dimensional electrospun scaffolds. Acta biomaterialia, 2012. 8(7): p. 2648-2658.*
9. *Graziano, A., et al., Secondary author, Concave pit-containing scaffold surfaces improve stem cell-derived osteoblast performance and lead to significant bone tissue formation. PloS one, 2007. 2(6): p. e496.*
10. *Bianchi, M., et al., Secondary author, Substrate geometry directs the in vitro mineralization of calcium phosphate ceramics. Acta biomaterialia, 2014. 10(2): p. 661-669.*
11. *Ma, J., et al., Secondary author, Bone forming capacity of cell- and growth factor-based constructs at different ectopic implantation sites. Journal of Biomedical Materials Research Part A, 2014: p. n/a-n/a.*
12. *Helder, M.N., et al., Secondary author, Stem cells from adipose tissue allow challenging new concepts for regenerative medicine. Tissue engineering, 2007. 13(8): p. 1799-1808.*
13. *Prodanov, L., et al., Secondary author, The effect of nanometric surface texture on bone contact to titanium implants in rabbit tibia. Biomaterials, 2013. 34(12): p. 2920-2927.*
14. *Ripamonti, U., Secondary author, Biomimetism, biomimetic matrices and the induction of bone formation. Journal of cellular and molecular medicine, 2009. 13(9b): p. 2953-2972.*

CALCIUM PHOSPHATE CERAMICS FOR BONE REGENERATION

15. Scarano, A., et al., Secondary author, *Experimental evaluation in rabbits of the effects of thread concavities in bone formation with different titanium implant surfaces. Clinical implant dentistry and related research*, 2013.
16. Sun, Y., C.S. Chen, and J. Fu, Secondary author, *Forcing stem cells to behave: a biophysical perspective of the cellular microenvironment. Annual review of biophysics*, 2012. 41: p. 519-542.
17. Oedayrajsingh-Varma, M., et al., Secondary author, *Adipose tissue-derived mesenchymal stem cell yield and growth characteristics are affected by the tissue-harvesting procedure. Cytotherapy*, 2006. 8(2): p. 166-177.
18. Ma, J., et al., Secondary author, *Osteogenic capacity of human BM-MSCs, AT-MSCs and their co-cultures using HUVECs in FBS and PL supplemented media. Journal of tissue engineering and regenerative medicine*, 2013.
19. Bolte, S. and F.P. CordeliÈRes, Secondary author, *A guided tour into subcellular colocalization analysis in light microscopy. Journal of Microscopy*, 2006. 224(3): p. 213-232.
20. Grellier, M., L. Bordenave, and J. Amedee, Secondary author, *Cell-to-cell communication between osteogenic and endothelial lineages: implications for tissue engineering. Trends in biotechnology*, 2009. 27(10): p. 562-571.

21. Ben-Shlomo, I., et al., Secondary author, *Signaling receptome: a genomic and evolutionary perspective of plasma membrane receptors involved in signal transduction*. *Science Signaling*, 2003. 2003(187): p. re9.
22. Kollmannsberger, P., et al., Secondary author, *The physics of tissue patterning and extracellular matrix organisation: how cells join forces*. *Soft Matter*, 2011. 7(20): p. 9549-9560.
23. Vogel, V. and M.P. Sheetz, Secondary author, *Cell fate regulation by coupling mechanical cycles to biochemical signaling pathways*. *Current opinion in cell biology*, 2009. 21(1): p. 38-46.
24. Joly, P., et al., Secondary author, *Geometry-driven cell organization determines tissue growths in scaffold pores: consequences for fibronectin organization*. *PloS one*, 2013. 8(9): p. e73545.
25. Bershadsky, A., M. Kozlov, and B. Geiger, Secondary author, *Adhesion-mediated mechanosensitivity: a time to experiment, and a time to theorize*. *Current opinion in cell biology*, 2006. 18(5): p. 472-481.
26. Yuan, H., et al., Secondary author, *Bone induction by porous glass ceramic made from Bioglass®(45S5)*. *Journal of biomedical materials research*, 2001. 58(3): p. 270-276.
27. Ripamonti, U., J. Crooks, and A. Kirkbride, Secondary author, *Sintered porous hydroxyapatites with intrinsic osteoinductive activity: geometric induction of bone formation*. 1999.

CALCIUM PHOSPHATE CERAMICS FOR BONE REGENERATION

28. Yuan, H., et al., Secondary author, *Tissue responses of calcium phosphate cement: a study in dogs. Biomaterials*, 2000. 21(12): p. 1283-1290.
29. Barradas, A., et al., Secondary author, *Osteoinductive biomaterials: current knowledge of properties, experimental models and biological mechanisms. European cells & materials*, 2011. 21: p. 407-429.
30. Hakkinen, K.M., et al., Secondary author, *Direct comparisons of the morphology, migration, cell adhesions, and actin cytoskeleton of fibroblasts in four different three-dimensional extracellular matrices. Tissue Engineering Part A*, 2010. 17(5-6): p. 713-724.

8

ENGLISH SUMMARY, DUTCH SUMMARY, CLOSING REMARKS, AND FUTURE PERSPECTIVES

CALCIUM PHOSPHATE CERAMICS FOR BONE REGENERATION

English summary and address to the aims

The aim of the current thesis was to investigate the physicochemical and biological properties of various calcium phosphate (CaP) ceramics as either CaP coatings or bulk CaP ceramics for biomedical applications, with major focus on CaP composition and surface morphology. Specifically, **Chapter 1** provides a general introduction on properties of bioceramics, the characteristics of each bioceramic, their use as coatings, coating deposition techniques, and physical and biological interaction of these implants with bone tissue. This summary addresses the research questions as described in the first chapter in successive order.

1. What is the current knowledge on coatings using inorganic and/or organic materials and which techniques are available for the deposition of such coatings on metallic materials?

Synthetic inorganic and organic materials have been extensively investigated in the field of bone regeneration in an attempt to mimic the composition and structure of the extracellular matrix (ECM) of bone tissue with the ultimate aim of generating suitable synthetic bone substitute materials and modifying the surface of bone implants. For load-bearing applications, bone implants are generally made of a bioinert metal with appropriate mechanical properties and a modified surface (i.e. roughened, coated or a combination thereof), to enhance the surface biocompatibility and osteoconductivity.

Currently, biomaterials research is evolving from the use of bioinert and biologically passive implants toward interactive implants that stimulate tissue regeneration. Therefore, surface physico-chemical properties of bone implants need to be optimal and capable to biologically instruct and stimulate the regeneration of bone tissue.

Chapter 2 was focused on surface modification approaches in the field of bone regeneration for load-bearing bone implants with emphasis on the use of inorganic and organic coating compounds that actively participate in the biological processes that occur upon implantation. The review shows that appropriate surface modifications can be helpful to achieve desired tissue responses in healthy as well as compromised conditions.

2. What are the effects of CaP composition in sputter coatings on in vitro and in vivo performance?

Calcium phosphate (CaP) ceramic coatings have been used to enhance the biocompatibility and osteoconductive properties of metallic implants. The chemical composition of these ceramic coatings is an important parameter, which can influence the final bone performance of the implant. In **Chapter 3**, the effect of phase composition of CaP-sputtered coatings was investigated on in vitro dissolution behavior and in vivo bone response. Coatings were prepared by a radio frequency (RF) magnetron sputtering technique; three types of CaP target materials were used to obtain coatings with different stoichiometry and calcium to phosphate ratios (hydroxyapatite (HA), α -tricalciumphosphate (α -

CALCIUM PHOSPHATE CERAMICS FOR BONE REGENERATION

TCP), and tetracalciumphosphate (TTCP)) were compared with non-coated titanium controls. The applied ceramic coatings were characterized by X-ray diffraction, Fourier transform infrared spectroscopy, scanning electron microscopy, and inductively coupled plasma optical emission spectroscopy. The in vitro dissolution/precipitation of the CaP coatings was evaluated using immersion tests in simulated body fluid (SBF). To mimic the in vivo situation, these compositionally different CaP coatings were also evaluated in a femoral condyle rabbit model. TCPH and TTCPH showed morphological changes during 4-week immersion in SBF. The results of bone implant contact (BIC) and peri-implant bone volume (BV) showed a similar response for all experimental coatings. An apparent increase in tartrate-resistant acid phosphatase (TRAP) positive staining was observed in the peri-implant region with decreasing coating stability. In conclusion, the experimental groups showed different coating properties when tested in vitro and an apparent increase in bone remodeling with increasing coating dissolution in vivo.

3. What is the effect of different micrometer hydroxyapatite coating thicknesses on residual stress?

Bioceramic coatings, including calcium phosphate coatings composed of hydroxyapatite (HA), represent a common surface modification for metallic bone implants. In view of the mismatch in material properties between the ceramic coating material and the metallic substrate material, **Chapter 4** aimed to evaluate the residual stress within an HA-coating deposited using RF

magnetron sputtering via two different analyses, based on either the Stoney formula (i.e. based on curvature measurements of the substrate [Stoney, 1909]) or the $\sin^2 \psi$ method (i.e. based on X-ray diffraction patterns of the coating). Additionally, the effect of HA-coating thickness (i.e. 1 or 4 μm) on residual stress and surface topography were addressed. We hypothesized that (i) both methods to determine residual stress would show similar results, and that (ii) thick coatings would increase residual stress compared to thin coatings. The curvature measurements showed low residual stress values (ranging from -60 to 80 MPa), which showed relaxation upon post-deposition heat treatment at 650 °C. Similarly, lattice-based measurements of residual stress showed relaxation of HA coatings upon post-deposition heat treatment. Coating thickness variation in the micrometer scale showed no major effects on residual stress magnitude. For reasons of accuracy and similarity to the actual conditions, determination of residual stress via lattice-based techniques is preferable.

4. What is the role of hemispherical concavities on the in vitro mineralization of bioceramic materials?

Repetitive concavities on the surface of bone implants have recently been demonstrated to foster bone formation when implanted at ectopic locations *in vivo*. In **Chapter 5**, we aimed to evaluate the effect of surface concavities on the surface mineralization of hydroxyapatite (HA) and β -tricalcium phosphate (β -TCP) ceramics *in vitro*. Hemispherical concavities with different diameters were prepared at the surface of HA and β -TCP sintered

CALCIUM PHOSPHATE CERAMICS FOR BONE REGENERATION

disks: 1.8 mm (large concavity), 0.8 mm (medium concavity) and 0.4 mm (small concavity). HA and β -TCP disks were sintered at 1100 or 1200°C and soaked in simulated body fluid for 28 days at 37°C; the mineralization process was followed by scanning electron microscopy, energy-dispersive spectroscopy, X-ray diffraction and calcium quantification analyses. The results showed that massive mineralization occurred exclusively at the surface of HA disks treated at 1200°C and that nucleation of large aggregates of calcium phosphate started specifically inside small concavities instead of on the planar surface of the disks. Regarding the effect of concavity diameter size on surface mineralization, it was observed that small concavities induce 124- and 10-fold increased mineralization compared to concavities of large or medium size, respectively. The results of this study demonstrated that (i) *in vitro* surface mineralization of calcium phosphate ceramics with surface concavities starts preferentially within the concavities and not on the planar surface, and (ii) concavity size is an effective parameter to control the spatial position and extent of mineralization *in vitro*.

5. *What is the influence of SBF volume change, disk material, and surface hemispheres on mineralization?*

Calcium phosphate ceramics are the main mineral constituents of bone and teeth and hence have been extensively investigated for bone regenerative applications. Therefore, in **Chapter 6**, the effect of disk material, surface geometry, and SBF volume on mineralization capacity was investigated.

Hemispherical concavities were created on the surfaces of disks made of different materials (i.e. hydroxyapatite (HA), β -tricalcium phosphate (β -TCP), biphasic calcium phosphate (BCP) and titanium (Ti)), of which the ceramic materials were sintered at 1200°C. Mineralization of CaP was assessed on disk surfaces after immersion of the samples in different volumes of simulated body fluid (SBF) up to 14 days by means of calcium assay and scanning electron microscopy (SEM). This study showed that different SBF volumes have different effects on mineralization, with an optimum material/liquid ratio of 4.92 ml of SBF per cm² surface area. Additionally, at this volume, apparent differences based on disk material became obvious. Evidently, surface hemispherical concavities acted as initiator areas for nucleation and crystal growth.

6. How do cells populate hemispherical concavities and to what extent does concavity size influence 3-dimensional cellular organization?

Calcium phosphate ceramics in combination with implant surface geometry have been shown to influence biological performance. It is also known that micro- and nano-scale morphology of the calcium phosphate surface can strongly influence osteoblast and stem cell adhesion, proliferation, and differentiation. Therefore, in **Chapter 7**, hemispherical cavities with a size of 440, 800 and 1800 μ m were created on the surface of HA disks sintered at 1200°C and cultured with adipose tissue mesenchymal stem cells (AT-MSCs) in osteogenic medium for up to 28 days at 37°C. At selected time points (3, 7,

CALCIUM PHOSPHATE CERAMICS FOR BONE REGENERATION

14, 21, and 28 days), samples were removed and after fixation, cells were fluorescently labeled with phalloidin-Alexa 568 for filamentous (F-)actin and DAPI for nuclear staining. Cells were imaged and examined with a confocal laser scanning microscopy (CLSM). Immunofluorescence-based three-dimensional (3D) image analysis showed differences in cell number between concavities. The highest number of cell nuclei was found in the 440 μm cavity and the lowest number in the 1800 μm . Additionally, cells were able to migrate toward the concavities and adhere to their edges and walls. Preferential mineralization was observed inside the concavities. Cells spread over and to the bottom of concavities covering all their volume and creating multilayers on their surfaces. Results from this study suggest a correlation between concavity size, cellular organization, mineralization and osteogenic differentiation.

Dutch summary / Samenvatting

Het doel van dit proefschrift was te onderzoeken wat het effect is van de fysisch-chemische en biologische eigenschappen van verscheidene calciumfosfaat (CaP) keramieken voor biomedische toepassingen, met daarbij nadruk op CaP compositie en oppervlakte-morfologie. **Hoofdstuk 1** geeft een algemene introductie over de eigenschappen van biokeramiek, de eigenschappen van ieder type biokeramiek, het gebruik van biokeramiek als coating, coating depositie-technieken, en de fysische en biologische interactie van zulke implantaten met botweefsel. Deze samenvatting behandelt opeenvolgend de onderzoeksvragen zoals beschreven in het eerste hoofdstuk.

1. Wat is de huidige kennis van coatings o.b.v. inorganische en/of organische materialen, en welke technieken zijn beschikbaar voor het aanbrengen van dergelijke coatings op metalen?

Synthetische inorganische en organische materialen zijn veelvuldig onderzocht voor botregeneratie in een poging de compositie en structuur van de bot extracellulaire matrix (ECM) na te bootsen, met als uiteindelijk doel het genereren van geschikte, synthetische botvervangers en modificaties van botimplantaat-oppervlakken. Voor lastdragende toepassingen bestaan botimplantaten veelal uit bioinert metaal met geschikte mechanische eigenschappen en een aangepast oppervlak (bijv. opgeruwd, gecoat, of een combinatie daarvan) om de biocompatibiliteit en osteoconductive

CALCIUM PHOSPHATE CERAMICS FOR BONE REGENERATION

eigenschappen te verbeteren. Momenteel ondergaat het biomaterialen onderzoek een transitie van inerte, biologisch-passieve implantaten naar interactieve implantaten, welke weefselregeneratie bevorderen. Daartoe dienen de fysisch-chemische eigenschappen optimaal en in staat te zijn om de regeneratie van botweefsel te instrueren en stimuleren.

Hoofdstuk 2 was gericht op oppervlakte-modificaties voor lastdragende botimplantaten binnen de botregeneratie, met nadruk op het gebruik van inorganische en organische coatingbestanddelen, die actief deelnemen aan het biologisch proces dat in gang gezet wordt na implantatie. Dit overzicht toont dat met de juiste oppervlakte-modificaties een bijdrage geleverd kan worden om gewenste weefselreacties in zowel gezonde als gecompromitteerde condities te bewerkstelligen.

2. Wat zijn de effecten van CaP compositie in sputtercoatings op in vitro en in vivo prestatie?

Keramische calciumfosfaat (CaP) coatings zijn gebruikt om de biocompatibiliteit en osteoconductive eigenschappen van metalen implantaten te verbeteren. De chemische compositie van deze keramische coatings is een belangrijke parameter, die de uiteindelijke botprestatie van het implantaat kan beïnvloeden. In **Hoofdstuk 3** werd het effect van compositie van CaP-sputtercoatings op in vitro oplosgedrag en in vivo botprestatie onderzocht. De coatings werden gegenereerd via radio frequency (RF) magnetron sputtering; drie types CaP target materiaal werden gebruikt om coatings te maken met

verschillende stoichiometrie en calcium/fosfaat ratio's (hydroxyapatiet,(HA), alfa-tricalciumfosfaat (alfa-TCP), en tetra-calciumfosfaat (TTCP)) en vergeleken met ongecoat titaan. De aangebrachte coatings werden gekarakteriseerd via X-ray diffractie, Fourier transform infrared spectroscopie, scanning elektronen microscopie, en inductively coupled plasma optische emissie spectroscopie. Het in vitro oplossen/precipiteren van de CaP coatings werd bestudeerd middels incubatie testen in simulated body fluid (SBF). Om de in vivo situatie na te bootsen werden deze verschillende CaP coatings ook geevalueerd in een femorale condyle model in konijnen. TCPH en TTCPH vertoonden morfologische veranderingen gedurende de 4 weken incubatie in SBF. De resultaten van bot-implantaat contact (BIC) en peri-implantaat botvolume (BV) toonden een gelijke prestatie voor alle experimentele coatings. Een klaarblijkelijk verschil in tartrate-resistant acidic phosphatase (TRAP) positieve kleuring werd waargenomen in het peri-implantaat gebied met afnemende coating stabiliteit. Concluderend toonden de experimentele groepen in vitro verschillende eigenschappen en een duidelijke toename in botremodelering met toenemend oplossen van de coating in vivo.

3. Wat is het effect van verschillende micrometer dikke hydroxyapatietcoatings op de residual stress?

Biokeramische coatings, inclusief calciumfosfaat coatings o.b.v. hydroxyapatiet (HA), vertegenwoordigen een gebruikelijke oppervlakte-modificatie voor metalen botimplantaten. T.a.v. de mismatch in

CALCIUM PHOSPHATE CERAMICS FOR BONE REGENERATION

materiaaleigenschappen tussen het keramisch coatingmateriaal en het metalen substraatmateriaal had **Hoofdstuk 4** als doel om de residual stress in een HA-coatings gedeponereerd middels RF magnetron sputtering te evalueren via twee verschillende analyses, gebaseerd op enerzijds de Stoney formule (via meting van de curvatuur van het substraat [Stoney, 1909]) en anderzijds de $\sin^2 \psi$ methode (via röntgen diffractie patronen van de coating). Bovendien werd het effect van dikte van de HA-coating (1 or 4 μm) op residual stress en oppervlakte-topografie bekeken. We veronderstelden dat (i) beide methoden eenzelfde residual stress beeld zouden geven, en dat (ii) dikke coatings de residual stress zouden verhogen in vergelijking met dunne coatings. De curvatuur metingen toonden een lage residual stress (range: -60-80 MPa), welke relaxeerde na post-depositie hittebehandeling op 650 °C. Ook kristalstructuurmetingen van residual stress toonden relaxatie van HA coatings na post-depositie hittebehandeling. De coatingdikte variaties in de micrometer-range lieten geen duidelijke effecten op residual stress zien. O.b.v. nauwkeurigheid en gelijkheid met werkelijke condities is het bepalen van residual stress via kristalstructuur metingen aan te bevelen.

4. Wat is de rol van hemisferische concaviteiten op de in vitro mineralisatie van biokeramische materialen?

Voor herhalende concaviteiten op het oppervlak van botimplantaten is recentelijk aangetoond dat ze een rol spelen in ectopische botvorming in vivo. In **Hoofdstuk 5** was ons doel om te evalueren wat het effect van oppervlakte

concaviteiten op de oppervlakte-mineralisatie van hydroxyapatiet (HA) en β -tricalcium phosphate (β -TCP) keramiek in vitro is. Hemisferische concaviteiten met verschillende diameters werden aangebracht op het oppervlak van HA en β -TCP gesinterde discs: 1.8 mm (grote concaviteit), 0.8 mm (middelgrote concaviteit) en 0.4 mm (kleine concaviteit). HA en β -TCP discs werden gesinterd op 1100 of 1200 °C en geïncubeerd in SBF voor een periode van 28 dagen bij 37 °C; het mineralisatie proces werd gevolgd via scanning elektronen microscopie, energy-dispersive spectroscopie, X-ray diffractie en calcium quantificatie analyses. De resultaten toonden dat extreme mineralisatie plaatsvond alleen aan het oppervlak van HA discs gesinterd op 1200 °C en dat nucleatie van calciumfosfaat specifiek in de kleine concaviteiten startte en niet op het vlakke deel van de discs. T.a.v. het effect van de diameter van de concaviteiten op oppervlakte-mineralisatie werd gezien dat kleine concaviteiten 124 en 10 keer zoveel mineralisatie gaven dan grote of middelgrote. De resultaten van deze studie toonden dat (i) in vitro oppervlakte-mineralisatie voor CaP keramiek met concaviteiten preferentieel start in deze concaviteiten en niet op het vlakke oppervlak, en dat (ii) concaviteit grootte een effectieve parameter is om de ruimtelijke positie en mate van in vitro mineralisatie te beïnvloeden.

5. Wat is de invloed van SBF volume verandering, disc materiaal, en oppervlakte hemisferen op mineralisatie?

CALCIUM PHOSPHATE CERAMICS FOR BONE REGENERATION

Calciumfosfaat keramiek is het belangrijkste bestanddeel van bot- en tandweefsel en derhalve veel onderzocht voor toepassingen voor botregeneratie. Derhalve werd in **Hoofdstuk 6** het effect van disc materiaal, oppervlakte geometrie, en SBF volume op mineralisatie onderzocht. Hemisferische concaviteiten werden aangebracht aan het oppervlak van discs (HA, β -TCP, BCP, en titaan), waarvan de keramische materialen werden gesinterd op 1200°C. CaP mineralisatie aan het oppervlak van de discs werd bestudeerd na incubatie van de discs in verschillende volumina SBF voor een periode tot 14 dagen middels een calcium assay en scanning electronen microscopie (SEM). Deze studie toonde dat verschillende SBF volumina een verschillende effect hebben op mineralisatie, met een optimale materiaal/vloeistof ratio van 4.92 ml SBF per cm² oppervlak. Bovendien toonde deze ratio een duidelijk verschil in mineralisatie o.b.v. disc materiaal. Het was duidelijk dat oppervlakte hemisferen fungeerden als initiator voor nucleatie en kristalgroei.

6. Hoe bevolken cellen hemisferische concaviteiten en in welke mate beïnvloedt concaviteit grootte de 3D cellulaire organisatie?

CaP keramiek gecombineerd met implantaat oppervlakte geometrie heeft aangetoond een rol te spelen in de biologische prestatie. Daarnaast is bekend dat micro- en nano-schaal morfologie van CaP oppervlakken sterk de adhesie, proliferatie en differentiatie van stamcellen kan beïnvloeden. Derhalve werden in **Hoofdstuk 7** hemisferische concaviteiten met een grootte van 440, 800 en 1800 μm aangebracht op het oppervlak van HA discs gesinterd op

1200°C en daarop celweekexperimenten met vetweefsel mesenchymale stamcellen uitgevoerd in osteogeen medium voor een periode van 28 dagen. Op geselecteerde momenten (3, 7, 14, 21 en 28 dagen) werden samples genomen en de cellen, na fixatie, fluorescerende gelabeld met phalloidin-Alexa 568 voor filamenteus (F-actine) en DAPI voor kernkleuring. Analyses werden uitgevoerd middels confocal laser scanning microscopie (CLSM). 3D immunofluorescentie beelden toonden verschillen in celaantal tussen de concaviteiten. Het hoogste aantal celkernen werd gezien in de 440 µm concaviteiten en het laagste aantal in die van 1800 µm. Bovendien bleken cellen in staat te migreren naar de concaviteiten en te hechten aan de randen en wanden ervan. Preferentiële mineralisatie werd waargenomen in de concaviteiten. Cellen spreidden zich in de concaviteiten, waarbij ze multilagen maakten op het oppervlak. De resultaten van deze studie suggereren een correlatie tussen concaviteit grootte, cellulaire organisatie, mineralisatie en osteogene differentiatie.

Afsluitende opmerkingen en toekomstperspectief

Dit proefschrift beschrijft onderzoek naar calciumfosfaat (CaP) keramiek in laboratorium en dierexperimenten gericht op uiteindelijke toepassing in de kliniek. CaP keramiek wordt gebruikt als coating materiaal om de biocompatibiliteit en osteoconductieve eigenschappen van metalen te verbeteren. De ontwikkeling van substantieel (inter)actievere CaP implantaat coating materialen heeft significant bijgedragen aan de voortgang in de wetenschap van oppervlakte-modificatie. Echter, vele wetenschappelijke en technologische uitdagingen blijven bestaan binnen het biomaterialen onderzoek. De laatste ontwikkelingen hierin, inclusief CaP coatings met kristalstructuur vervangingen, CaP coatings gebruikt als therapeutische coatings, en meer interactieve CaP coatings voor gebruik in gecompromiteerde condities werden beschreven in ons overzichtshoofdstuk. T.a.v. de klinische en commerciële toepassing van coatings ontwikkeld voor ons onderzoek dient te worden opgemerkt dat CaP sputtercoatings (in de vorm van 1-2 μm dikke hydroxyapatiet coatings op dentale implantaten) reeds klinisch gebruikt worden. Wij hebben aangetoond dat verschillende targetcomposities een effect hebben op het oplos- en precipitatiegedrag van de resulterende CaP coatings in vitro. Voorts werd in vivo een toename in botremodelering gezien voor CaP coatings met een hoger oplosgedrag, bijv. voor coatings gemaakt met tetracalciumfosfaat (TTCP) als target materiaal. De weinige onderzoeken die TTCP gebruikt hebben als coating materiaal hebben een veelbelovende

biologische prestatie laten zien [1,2]. Verder onderzoek dient zich te richten op het gebruik van radio-frequency (RF) magnetron sputtering voor het maken van TTCP coatings in fase-combinatie met hydroxyapatiet (bijv. HA/TTCP coatings) om zich te verzekeren van coatingstabiliteit, alsook het gebruiken van het oplosgedrag van TTCP voor biologische optimalisatie.

Naast de compositie van CaP keramiek zijn ook andere parameters van belang voor de optimalisatie van oppervlakte-eigenschappen van implantaten. Dit proefschrift heeft de relevantie aangetoond van oppervlakte topografie gecombineerd met CaP keramiek als bulk materiaal voor de promotie van mineralisatie in vergelijking met vlakke oppervlakken. Dat dergelijke oppervlakte topografie in staat was celgedrag te beïnvloeden, waaronder proliferatie en osteogene differentiatie, werd ook aangetoond. Daarom is de combinatie van oppervlakte topografie in een mechanisch sterk materiaal met een bioactieve CaP coating veelbelovend; toekomstig onderzoek is noodzakelijk om de fundamentele principes verantwoordelijk voor cel- en weefselresponse op ‘off-the-shelf’ beschikbare medische hulpmiddelen (bijv. botimplantaten) te ontrafelen.

Hoewel het gebruik van SBF als een voorspellende in vitro test voor onderzoek naar botbinding algemeen geaccepteerd is, hebben sommige onderzoekers bezwaren tegen de vermeende voorspellende waarde ervan, waardoor inspanningen hebben geleid tot een aangepast protocol voor dergelijk onderzoek. Echter, parameters zoals het optimale volume SBF blijven onduidelijk. Onze inspanningen poogden duidelijkheid te verkrijgen hierin door

CALCIUM PHOSPHATE CERAMICS FOR BONE REGENERATION

drie verschillende volumina SBF te vergelijken. Een optimale ratio werd gevonden voor het intermediaire volume, hetgeen de mineralisatie van CaP keramiek bevorderde. Ondanks deze opvallende vondst blijft het mechanisme hierachter onduidelijk en is er dus meer onderzoek noodzakelijk.

Zoals eerder aangegeven lijkt het gebruik van optimaal CaP keramiek gecombineerd met optimale oppervlakte geometrie veelbelovend en waarschijnlijk te leiden tot de ontwikkeling van een nieuwe generatie CaP keramische biomaterialen met verbeterde biologische prestaties. Toch is meer aandacht nodig voor onderzoek naar hoe cellen een interactie aangaan met 3D matrices, hun oppervlakte-eigenschappen herkennen, en intracellulaire signaling netwerken gebruiken. Deze kennis t.a.v. fundamentele cel-materiaal interacties is uitermate belangrijk om te begrijpen waarom een CaP keramiek met specifieke eigenschappen (e.g. compositie, oppervlakte morfologie, etc.) een bepaalde response teweegbrengt i.p.v. het enkel aantonen van een verbeterde biologisch prestatie. Bovendien zijn slechts enkele dierstudies beschikbaar waarin CaP keramiek gecombineerd met gewenste oppervlakte geometrie werd gebruikt. Echter, enkele CaP keramieken hebben aangetoond osteoinductieve eigenschappen te hebben (het materiaal induceert de novo botvorming) wanneer geïmplantéerd op een ectopische locatie (subcutaan of intramusculair) [3-5]. Het ontrafelen van de grondslag van dit osteoinductieve fenomeen zal leiden tot breed gebruik van CaP keramiek eigenschappen voor de ontwikkeling van instructieve implantaten. Hierdoor kan het in de toekomst mogelijk worden om synthetische materialen te ontwikkelen met een

biologische prestatie gelijk aan die van autoloog bot.

Closing remarks and future perspectives

In this thesis, calcium phosphate (CaP) ceramic materials were investigated in a laboratory and preclinical setting for their eventual use in clinical applications. CaP ceramics are used as coating materials to enhance the biocompatibility and osteoconductive properties of metallic implants. Development of substantially more (inter)active CaP implant coating materials has significantly propelled the science of surface modification. However, many scientific and technological challenges remain in biomaterials research. The latest developments in biomaterials research, including CaP coatings with crystal lattice substitutions, CaP coatings employed as therapeutic coatings, and more interactive CaP coatings for use in compromised conditions were explored in our review chapter. Concerning the clinical and commercial application of the coatings developed in this thesis, it is important to mention that sputter deposited CaP coatings (in the form of 1-2 μm thick hydroxyapatite coatings on dental implants) are already clinically used. We showed that different target phase composition influences dissolution and precipitation formation of the resulting CaP coatings when tested *in vitro*. Moreover, when these coatings were tested *in vivo*, an increase in bone remodelling was observed for CaP coatings with higher dissolution rate, such as coatings deposited using tetracalcium phosphate (TTCP) as target material. The very few studies that have used TTCP as a coating material have shown promising biological performance [1, 2]. Further research should focus on the use of

CALCIUM PHOSPHATE CERAMICS FOR BONE REGENERATION

radio-frequency (RF) magnetron sputter deposition to generate TTCP coatings in phase combination with hydroxyapatite (i.e. HA)/TTCP coatings) to ensure long-term stability of the coating, while exploiting the higher dissolution properties of TTCP for biological optimization.

In addition to the composition of CaP ceramics, other parameters are critical to optimize surface properties of implants. This thesis has shown the relevance of surface topography in combination with CaP ceramics as bulk material to promote mineralization compared to a planar surface. That this surface topography was able to affect cell behavior in terms of proliferation and osteogenic differentiation was also demonstrated. Therefore, the combination of surface topography in a mechanically strong material with a bioactive CaP coating is promising and should be considered for future studies to unravel the fundamental basics responsible for cell and tissue response to off-the-shelf available medical devices (i.e. bone implants).

Although the use of simulated body fluid (SBF) as a predictive *in vitro* test for examining bone bonding potential is widely accepted, some researchers have argued the predictive validity of this test, and efforts have been made to improve the current protocol. However, parameters such as the optimal SBF volume ratio remain unclear. Our efforts attempted to reveal an optimal SBF volume/surface area ratio using three different SBF volumes. An optimal ratio was found for the intermediate volume, which favoured mineralization of CaP ceramic materials. Despite this remarkable finding, the mechanism behind this

optimal calcium deposition at the intermediate volume is still unclear and further research is needed.

As mentioned above, the use of optimal CaP ceramics in combination with optimized surface geometry seems promising and likely to attain a novel generation of CaP ceramic biomaterials with further improved biological performance. Still, more attention should be paid to specifics of how cells interact with 3D matrices, recognize their surface properties, and use intracellular signaling pathways. This knowledge on the fundamentals of cell/material interactions is pivotal to understand why a CaP ceramic with certain characteristics (i.e. composition, surface morphology, etc.) induces a certain response rather than empirically demonstrate superior biological performance. Moreover, few animal studies are available in which CaP ceramics in combination with (intended) substrate geometry were used. However, several CaP materials have shown osteoinductive capacity (i.e. potential of a material to induce bone formation while implanted in an animal at ectopic sites (e.g. subcutaneously or intramuscularly)) [3-5]. Unraveling the nature of this osteoinductive phenomenon will pave the way for broad utilization of CaP ceramic characteristics for instructive implant manufacturing, for which accounts that rapprochement to synthetic materials with equal biological performance as autologous bone can become realistic.

CALCIUM PHOSPHATE CERAMICS FOR BONE REGENERATION

References

1. *J.D. de Bruijn, Y.P. Bovell, C.A. van Blitterswijk, Biomaterials, 15 (1994) 543-550.*
2. *C.P. Klein, P. Patka, J.G. Wolke, J.M. de Blicck-Hogervorst, K. de Groot, Biomaterials, 15 (1994) 146-150.*
3. *Ripamonti U. et al., J. Cell. Mol. Med. 13, 2953, 2009*
4. *Scarano A., et al., Clin. Implant Dent. Rel. Res, 2009*
5. *Ripamonti U. et al., Biomaterials, 3813, 2012*

9

ACKNOWLEDGMENTS, CURRICULUM VITAE, AND LIST OF PUBLICATIONS

CALCIUM PHOSPHATE CERAMICS FOR BONE REGENERATION

Acknowledgments:

First of all I would like to thank Prof. Jansen for giving me the opportunity to conduct this research in his department. This Ph.D. has been a lot of work but I enjoyed being a part of your department and I learned a lot. I was given the freedom to satisfy my curiosity and sometimes I was so focused that time really flew by. I wanted to thank you especially for our scientific discussions and the advice you gave me that bettered my work. I also want to thank you for your professionalism and your aid in all aspects of my Ph.D. journey.

Dr. Wolke, Joop, it has been a pleasure to work with you; your passion for research and biomaterials is really contagious. You are the person that I have learned the most from during my research, you always had time to discuss and explain things to me. I greatly enjoyed those conversations and I am sure I am going to miss them and miss you. Thank you very much Joop for encouraging, supporting, and motivating me again in the most difficult moments, you were a real supervisor to me and a good friend and I will always remember you!

Dr. van den Beucken, Jeroen, thank you very much for helping me and motivating me to start and to finish this thesis. You were always impressively fast reviewing my articles and had very good comments about my work which helped to greatly improve the quality of my research. I know we didn't always

agree with each other but I am glad we kept working together and that you didn't give up on me.

Dr. Yang, Fang, just thinking of you makes me smile! Thank you for encouraging and supporting me to carry on in this research. You were always there to help and to bring a good atmosphere and interesting conversations.

Dr. Sanne Both, Dr. Frank Walboomers, Dr. Sander Leeuwenburgh, and Dr. Adelina S. Plachokova-Damyanova. It has been great to meet you in the department!

I would like to express my gratitude to Kim, Vincent, Martijn, Monique, Natasja, and Henriette for all your help and support during my Ph.D.

Especial thanks to Astghik, Hamdan, and Alexey, I really enjoyed working with you and I learned lots of things from all of you. Dear Astghik, working on my last article with you was the most challenging, exhausting, and fascinating time of my research, we were so stubborn about it that we made it work! I loved our scientific discussions and all of our conversations and I will miss working with you but mostly I will miss my friend!

I would like to thank all my biomaterial colleagues, but especially Cristina, Daniel, Reza, Marco, Jiankang, Claire, Matilde, Ljupcho, Kemal, Edwin, Huanan, Ruggero, Arnold, Floor, Bart, Paulo, Simone, Jan, Xinjie, Kambiz, Antonio, Mani, Alessandro, Pedro, Carla, Take, Yue, Jing, and Hongbing. It was great to meet you all and to have you there!

I've encountered a number of kind souls along the way. Rosa, Wanxun, Na, Wei, Jingling, Ana, Manuela, Xiangzhen, and Paula, thank you

CALCIUM PHOSPHATE CERAMICS FOR BONE REGENERATION

for all the memories and great times together. Jingling and Wei you made me laugh every day in the office! Wanxun and Na I will never forget our amazing trip together, thank you for being always there for me! Rosa, Ana y Paula chicas sois increíbles, qué más puedo decir? De verdad que no me imagino estos cuatro años sin vosotras, gracias por sacarme siempre una sonrisa y por recordarme porque me gusta tanto la gente del sur jeje!

A mis amigos de siempre, Lore, Virgi, Anita, Anamari, Alvaro, Alberto, Rosi y Pablo. Gracias por estar siempre ahí, no importa la distancia o el tiempo que pase sin vernos, cuando hablamos es como si los años no hubieran pasado.

A nuestros amigos de “los Pinos”, Alex, Verity, Quentin, Javier, María, Inés, Anna, Theo, Patricia y Gabriel gracias chicos por hacernos pasar unos seis meses inolvidables en Madrid!

To our Dutch family, some of you we knew before we arrived in The Netherlands, Marjolein, Arjan, Lars, Sheila, and Charlie. Some we met later Roland and Carolina, Milja and Vlado, Simon and Ana, and Hanneke and Nils. Thank you all for sharing with us so many priceless memories you will always be part of us.

To my family in Canada including our family in Dresden thank you always for being there for us and for always coming to see us!

A mi familia de Cádiz y Madrid y en especial a mis abuelos los que se han ido en estos últimos años y los que todavía están conmigo. Gracias por vuestro amor incondicional y por todas las cosas que me habéis enseñado. A

mis hermanos Fernan, Carlos y David, cuñadas Anmari, Carmen y Cristina y a mis sobrinitos Elsa y Dani. Gracias por estar siempre ahí y por hacer que nuestras vacaciones en España se pasen tan rápido!

Nacho me faltan las palabras para agradecerte tu esfuerzo en el diseño de esta tesis, como se dice por Cádiz tu sí que tienes arte, y mucho talento!!

Nuria, gracias por ser un ejemplo para mí y por ayudarme siempre de corazón. El año que viví contigo en Roma es inolvidable para mí por muchos motivos...

A mi madre, sin cuyo esfuerzo, dedicación y apoyo incondicional no hubiera podido terminar esta tesis. Tu fe en mí es lo que me ha ayudado a seguir adelante en los momentos difíciles. Te echo de menos cada día.

This book is dedicated to Steve, Dafne and Audrey. Dafne y Audrey solo una sonrisa vuestra me llena de felicidad, vosotras sois mi mayor motivación y lo más importante en mi vida. Steve gracias por tu amor, por tu apoyo diario, por tu paciencia, por creer en mí y por hacerme tan feliz. La vida contigo es toda una aventura!

Curriculum vitae:

Eva R. Urquía Edreira was born on the 7th of March, 1981 in Madrid, Spain. She received her M.Sc. and Honours Bachelor of Chemical Engineering degrees from the Faculty of Science, University of Cádiz, Spain (2009). She was also a research volunteer at the Food and Agriculture Organization of the United Nations (FAO), Italy (2005) and interned at the University of Rennes, France for one year under the Erasmus program (2007). Her final M.Sc. project was then conducted in the Department of Process and Technology at Akzo Nobel Chemicals, The Netherlands (2010). In October 2010 she began her Ph.D. research on the development and biological evaluation of ceramic coatings, in the Department of Biomaterials of Prof. Dr. John Jansen at Radboud University Nijmegen, The Netherlands.

Publications related to this thesis:

Urquia Edreira, E.R., Alghamdi, H., Wolke, J.G.C., van den Beucken, J.J.J.P., Jansen JA. Material and Biological Issues Related to the Use of Inorganic Materials at the Bone–Implant Interface. (*Reference Module in Chemistry, Molecular Sciences and Chemical Engineering Comprehensive Inorganic Chemistry II (Second Edition). From Elements to Applications Volume 4: Solid-State Materials, Including Ceramics and Minerals. Pages 417-430, 2013.*)

Urquia Edreira, E.R.*, Bosco, R.*, Wolke, J., Leeuwenburgh, S.C.G., van den Beucken, J.J.J.P., Jansen, J.A.. Instructive coatings for biological guidance of bone implants. (*Surface and Coatings Technology, 2013. 233: p. 91-98*)

Urquia Edreira, E.R., Wolke, J.G., Aldosari, A.A., Al-Johany, S.S., Anil, S., Jansen, J.A., van den Beucken, J.J.J.P.. Effects of calcium phosphate composition in sputter coatings on *in vitro* and *in vivo* performance. (*Journal of Biomedical Materials Research Part A, 2014*)

Bianchi, M., Urquia Edreira, E.R., Wolke, J.G., Birgani, Z.T., Habibovic, P., Jansen, J.A., Tampieri, A., Marcacci, M., Leeuwenburgh, S.C., van den Beucken, J.J.J.G. Substrate geometry directs the *in vitro* mineralization of calcium phosphate ceramics. (*Acta Biomaterialia. 10:661-9, 2014*)

Urquia Edreira, E. R., Wolke, J.G., Jansen, J.A., van den Beucken, J.J.J.P. Influence of ceramic disk material, surface hemispheres, and SBF volume on *in vitro* mineralization. (*Journal of Biomedical Materials Research Part A, 2015*)

Urquia Edreira, E. R., Wolke, J.G., Jansen, J.A., van den Beucken, J.J.J.P.. Residual stress evaluation within hydroxyapatite coatings of different micrometer thicknesses. (*Surface and Coatings Technology, 2015*)

Urquia Edreira, E. R.*, Hayrapetyan, A.*, Wolke, J., Croes, H.J.E., Klymov, A., Jansen, J.A., van den Beucken, J.J.J.P. Effect of Calcium

CALCIUM PHOSPHATE CERAMICS FOR BONE REGENERATION

Phosphate Ceramic Substrate Geometry on MSC Organization and Osteogenic Differentiation. (*Submitted*)

* These authors contributed equally.

**CALCIUM
PHOSPHATE
CERAMICS
FOR BONE
REGENERATION**

Eva R. Urquía Edreira